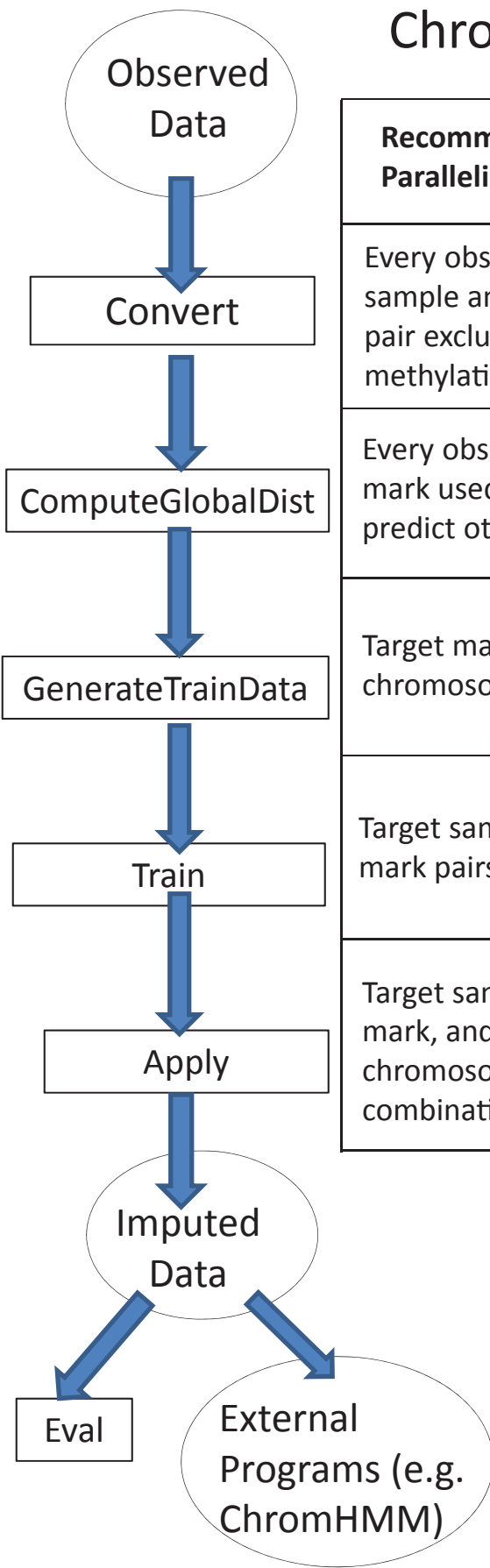


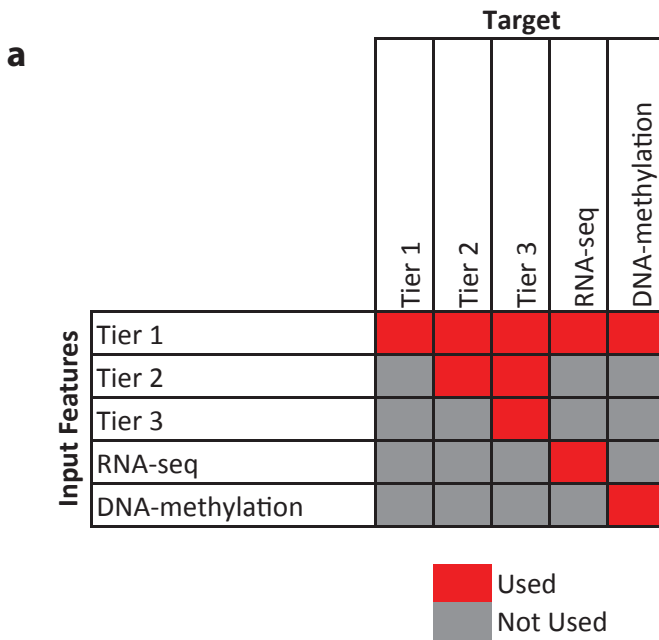
ChromImpute Workflow



Recommended Parallelization	Number of Jobs	Approximate CPU time for hardest jobs	Approximate CPU time for average job
Every observed sample and mark pair excluding DNA-methylation	1088	10min	10min
Every observed mark used to predict other marks	32	2hr	1hr
Target mark and chromosome	782	2hr	1hr
Target sample and mark pairs	4315	4hr	1hr
Target sample, mark, and chromosome combinations	99245	3hr	1hr

Supplementary Figure 1: Workflow of ChromImpute.

On left is a flow chart illustrating the various steps to generate the imputed data using the ChromImpute software. First the observed data is converted into the desired target resolution. Second a global distance for each mark between all pairs of samples is computed based on correlation. Third the training data is generated. Fourth the regression predictors are trained. Finally the regression predictors can be applied to generate imputed data for which additional analysis can be conducted. On the right is a recommended parallelization strategy for each command, and then for the imputation application considered here the number of compute jobs that would lead to and the approximate maximum and average CPU time for each job.



b

Tier	Marks	# of Marks	# Samples Represented	Min # Samples Per Mark	Max # of Samples Per Mark	Average # of Samples Per Mark	Total # of Observed Datasets	Total # of Imputed Datasets	Tiers of Other Marks Used in Primary Imputation
1	DNase,H3K27ac,H3K27me3, H3K36me3,H3K4me1,H3K4me3, H3K9ac,H3K9me3	8	127	53	127	106	848	1016	1
2	H2A.Z,H3K4me2,H3K79me2, H4K20me1	4	26	19	23	21.75	87	508	1,2
3	H2AK5ac,H2AK9ac,H2BK120ac, H2BK12ac,H2BK15ac,H2BK20ac, H2BK5ac,H3K14ac,H3K18ac, H3K23ac,H3K23me2,H3K4ac, H3K56ac,H3K79me1,H3K9me1, H3T11ph,H4K5ac,H4K8ac, H4K12ac, H4K91ac	20	10	1	7	4.85	97	2537	1,2,3
	DNA Methylation	1	37	37	56	37	37	127	1
	RNA-seq	1	56	56	56	56	56	127	1

Supplementary Figure 2: Relationship between Mark Tiers for the Main Imputation.
(a) The rows of the matrix correspond to subsets of marks for input defined in **b**, and the columns the set of target marks. A cell in the matrix is colored red if the corresponding set of marks of the row is used to predict the set of marks of the column for the main imputation. **(b)** The table reports statistics on the different tiers of marks as used for the primary imputation.

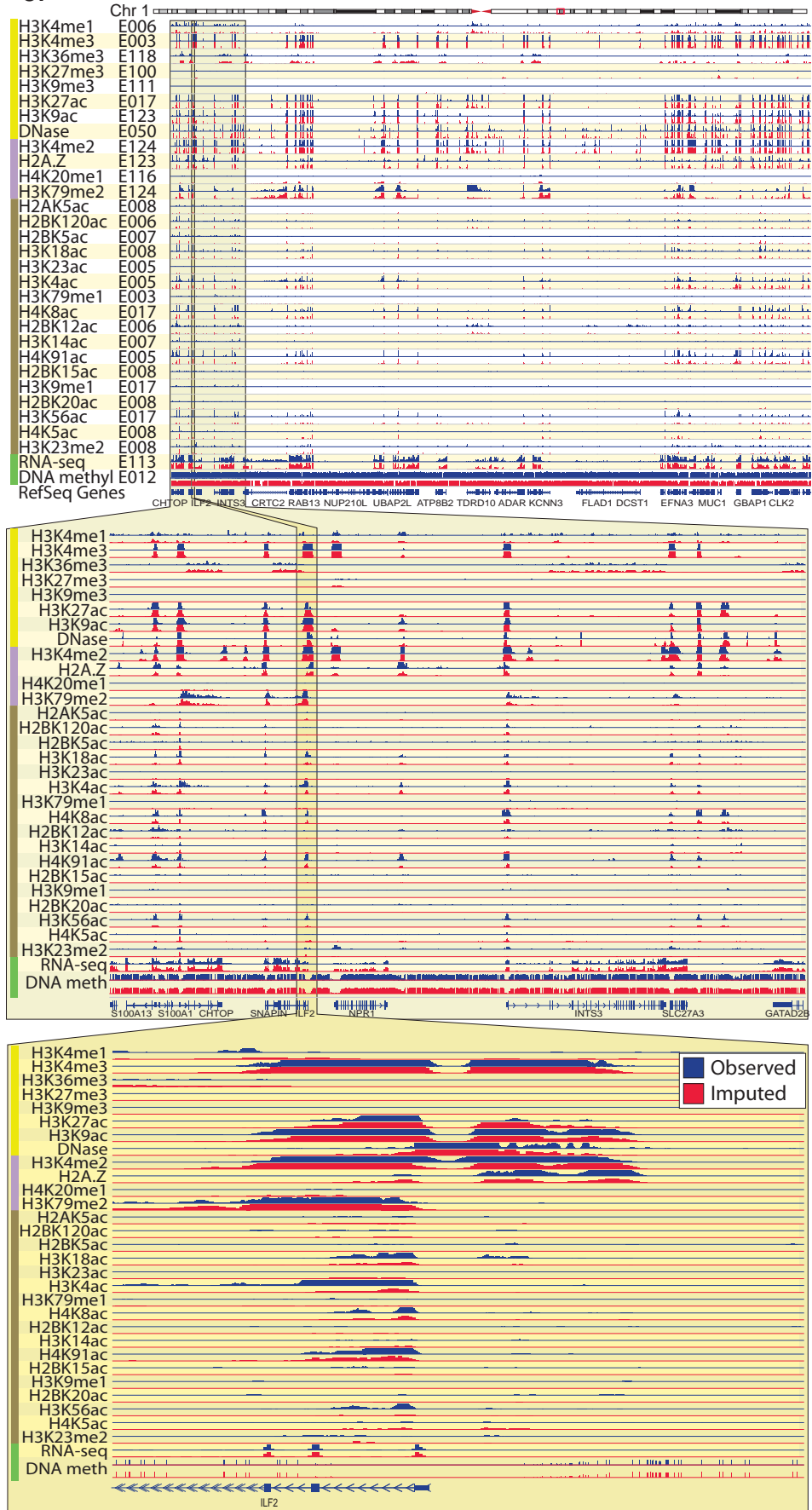
a

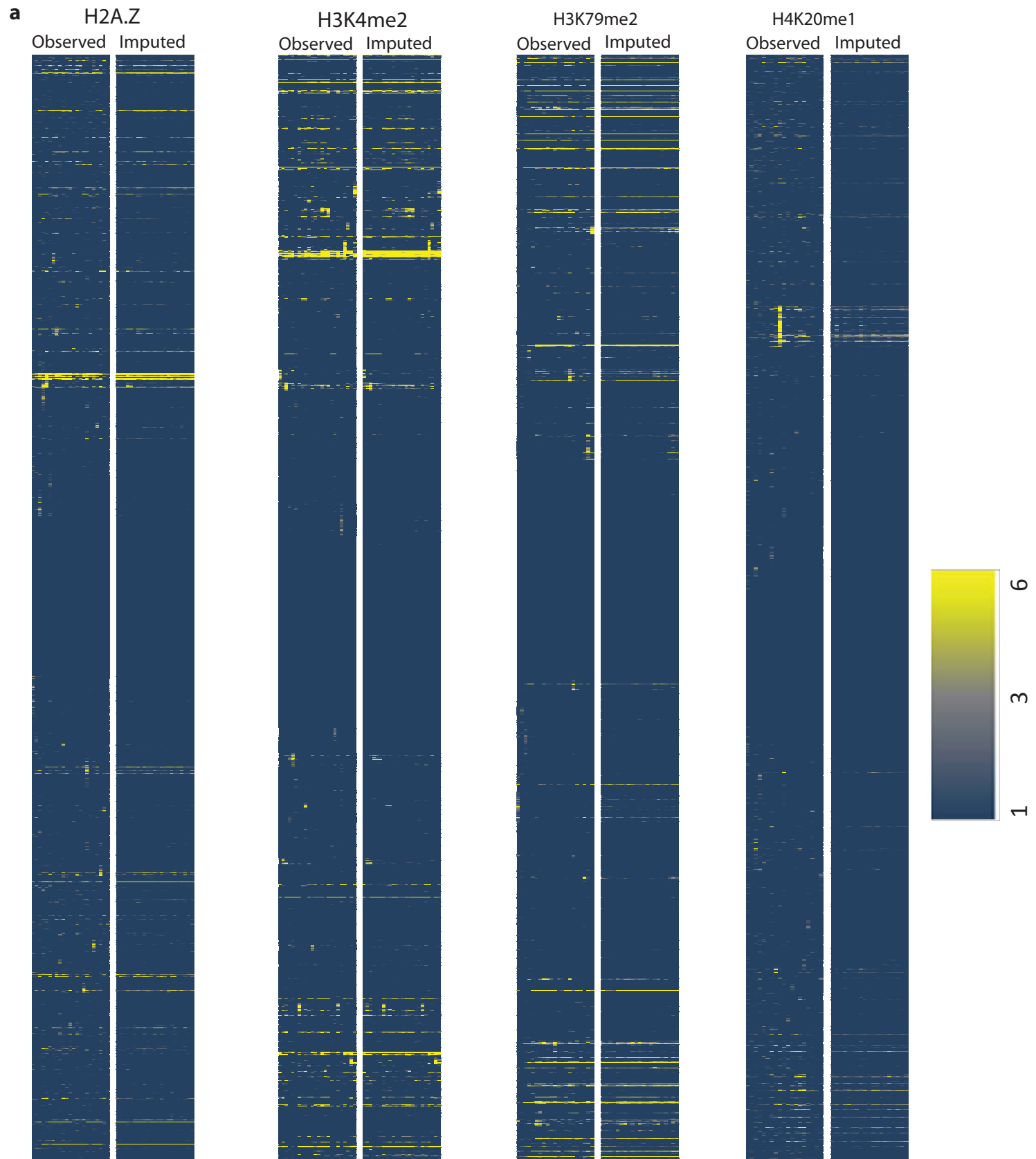
Supplementary Figure 3: Browser Images for Random Loci

(a) The figure shows browser screenshots for all Tier 1,2 marks, DNA-methylation, and RNA-seq at nine randomly selected 200kb loci of which the one with the most signal is also shown in **Fig. 2**. In blue is the signal for a randomly selected observed track for the mark and below it in red is the corresponding imputed track. DNA methylation values below the horizontal line correspond to missing values. **(b)** The same as shown in a, but for the Tier-3 marks. **(c)** Larger 1.5Mb context, and example 5kb close-up also shown for the randomly selected loci with the most signal associated with it. In the bottom set of tracks, note the dip in the nucleosome-free region of the ILF2 gene promoter, and the nucleotide-level concordance in CpG methylation information.

b

C.

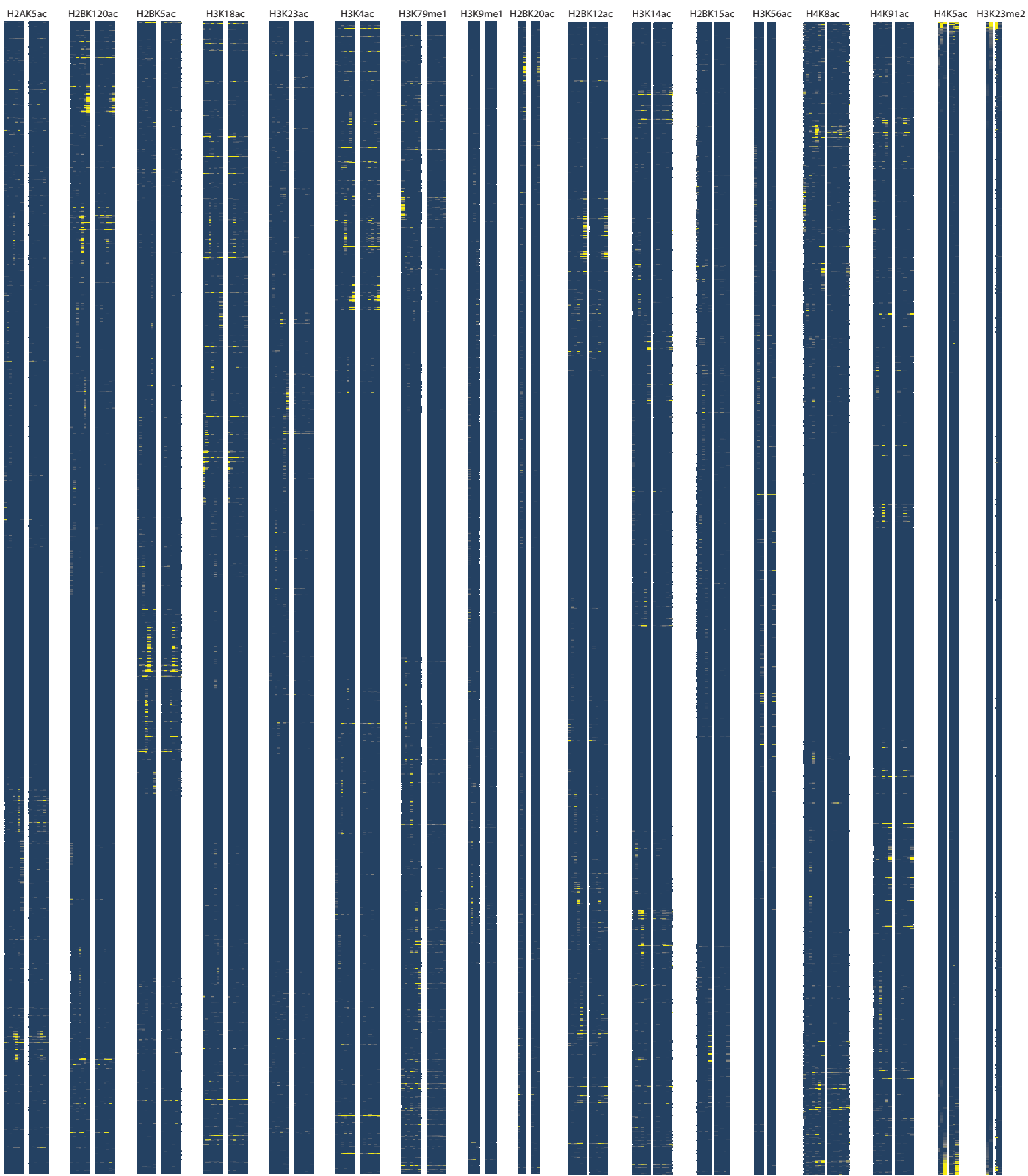


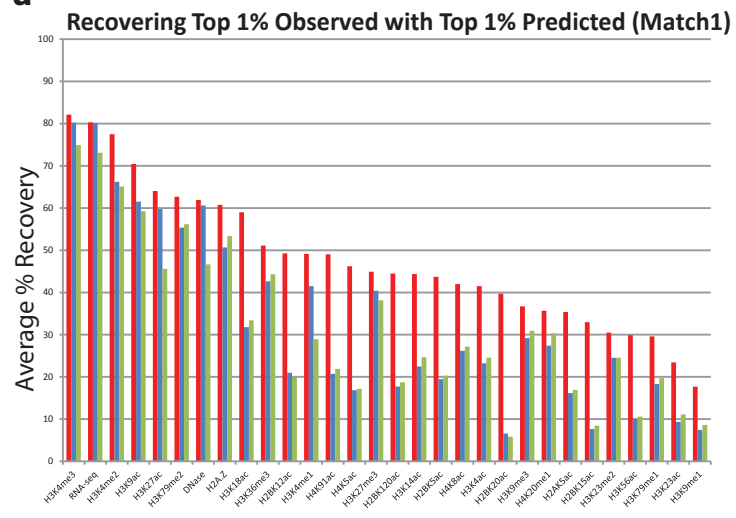
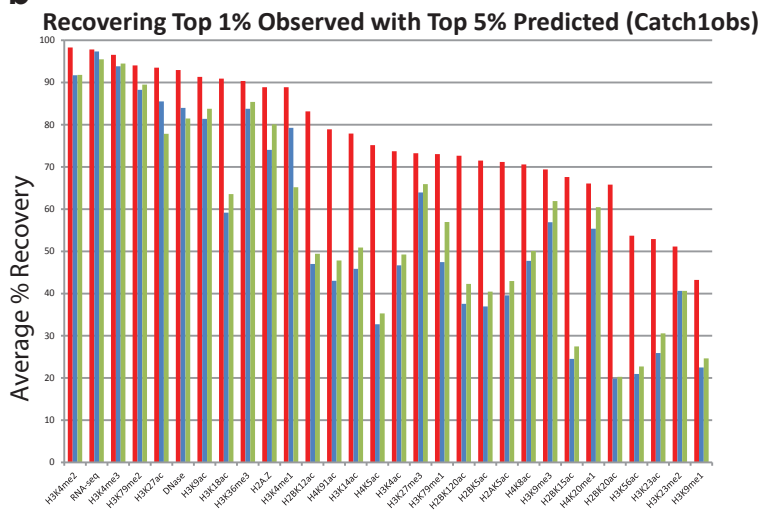
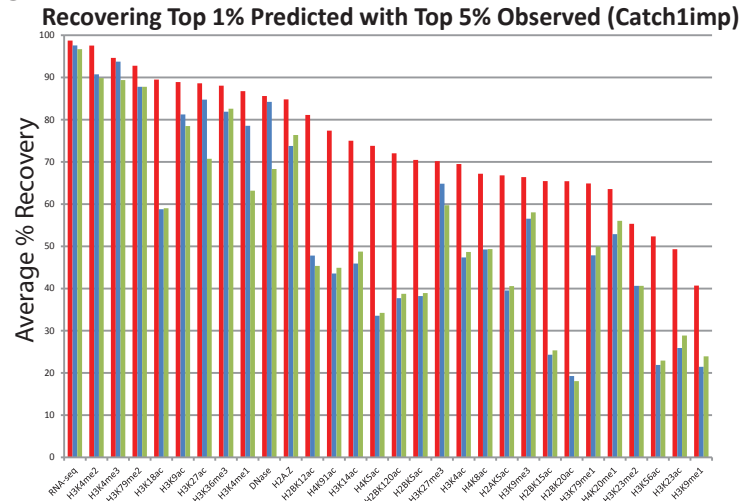
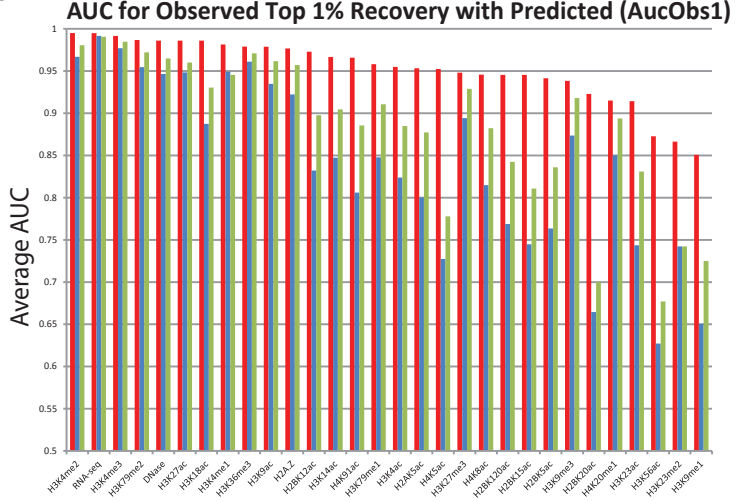
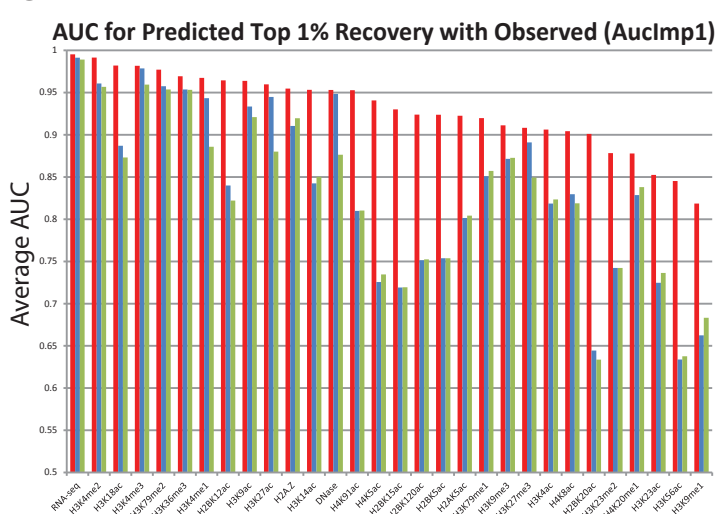


Supplementary Figure 4:

Heatmap of Clustering of Signal at Randomly Selected Positions for Tier-2 and Tier-3 Marks.

Similar heatmaps to those in **Fig. 2b**. The individual columns correspond to samples and the rows correspond to 2,000 randomly selected 25bp intervals that were clustered based on the observed data (left) with the corresponding imputed data also shown (right) for **(a)** Tier-2 marks and **(b)** Tier-3 marks. Only samples for which observed data is available are shown. The coloring corresponds to the signal level as indicated in the legend. Visually the heatmap show an overall agreement though some differences associated with outlier data sets or highly cell type specific behavior can also be seen.

b

a**b****c****d****e**

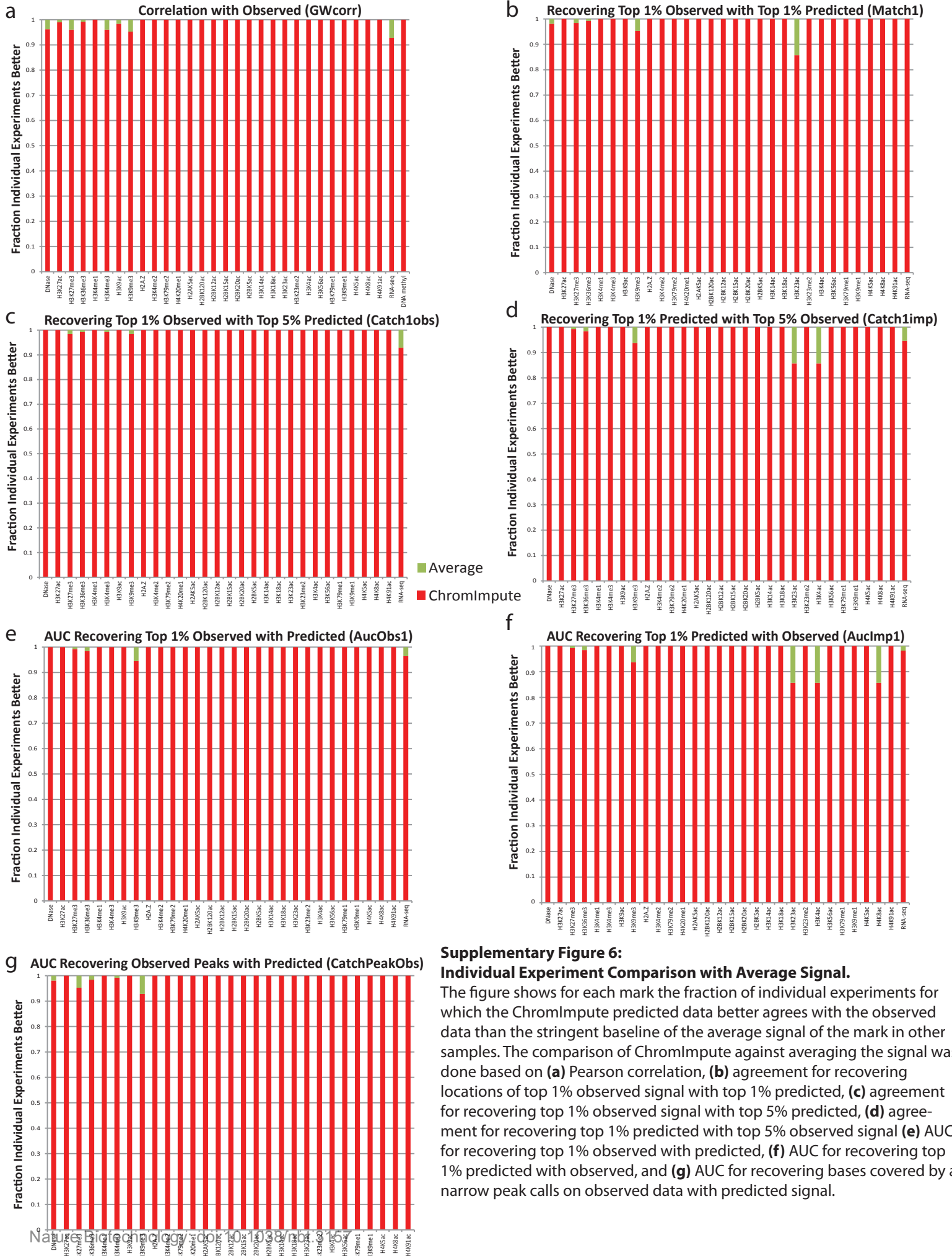
ChromImpute

Best Case Single Epigenome

Signal Average

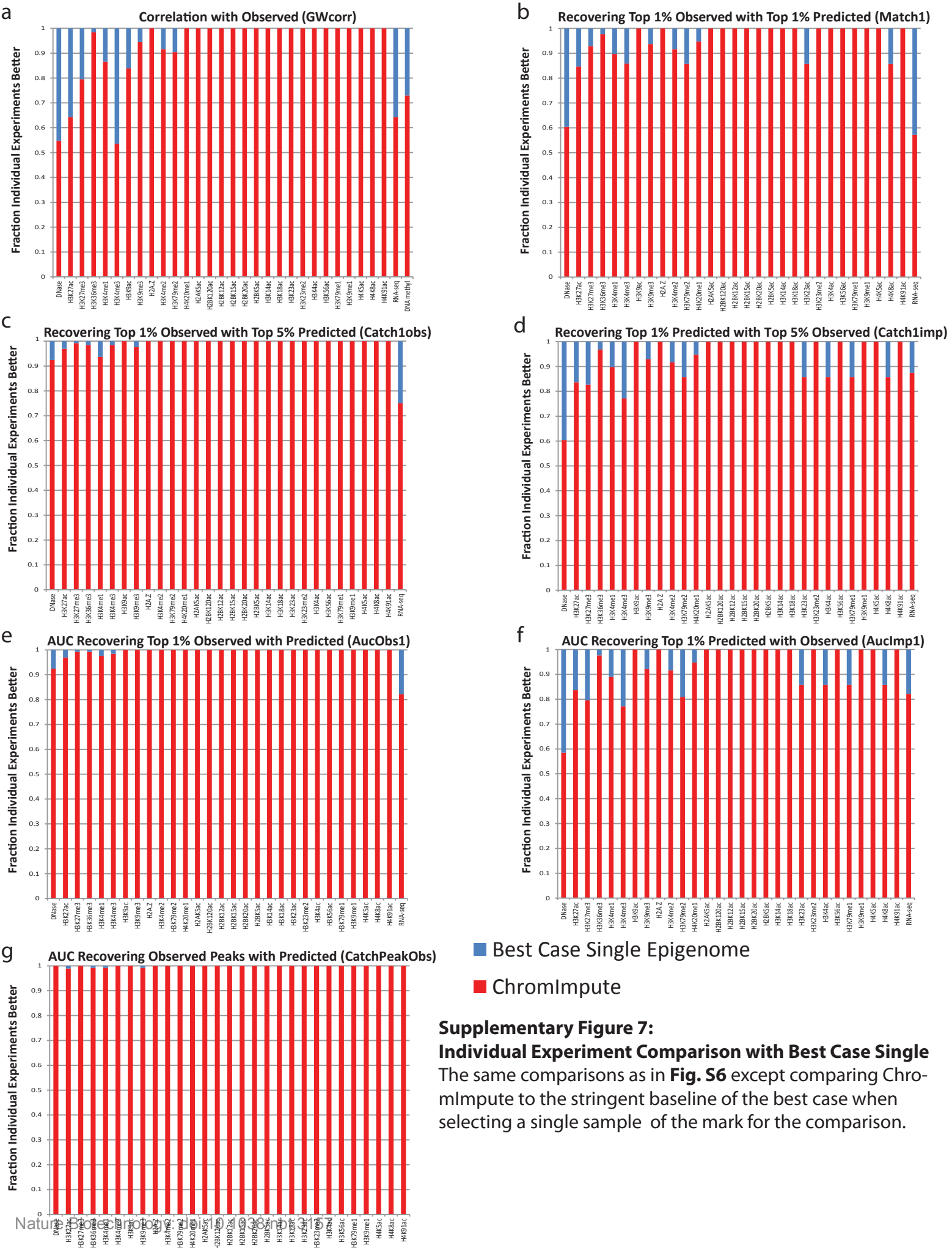
Supplementary Figure 5: Additional Aggregate Comparisons with Stringent Baselines.

These comparisons are similar to those shown in **Fig 2c,d** except showing the results based on different evaluation metrics: **(a)** average percent recovery of 25-bp bins in the top 1% observed signal with those in the top 1% of predicted signal **(b)** average percent recovery of top 1% observed signal with the top 5% predicted signal **(c)** average percent recovery of top 1% predicted signal with the top 5% observed signal **(d)** Area under the ROC curve (AUC) for recovering top 1% observed signal when ranking based on predicted signal level **(e)** AUC for recovering top 1% predicted signal when ranking based on observed signal.

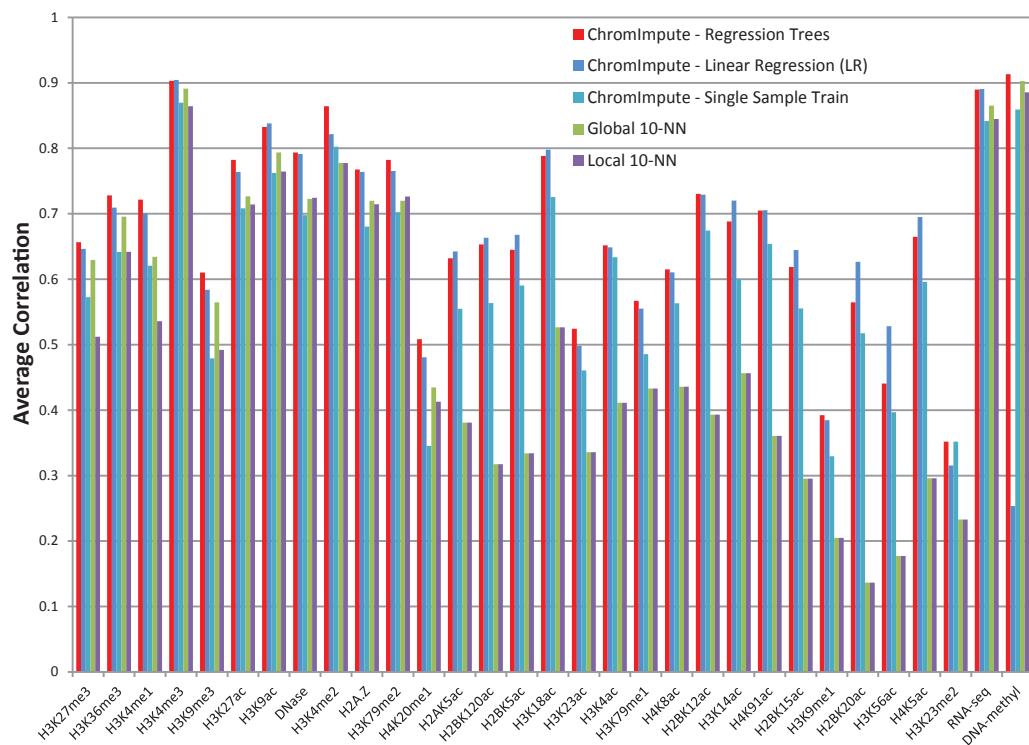
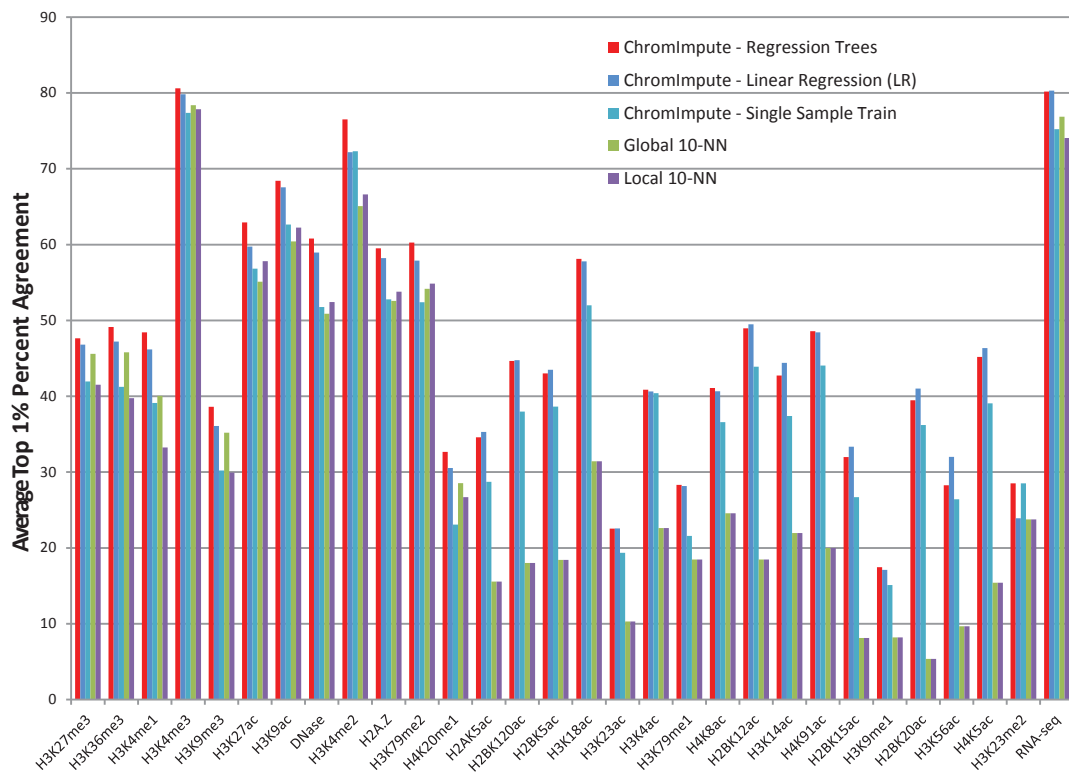


**Supplementary Figure 6:
Individual Experiment Comparison with Average Signal.**

The figure shows for each mark the fraction of individual experiments for which the ChromImpute predicted data better agrees with the observed data than the stringent baseline of the average signal of the mark in other samples. The comparison of ChromImpute against averaging the signal was done based on (a) Pearson correlation, (b) agreement for recovering locations of top 1% observed signal with top 1% predicted, (c) agreement for recovering top 1% observed signal with top 5% predicted, (d) agreement for recovering top 1% predicted with top 5% observed signal (e) AUC for recovering top 1% observed with predicted, (f) AUC for recovering top 1% predicted with observed, and (g) AUC for recovering bases covered by a narrow peak calls on observed data with predicted signal.

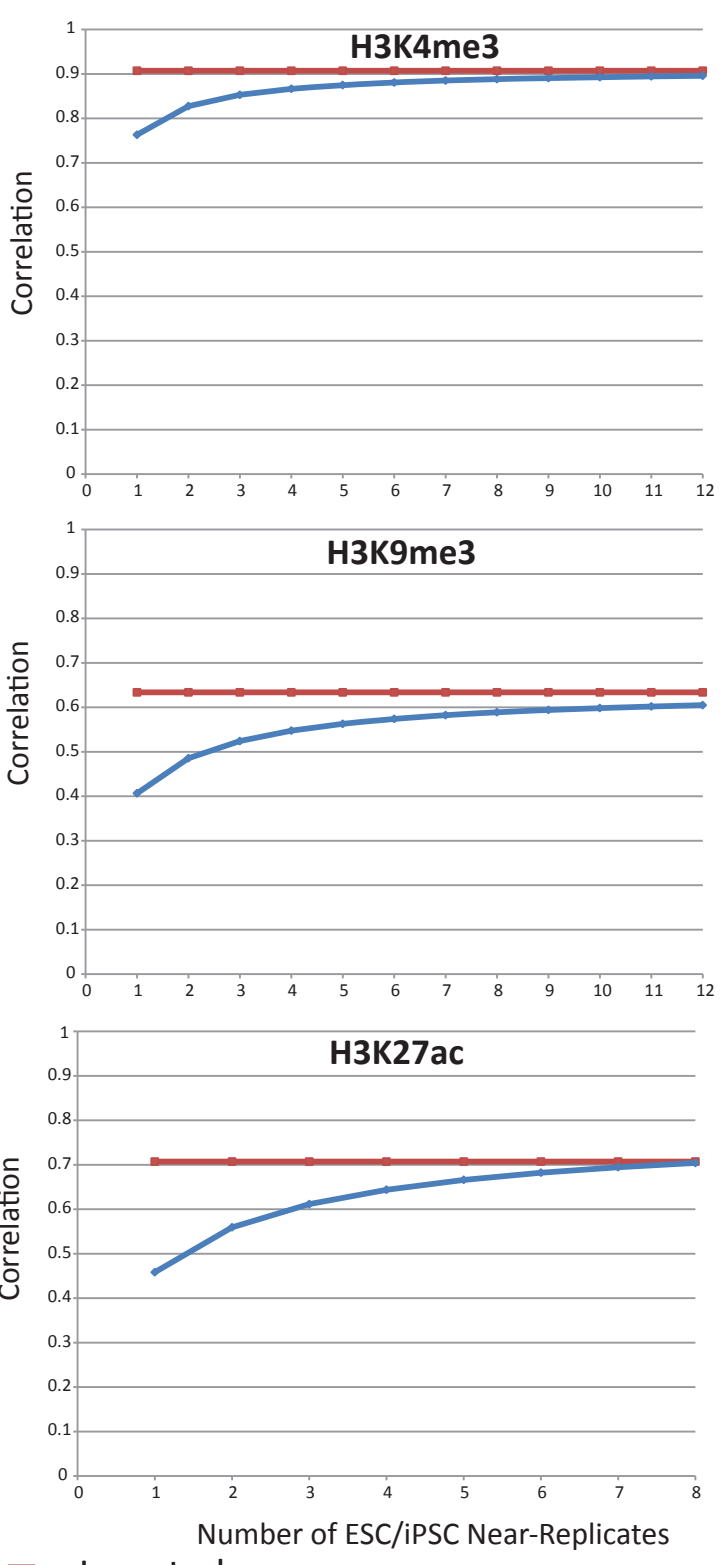
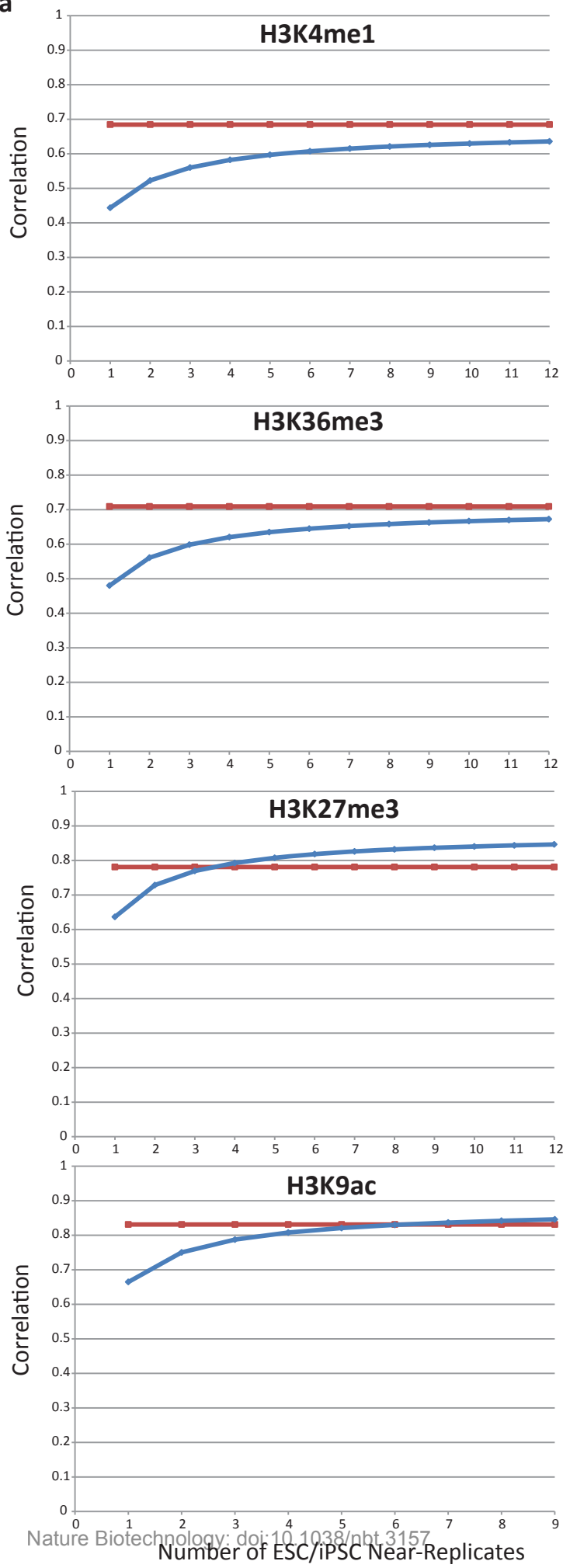


Supplementary Figure 7: Individual Experiment Comparison with Best Case Single
The same comparisons as in Fig. S6 except comparing ChromImpute to the stringent baseline of the best case when selecting a single sample of the mark for the comparison.

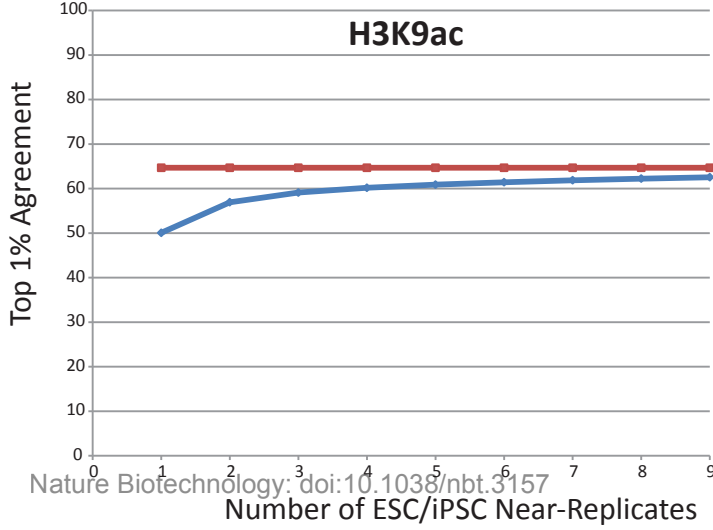
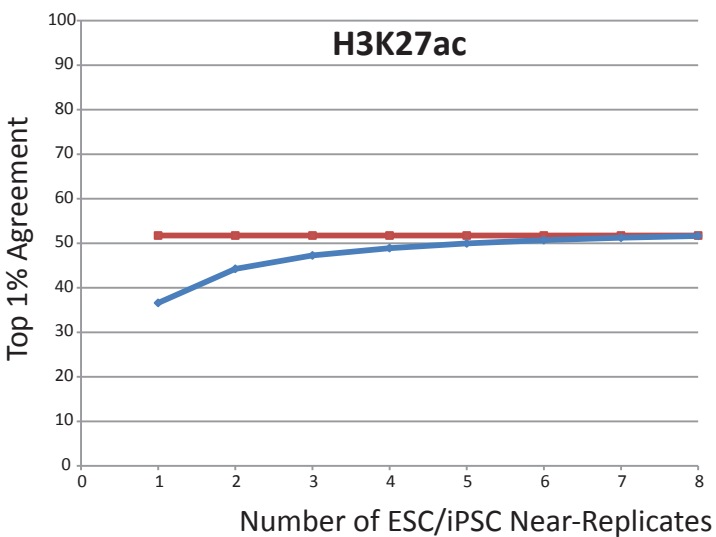
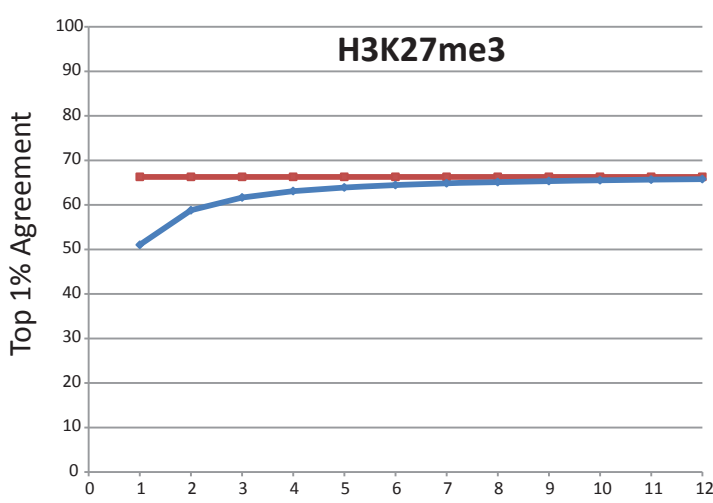
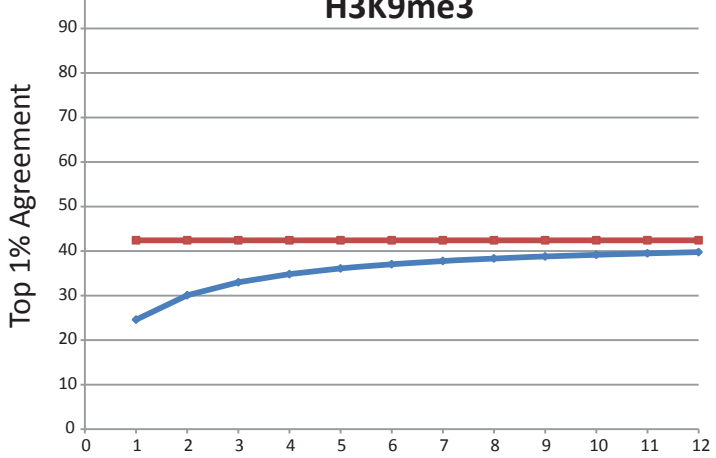
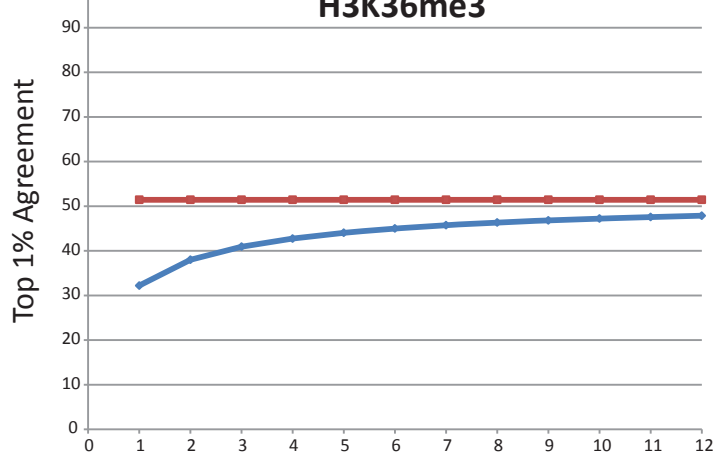
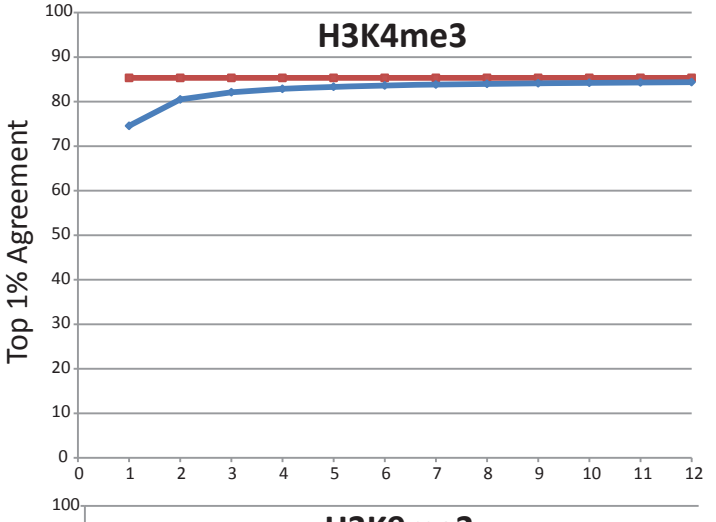
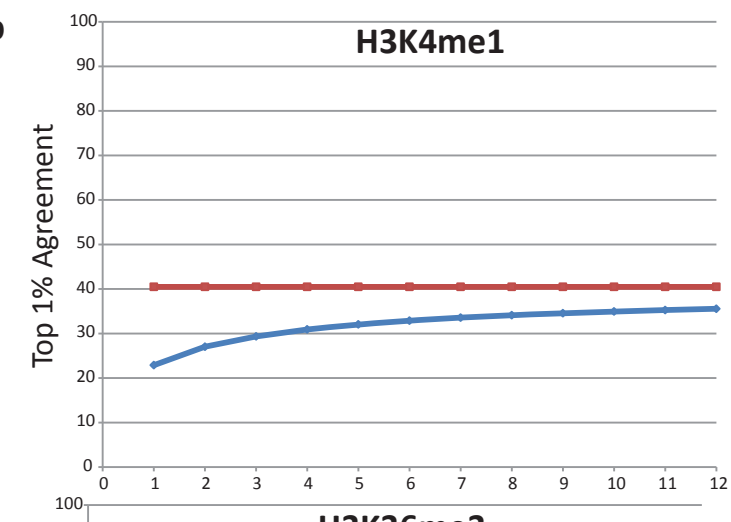
a**b**

Supplementary Figure 9: Methodological Comparisons.

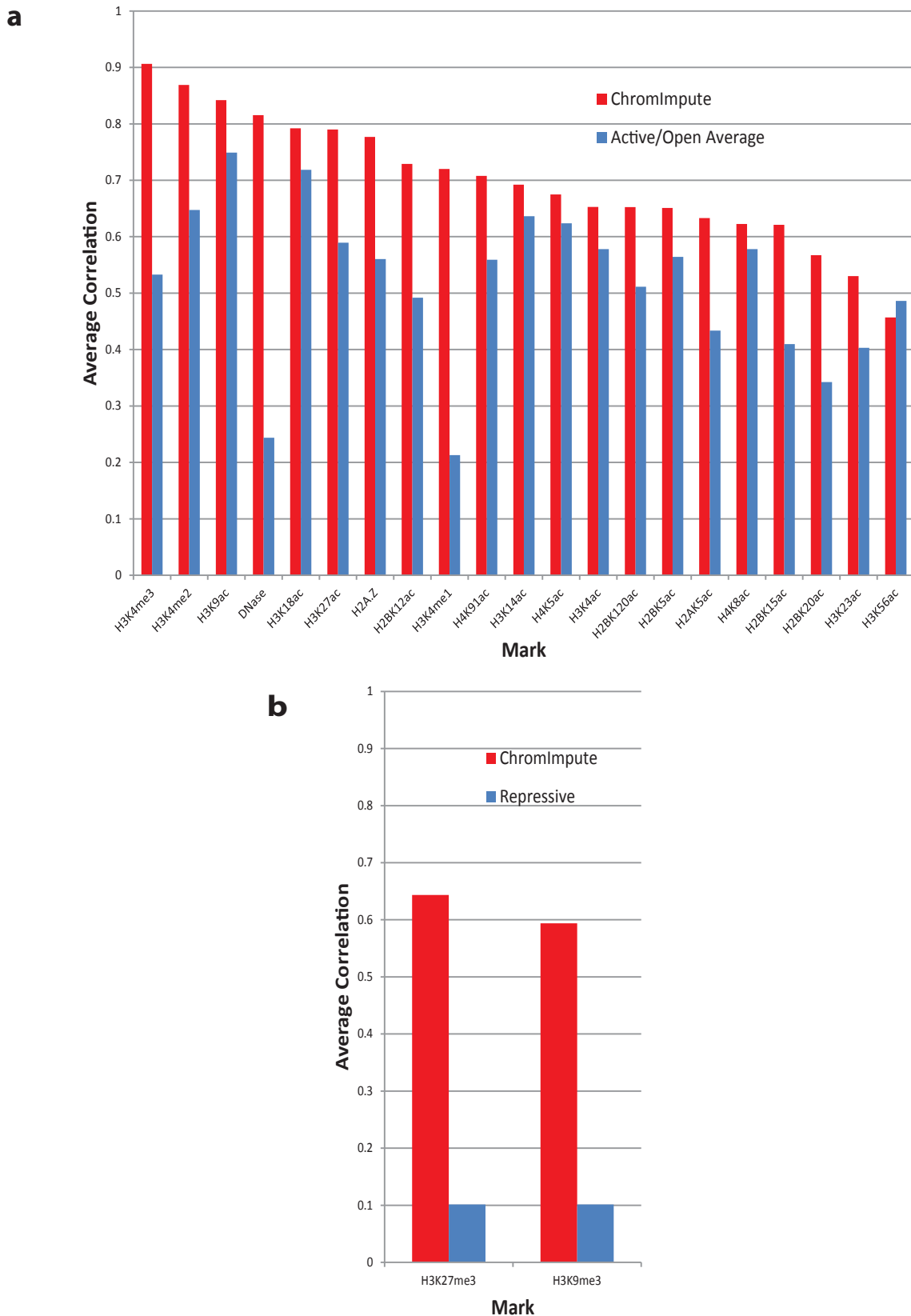
The graphs show a comparison based on (a) Correlation and (b) Top 1% agreement metrics for: (1) the standard ChromImpute which is based on an ensemble of regression trees, (2) ChromImpute with the same features and ensemble training strategy except using linear regression opposed to regression trees, (3) ChromImpute with regression trees trained on only on a single sample which was chosen to be the globally most correlated based on H3K4me1, except using H3K4me3 when training for H3K4me1. (4) Predictions based on averaging the target mark in up to the 10 nearest-neighboring samples having the target mark where the distance is determined based on the global correlation distance measure with H3K4me1, except using H3K4me3 when trying to predict H3K4me1. (5) The same as in (4) except using the local Euclidean distance opposed to the global correlation. Evaluation was limited to chr10.

a**Supplementary Figure 10:**

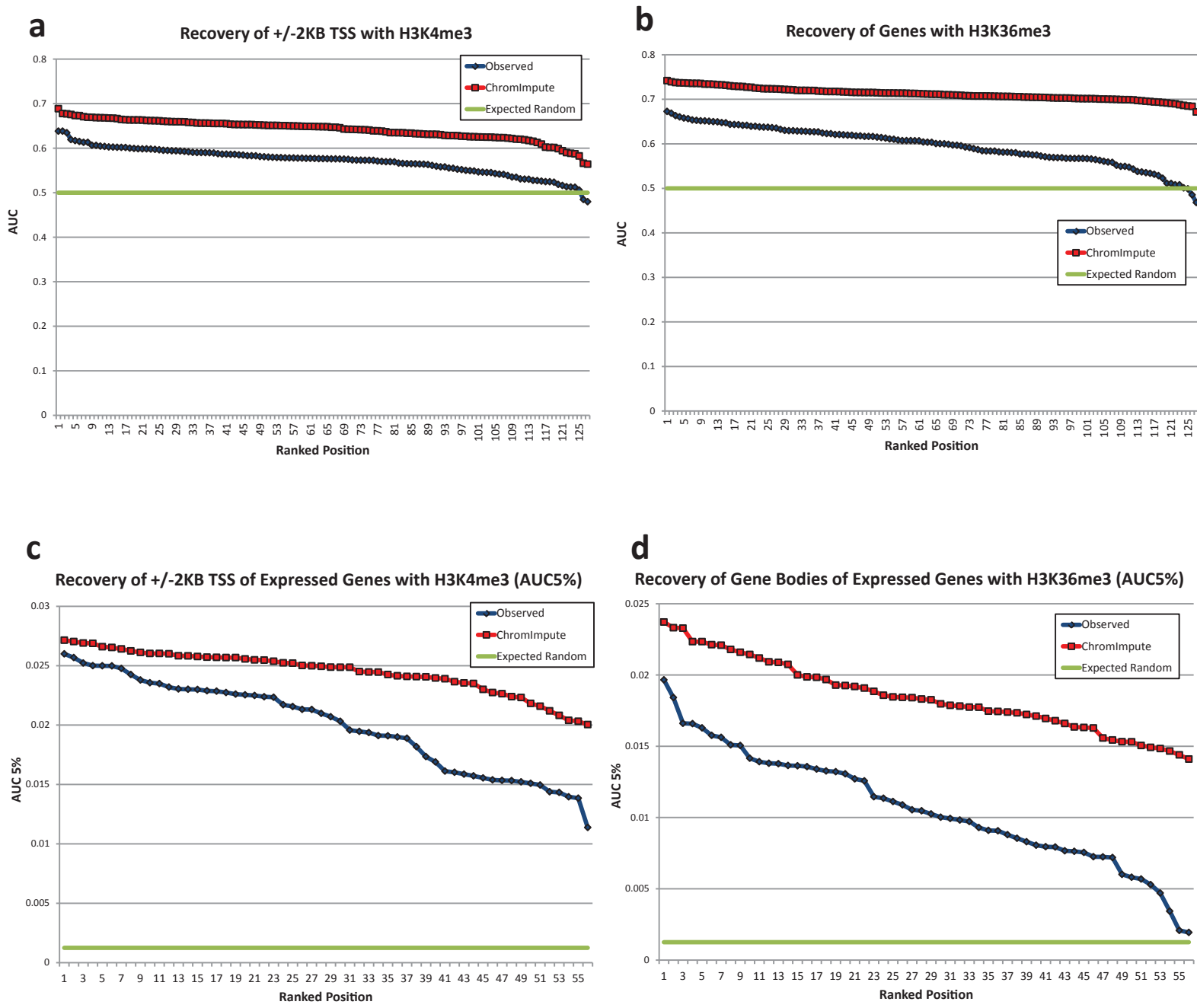
Comparison of Imputed Data and ESC/iPSC Near-Replicate Predictions. The figures show for the tier 1 histone marks a comparison of the performance of the imputed data on average for ESC and iPSC samples compared with what would be expected by treating the other ESC and iPSC samples as effective replicates and averaging their values as a function of the number of replicates in terms of (a) correlation and (b) top 1% agreement. To compute the expectation for k-replicates for each 25-bp interval we randomly selected k of the ESC and iPSC samples which had the mark mapped excluding the sample being evaluated. The performance of the imputed data in comparison is shown with the horizontal line in red.

b

■ Imputed
◆ ESC/iPSC Near-Replicates

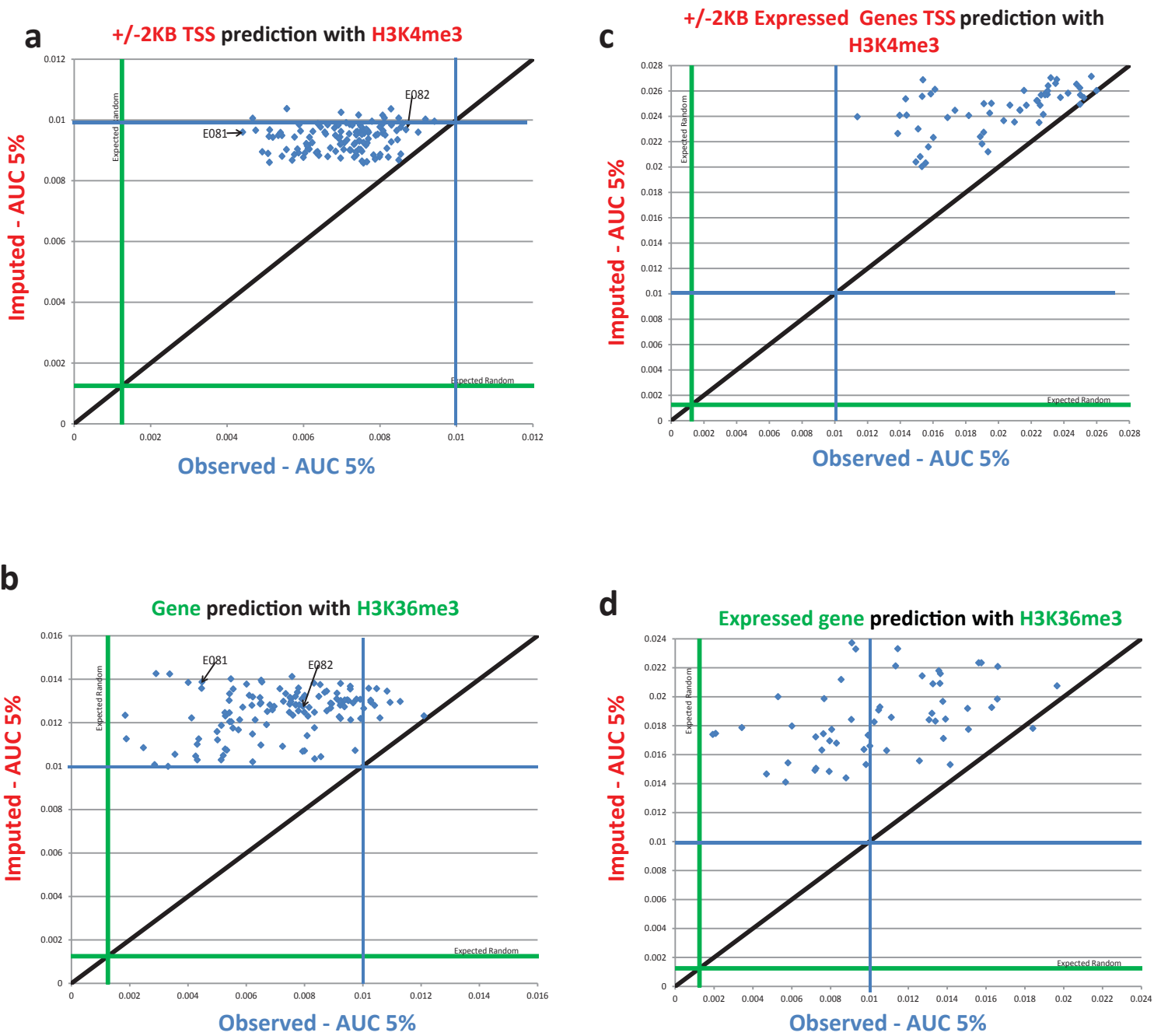


Supplementary Figure 11: Comparison with Averaging Subset of Other Marks in the Same Sample. **(a)** A comparison of predicting a set of putative active/open marks (H3K4me1/2/3, H2A.Z, DNase, and acetylations) by averaging all other such marks from the same sample compared with ChromImpute predictions evaluated based on average correlation with the observed data. **(b)** Predicting the repressive marks H3K9me3 and H3K27me3 with the other repressive mark in the same sample compared with ChromImpute predictions evaluated based on average correlation with observed data.

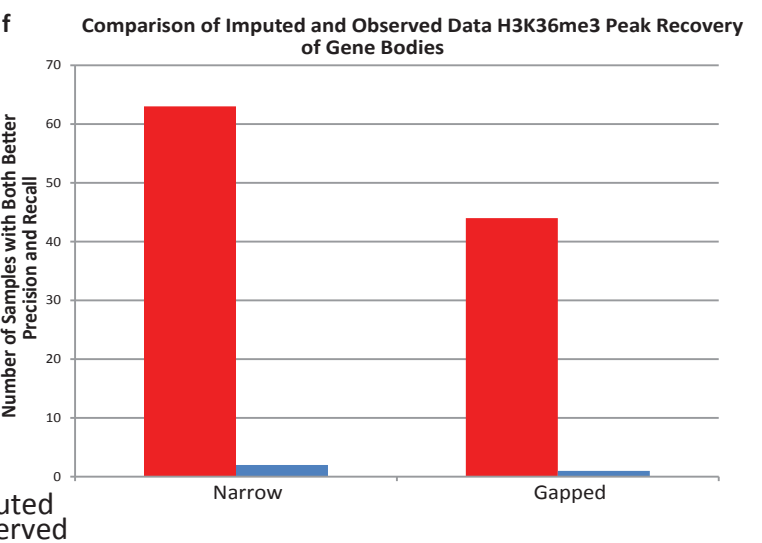
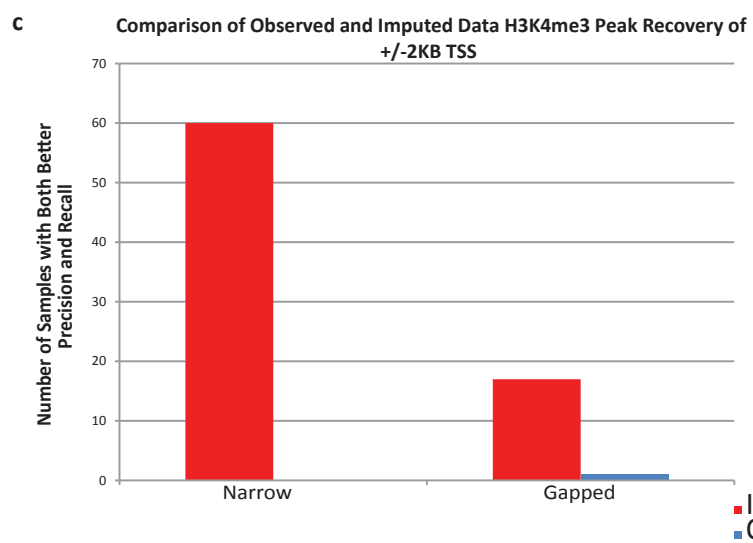
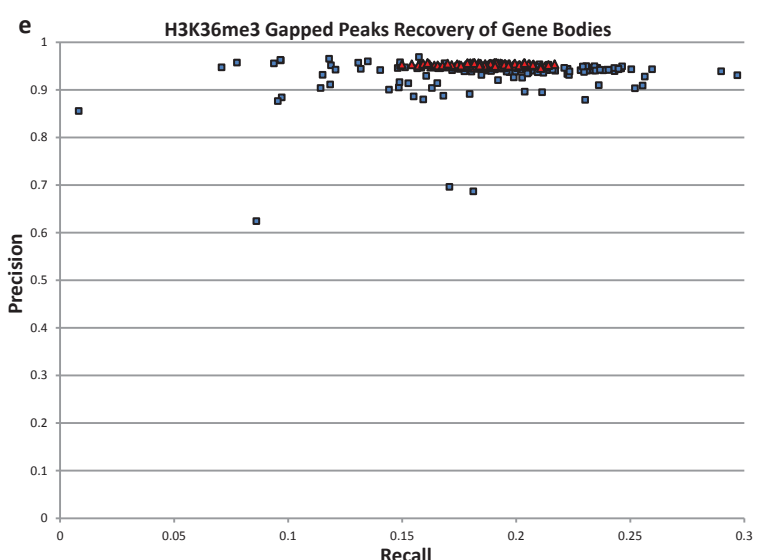
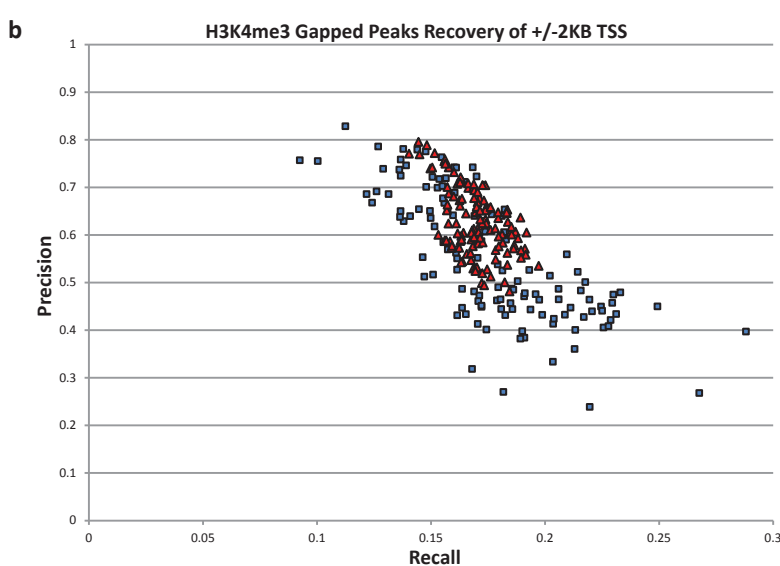
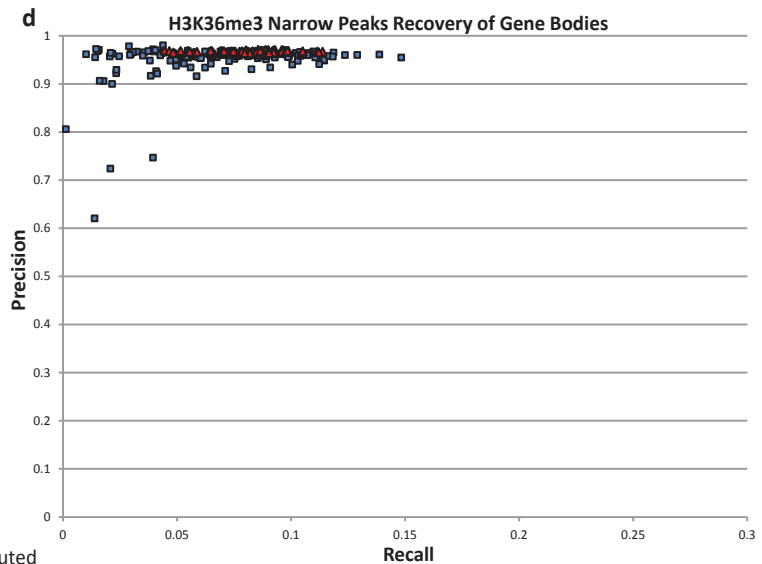
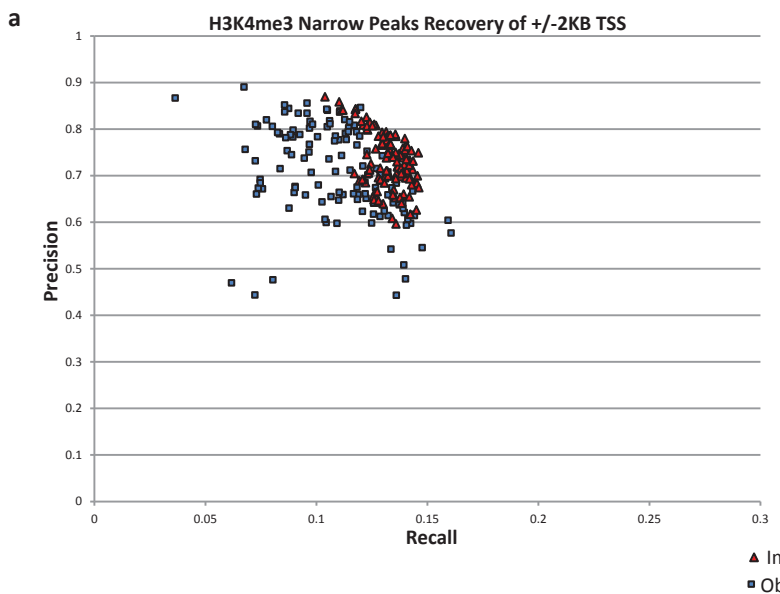


Supplementary Figure 12: Observed and Imputed Mark Recovery of Genomic Features

These are similar plots to main **Fig 3a,b** except **(a,b)** reporting the full AUC for **(a)** H3K4me3 recovery of +/-2KB TSS **(b)** H3K36me3 recovery of gene bodies **(c,d)** reporting the AUC up to a 5% false positive rate based on a set of expressed genes (see **Methods**) for **(c)** the H3K4me3 signal recovering locations within 2kb of the TSS of these genes for the 56 samples with gene expression data available and **(d)** the same as (c) except for gene regions and the H3K36me3 signal.

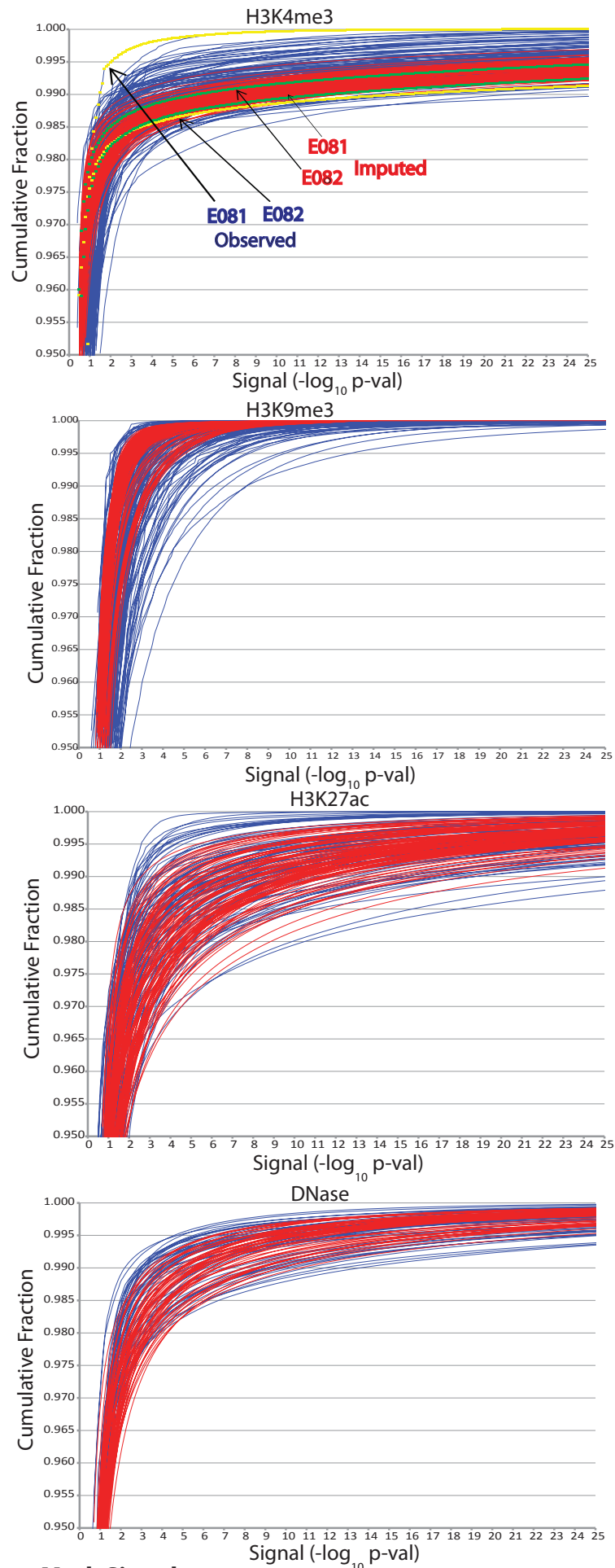
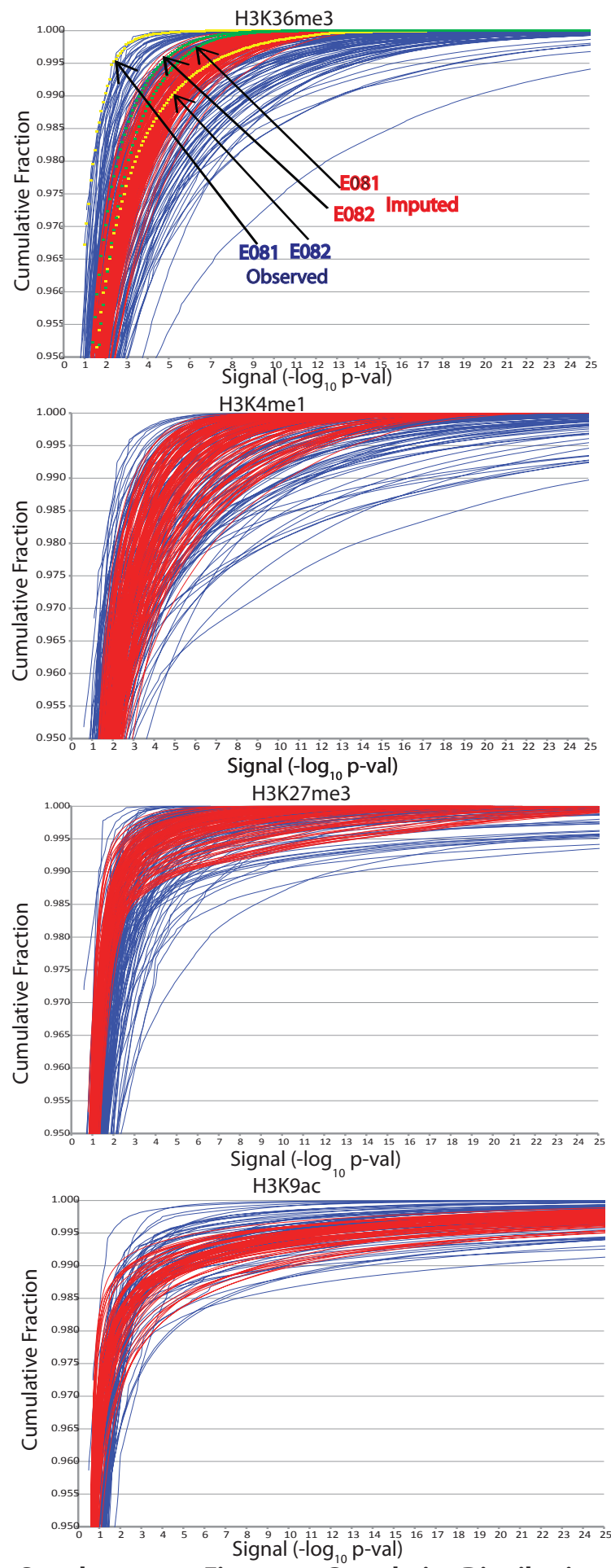


Supplementary Figure 13:
Scatter Plot Comparison of Observed vs. Imputed Signal at Recovery of Annotated Gene Features.
The x-axis of these plots correspond to the area under the ROC curve up to a 5% false positive rate for the observed signal, while the y-axis shows it for the imputed data for (a) H3K4me3 recovery of locations within 2kb of annotated transcription start sites (b) H3K36me3 recovery of locations within annotated genes (c) H3K4me3 recovery of locations within 2kb of annotated transcription start sites for an expressed gene set (see **Methods**) (d) H3K36me3 recovery of locations within the expressed gene set (see **Methods**). The black line shows the $y=x$ line, demonstrating in almost all cases the imputed data has better agreement with the annotated gene features. The green lines illustrate what would be expected by random guessing, and the blue lines mark consistently the 0.01 values in each figure.



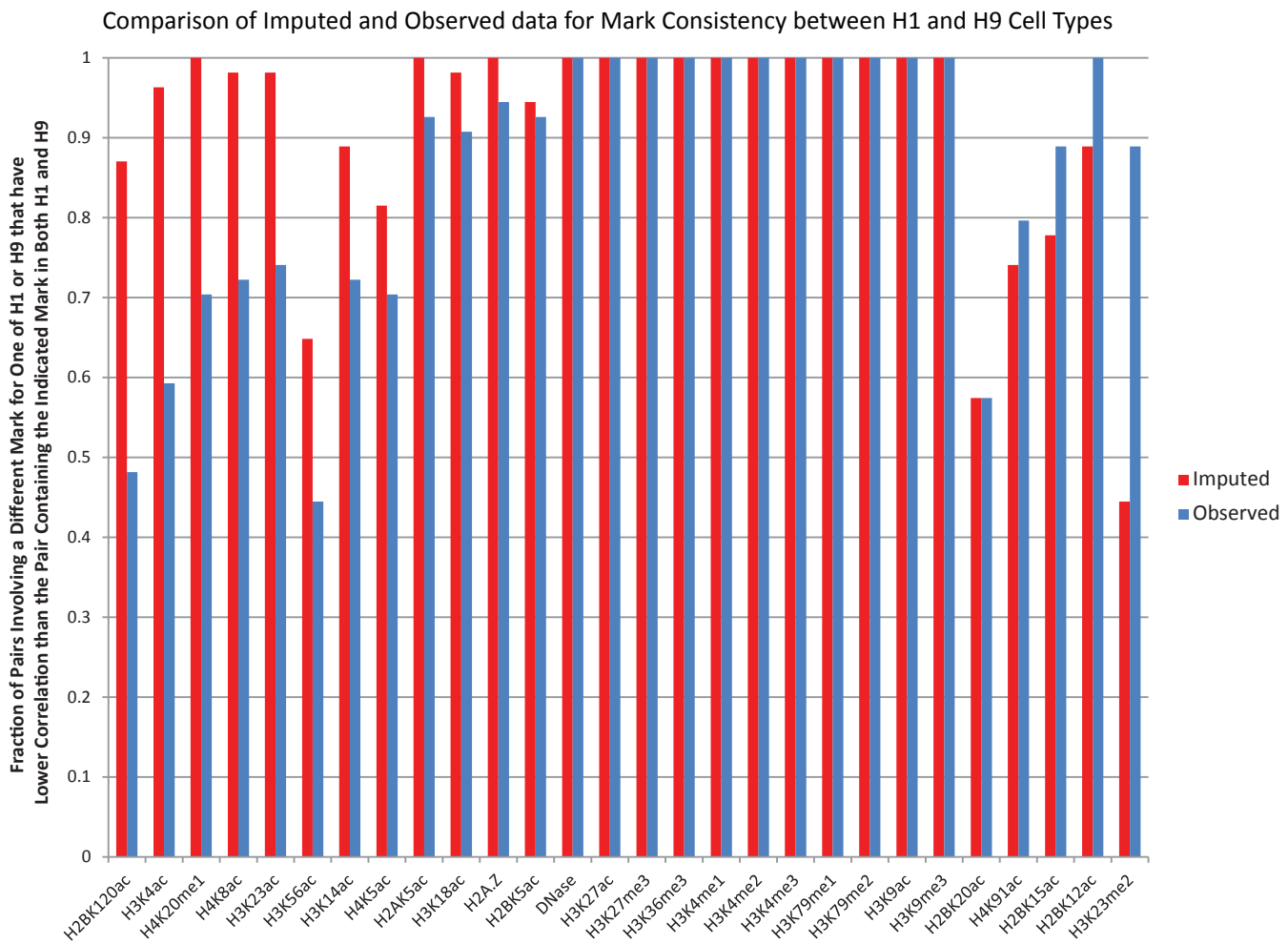
Supplementary Figure 14: Peak Calls Agreement with Annotated Features.

(a) Precision and recall of narrow peak calls for H3K4me3 overlap with locations within 2kb of annotated TSS. Each dot in red corresponds to a peak call set based on the imputed and in blue based on the observed data (b) Same as a except for gapped peaks. (c) The number of samples for which the peak calls based on imputed (observed) H3K4me3 data had both better precision and recall than the corresponding observed (imputed) data shown for separate comparisons based on narrow and gapped peak calls. Peak call sets which were not better in both precision and recall were not counted. (d-f) The same as a-c except for H3K36me3 overlap with locations within annotated genes.



Supplementary Figure 15: Cumulative Distribution of Tier-1 Mark Signals.

The figure shows the cumulative distribution function plots for the eight Tier-1 marks for each sample based on the observed data in blue and the imputed data in red. These plots show the imputed signal has a more consistent distribution across samples. For H3K4me3 and H3K36me3, in yellow are the cumulative distribution for the observed data of two Fetal brain samples (E081 and E082), while in green for the imputed data, showing even for the same tissue type that the distribution of observed signal can be very different.



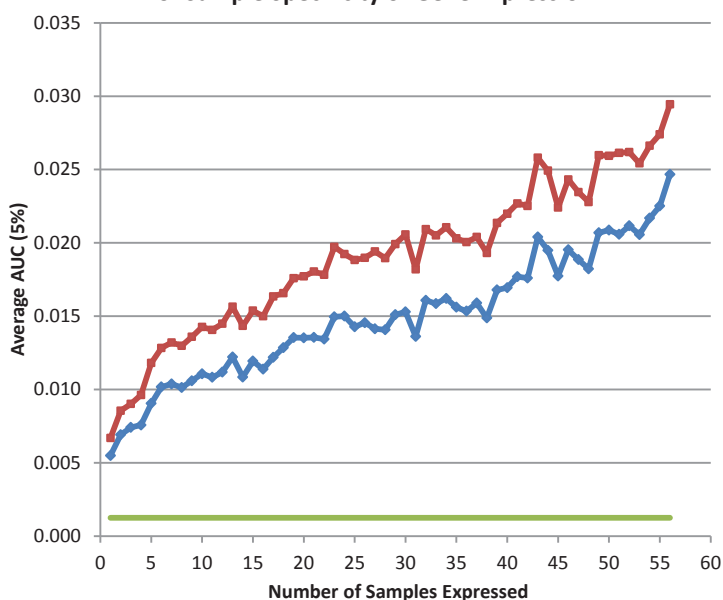
Supplementary Figure 16:

Comparison of Observed and Imputed Relative Mark Agreement Between H1 and H9.

This evaluates for a mark A, how frequently the correlation for the pair (A_{H1}, A_{H9}) is greater than the correlation of any other pair (A_{H1}, B_{H9}) or (B_{H1}, A_{H9}) where B is a mark other than A and the subscript indicates the sample of the experiment which is either of two embryonic stem cell samples, from the H1 or H9 cell lines. This evaluation is done separately for the observed and imputed data. In total the imputed and observed data had different relative agreement on 16 marks, with the imputed data having better relative agreement for 12 of these marks, which is significant ($p<0.04$) based on a binomial test.

a

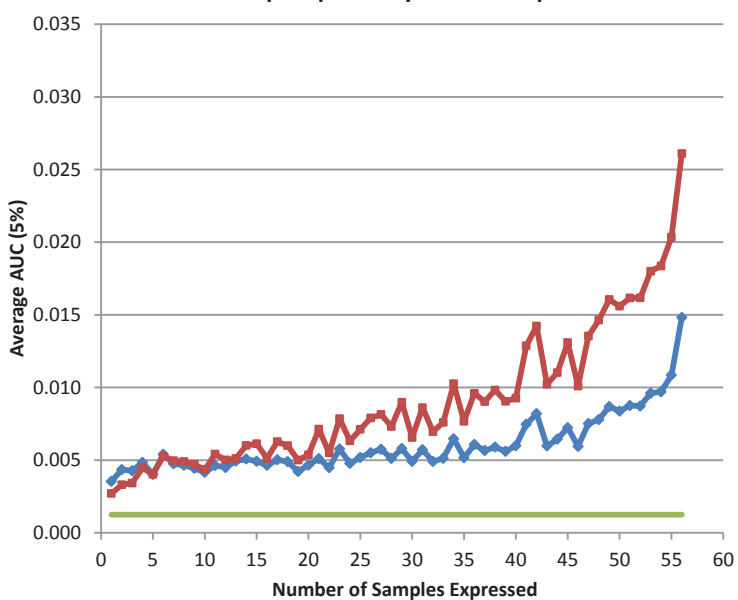
Average H3K4me3 Recovery of +/-2kb TSS as a Function of Sample Specificity of Gene Expression



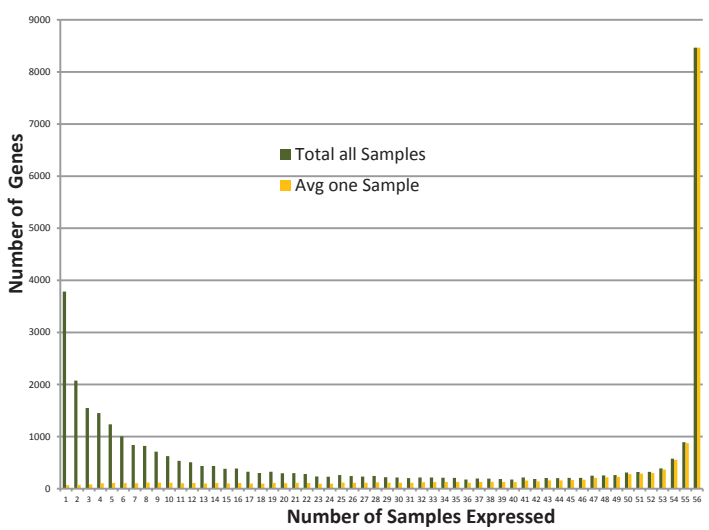
Observed
Imputed
Random

b

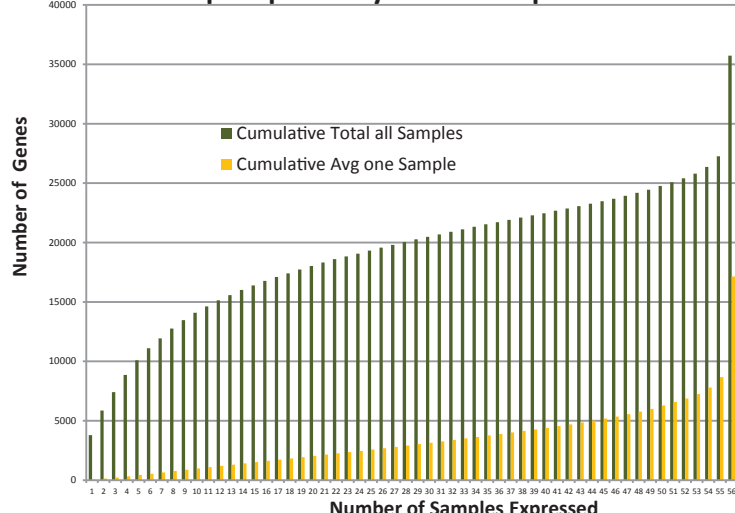
Average H3K36me3 Recovery of Gene Bodies as a Function of Sample Specificity of Gene Expression

**c**

Distribution of Sample Specificity of Gene Expression

**d**

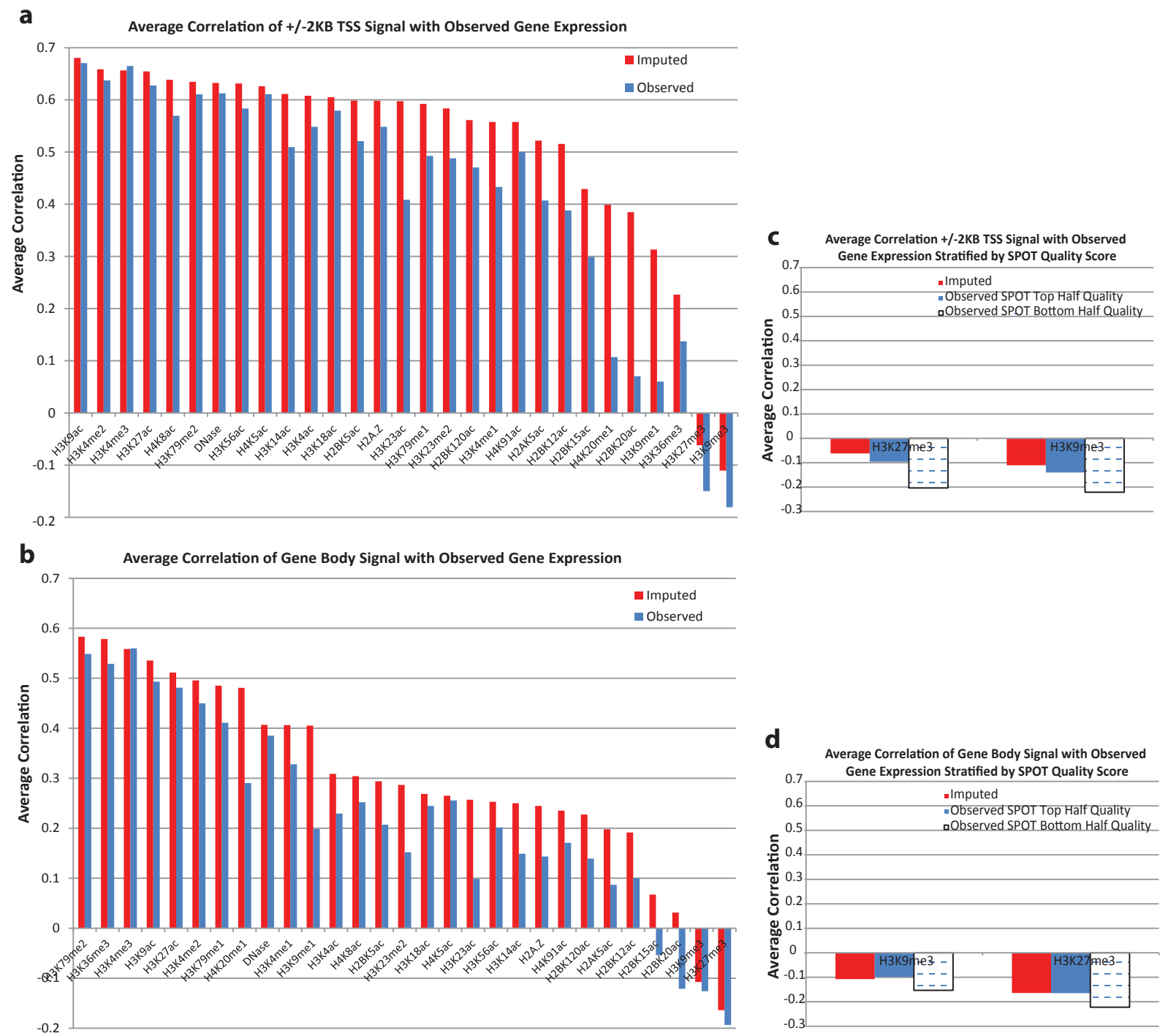
Cumulative Distribution of Sample Specificity of Gene Expression



Supplementary Figure 17:

Observed and Imputed Mark Recovery of Genomic Features as a Function of Sample Specificity.

(a) The area under the ROC curve up to a 5% false positive rate for recovering bases +/-2kb of a TSS of an expressed gene in a sample (defined as RPKM ≥ 0.5) conditioned on the number of samples in which the gene is expressed based on the imputed and observed H3K4me3 signal. The negative set is all other bases in the genome except positions corresponding to an expressed gene that are not expressed in the number of samples being conditioned on. The reported AUC is averaged over all the samples with expression data available. (b) The same as a except for H3K36me3 and gene bodies. (c) In green the count of the total number of genes expressed in the specified number of samples. In yellow the average count of the number of genes expressed in the specified number of samples among expressed genes in a given sample. The imputed data has better or similar performance in both evaluations except for recovering the gene bodies with H3K36me3 for a limited number of the most sample specific genes. (d) The same as c except showing the cumulative totals.

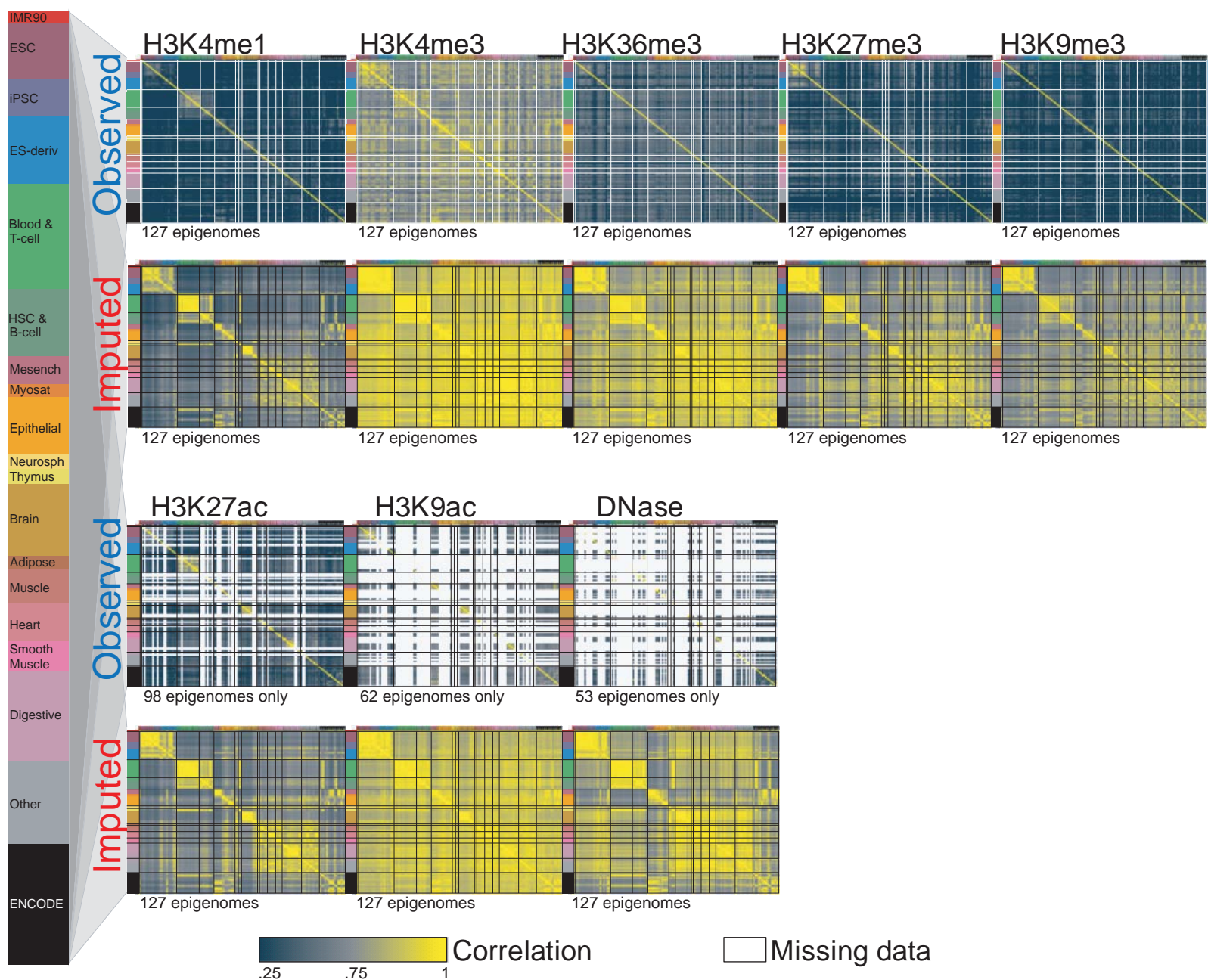


Supplementary Figure 18:

Comparison of Observed and Imputed Chromatin Mark Data Correlation with Observed Gene Expression.

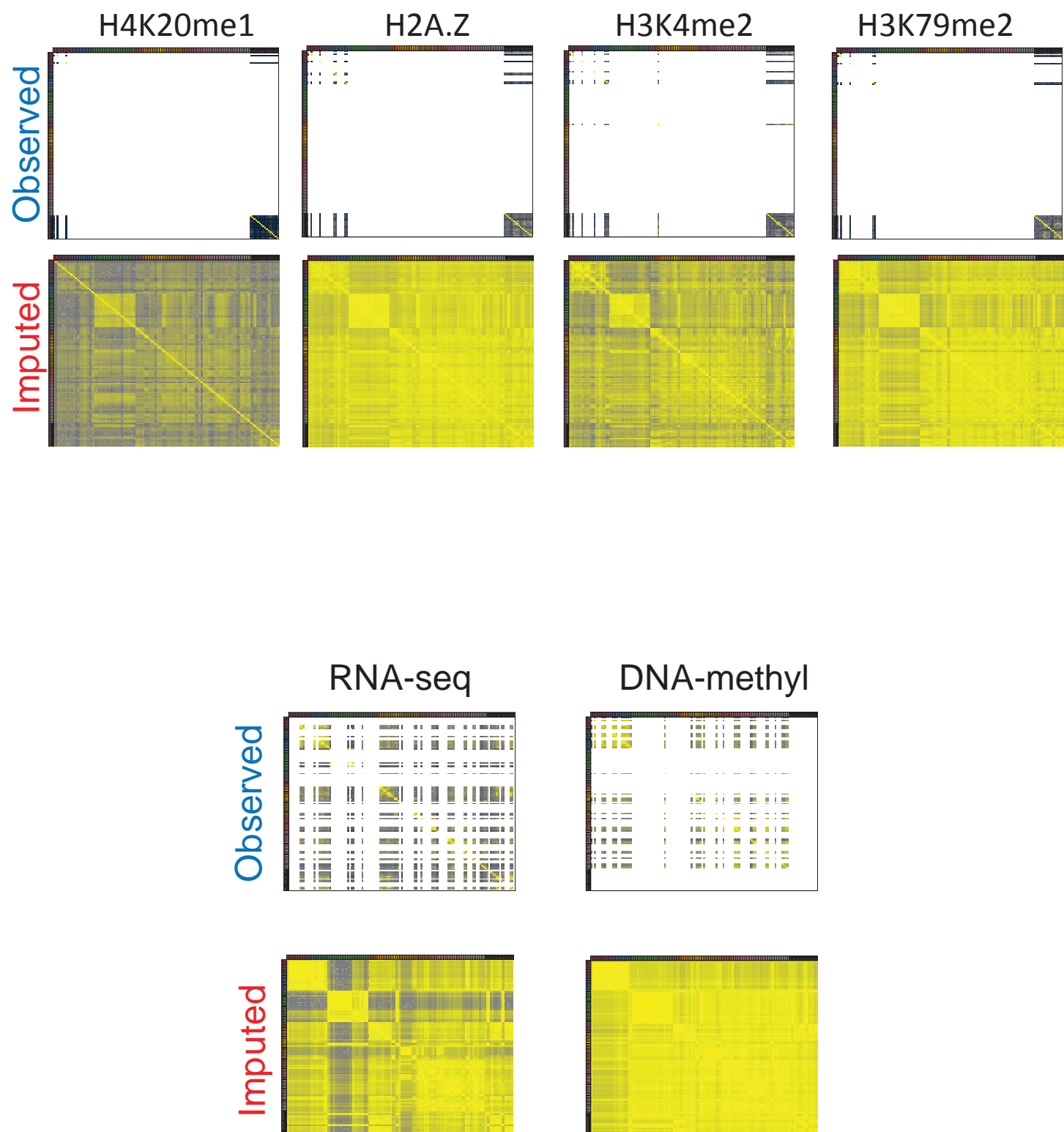
(a) For each of the tier 1-3 marks mapped in at least two samples for both the imputed and observed data the average correlation of the mark signal within +/-2KB TSS with gene expression. Signal was represented by computing the average of the signal values within the range adding one and then taking a log transformation. The correlations were computed separately for each sample with observed data available for the mark and gene expression, and then averaged. For most marks there was a greater positive correlation with gene expression for the imputed data compared to the observed data. (b) The same as a, but for annotated gene bodies. (c) The correlation of the two repressive marks, H3K27me3 and H3K9me3, for +/-2KB TSS signal with gene expression with the observed data stratified based on whether the sample is in the top half or bottom half of observed datasets considered by the SPOT quality score¹⁰ compared with the imputed data correlation. This shows the stronger negative correlation with gene expression for the observed data for the repressive marks is associated with data sets with lower quality as scored by SPOT. (d) The same as c but for gene bodies.

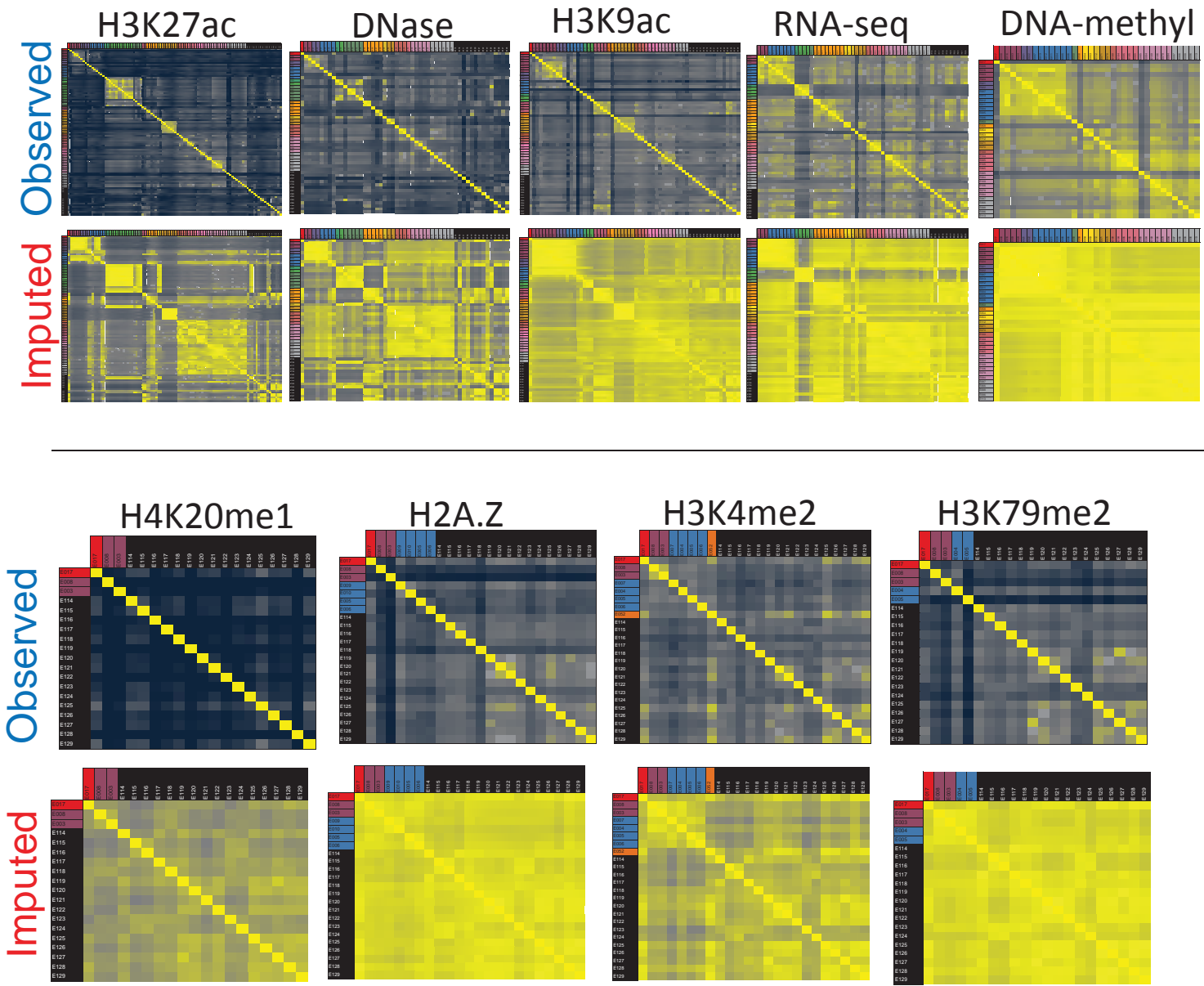
a

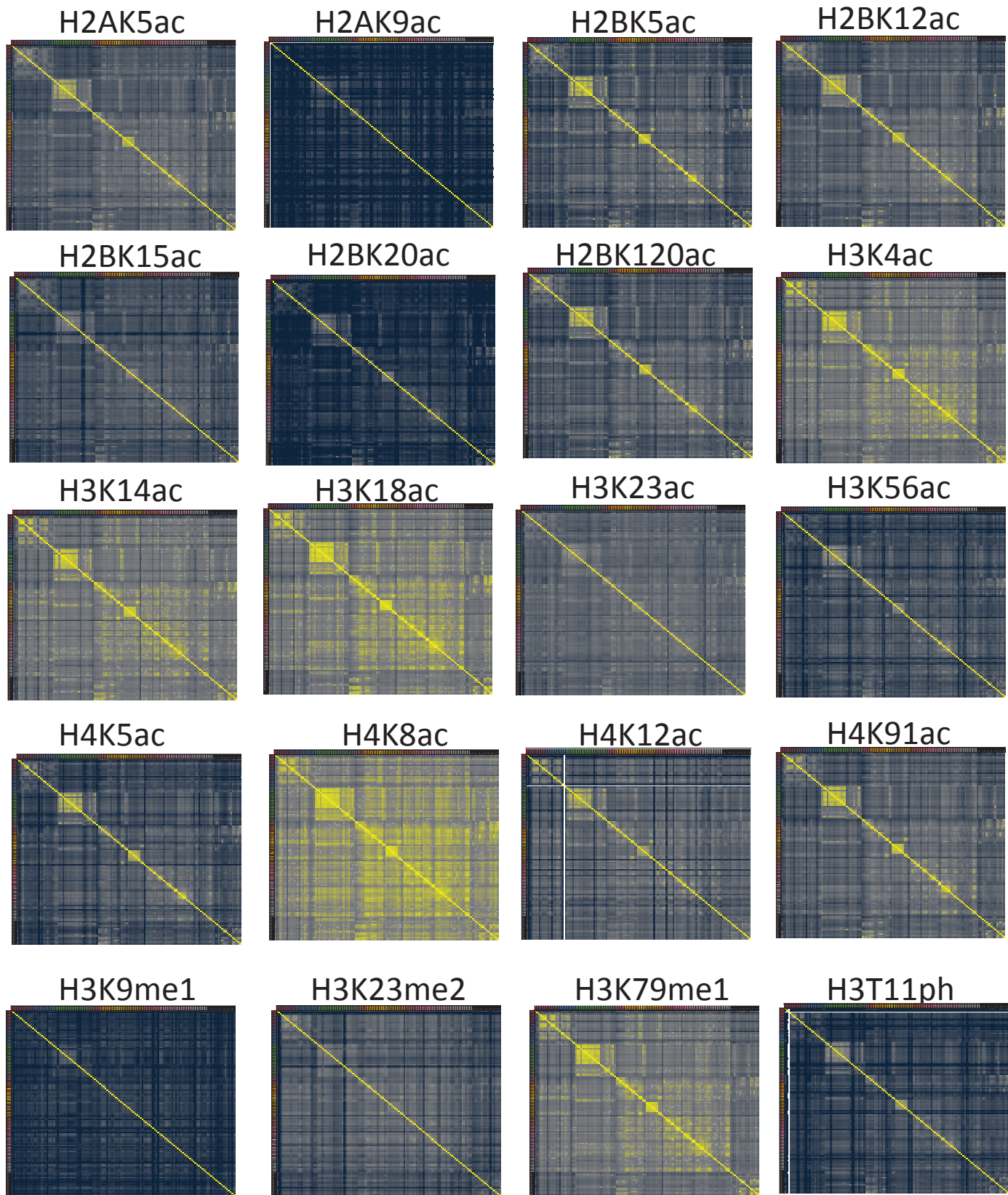


Supplementary Figure 19: Sample correlations for imputed vs. observed signal.

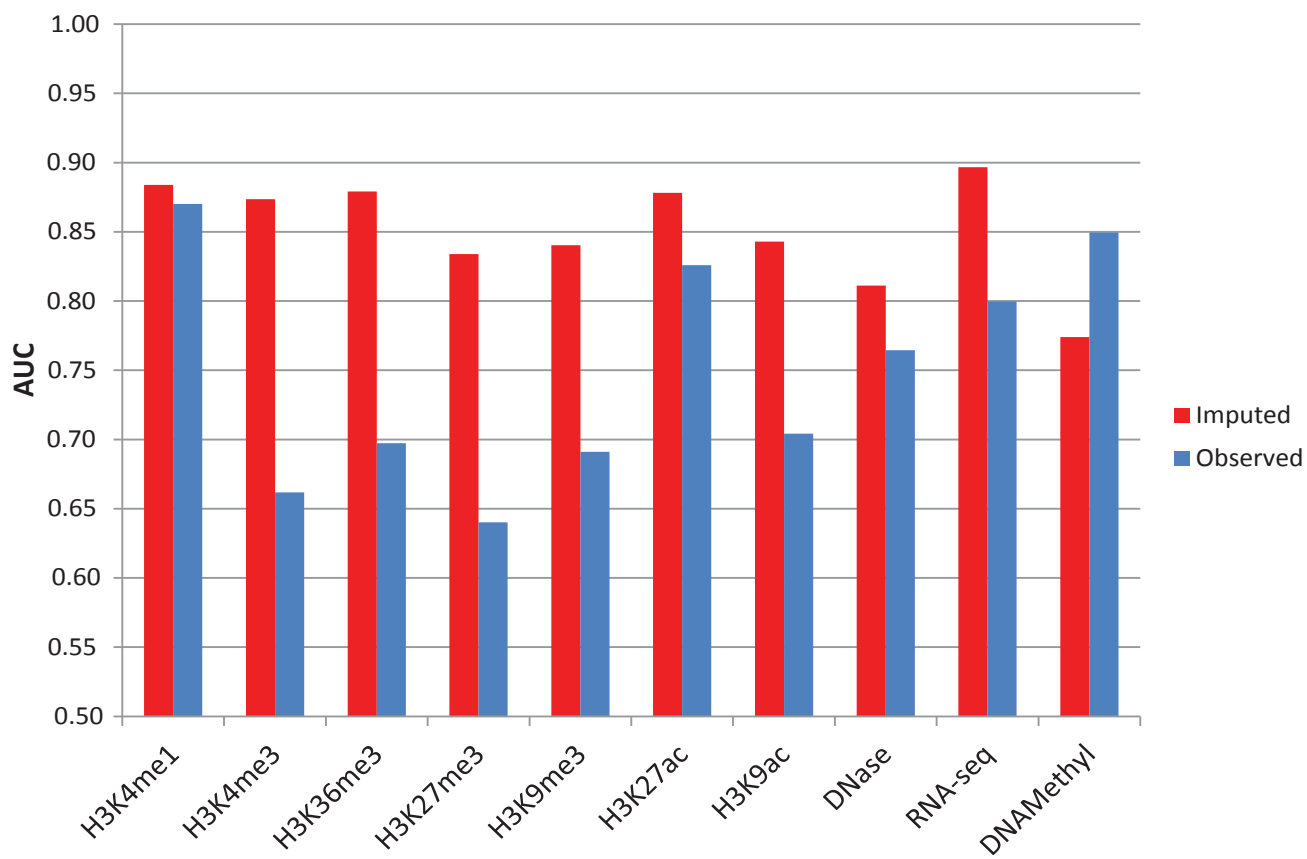
The same heatmap of pairwise correlations for observed and imputed data as shown in **Fig. 3e**, but showing **(a)** all the Tier-1 marks **(b)** the Tier-2 marks, RNA-seq, and DNA-methylation **(c)** heatmap of pairwise correlations for observed and imputed data of the Tier-1 marks not mapped in every sample, RNA-seq, DNA-methylation, and Tier-2 marks only showing the subset of samples for which there is observed data available **(d)** heatmap of pairwise correlations for the imputed data for the Tier-3 marks.

b

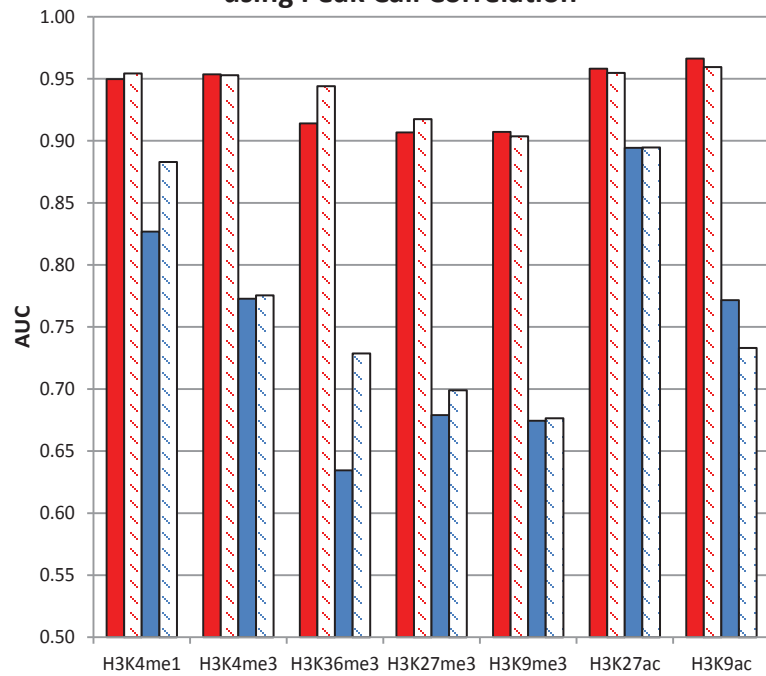
c

d

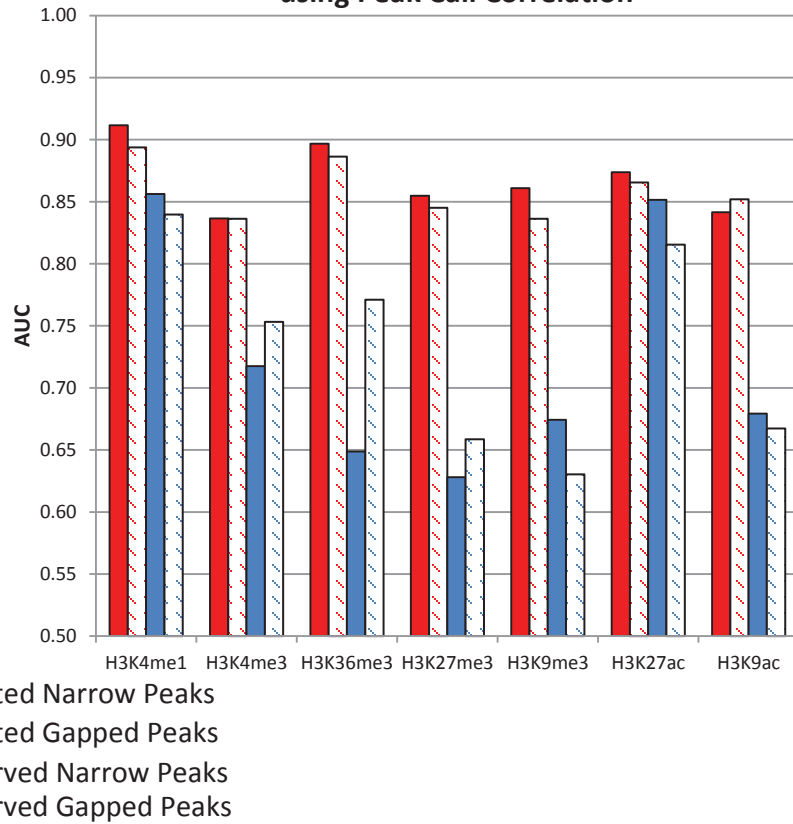
a AUC for Classifying Pairs as the Same Anatomy using Signal Correlation



b AUC for Classifying Pairs as the Same Group using Peak Call Correlation



c AUC for Classifying Pairs as the Same Anatomy using Peak Call Correlation



Supplementary Figure 20: Prediction of Same Anatomy and Group Pairs.

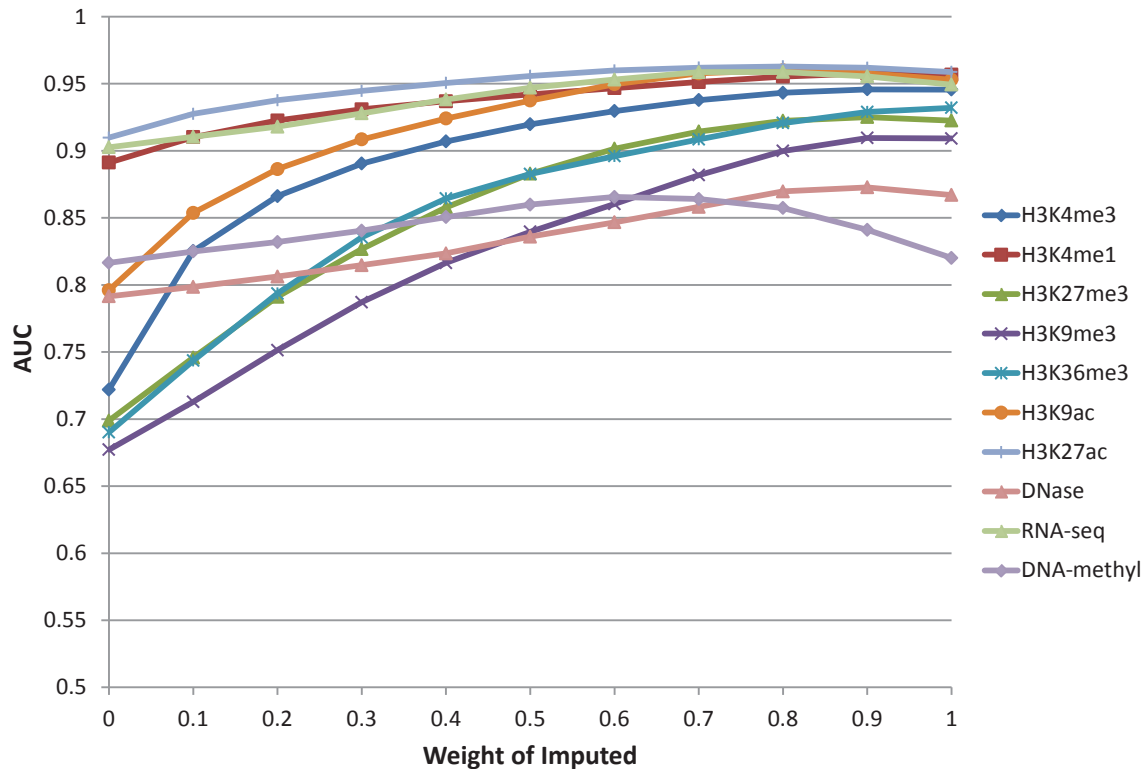
(a) This is the same evaluation of mark signal correlation pairs as in **Fig. 3f** except for anatomy annotations¹⁰ (**Table S1**) opposed to sample group annotations. (b) The same evaluation as in **Fig. 3f** except based on histone mark peak calls with results shown for both gapped and narrow peak calls. The correlations were computed the same as for the signal except being at the base level and treating a base as having a signal of 1 if it was covered by a peak call and 0 otherwise. (c) The same evaluation as in **b**, but for anatomy annotations.

	H3K27me3			H3K36me3			H3K4me1			H3K4me3			H3K9me3			H3K27ac		
	ChromImpute	Group Average	Difference															
ESC	0.73	0.74	-0.02	0.29	0.26	0.03	0.39	0.36	0.03	0.56	0.53	0.03	0.42	0.42	0.00	0.54	0.55	0.00
iPSC	0.88	0.97	-0.08	0.87	0.76	0.11	0.77	0.69	0.09	0.95	0.89	0.06	0.85	0.82	0.03	0.77	0.72	0.05
ES-deriv	0.42	0.40	0.03	0.56	0.48	0.07	0.58	0.48	0.10	0.88	0.87	0.01	0.57	0.47	0.10	0.59	0.50	0.08
Blood & T-cell	0.78	0.70	0.08	0.77	0.72	0.04	0.58	0.45	0.13	0.90	0.88	0.03	0.72	0.63	0.09	0.73	0.69	0.05
HSC & B-cell	0.87	0.76	0.11	0.85	0.81	0.04	0.81	0.65	0.17	0.89	0.89	0.00	0.63	0.58	0.04	0.72	0.56	0.17
Mesench	0.77	0.71	0.06	0.84	0.80	0.04	0.84	0.73	0.11	0.96	0.95	0.01	0.67	0.60	0.08	0.85	0.74	0.12
Epithelial	0.83	0.73	0.10	0.83	0.74	0.09	0.82	0.63	0.18	0.97	0.95	0.02	0.62	0.59	0.04	0.85	0.84	0.01
Neurosp	0.58	0.54	0.04	0.77	0.64	0.12	0.74	0.69	0.06	0.97	0.96	0.01	0.73	0.68	0.06	0.80	0.69	0.11
Thymus	0.69	0.58	0.12	0.67	0.57	0.10	0.67	0.65	0.02	0.90	0.82	0.08	0.29	0.26	0.03	0.80	0.69	0.11
Brain	0.76	0.71	0.05	0.81	0.79	0.02	0.85	0.80	0.05	0.97	0.95	0.02	0.72	0.67	0.05	0.91	0.90	0.01
Muscle	0.41	0.33	0.08	0.52	0.44	0.08	0.59	0.45	0.14	0.91	0.79	0.12	0.47	0.34	0.12	0.80	0.65	0.15
Heart	0.56	0.27	0.28	0.37	0.28	0.09	0.67	0.51	0.16	0.57	0.41	0.16	0.41	0.19	0.22	0.88	0.87	0.00
Sm. Muscle	0.80	0.70	0.10	0.83	0.74	0.08	0.73	0.67	0.07	0.95	0.93	0.02	0.78	0.62	0.17	0.79	0.66	0.13
Digestive	0.84	0.76	0.08	0.83	0.78	0.04	0.72	0.46	0.26	0.96	0.94	0.02	0.77	0.76	0.02	0.86	0.75	0.11
Other	0.69	0.63	0.07	0.69	0.62	0.07	0.63	0.47	0.16	0.85	0.84	0.01	0.39	0.31	0.07	0.47	0.38	0.10
ENCODE	0.39	0.39	0.00	0.71	0.66	0.05	0.73	0.51	0.22	0.91	0.87	0.04	0.58	0.52	0.06	0.69	0.57	0.12

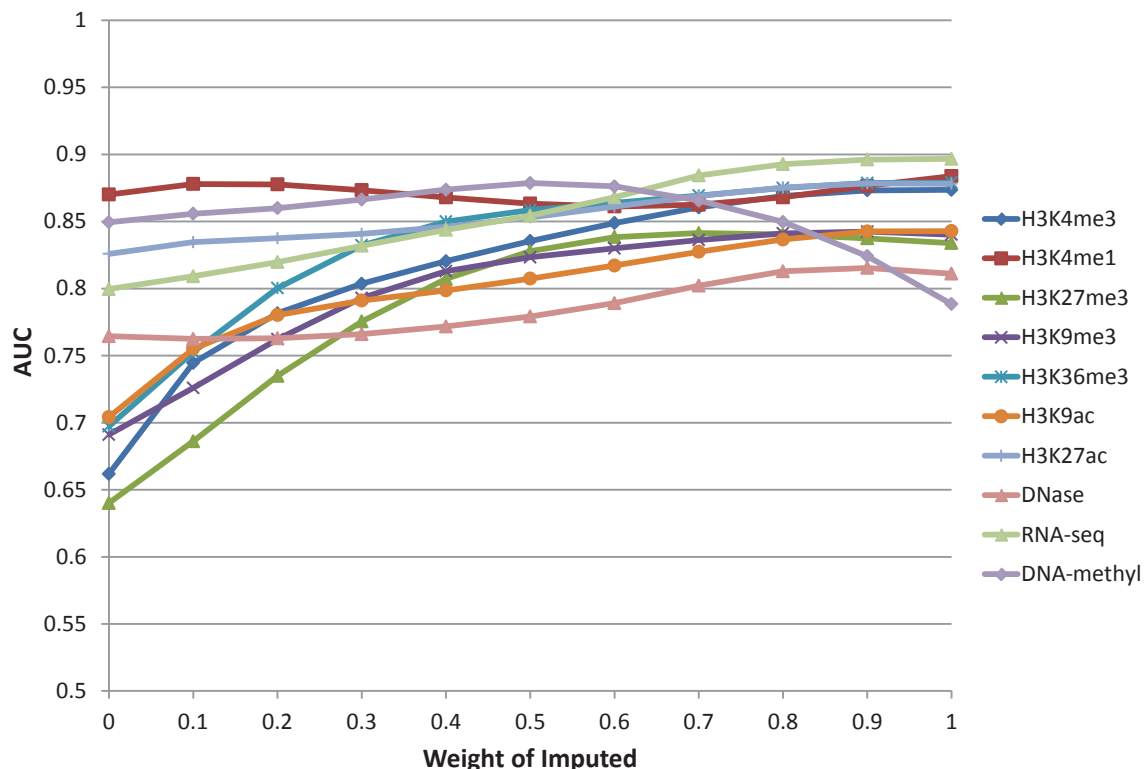
Supplementary Figure 21: Comparison of ChromImpute Predictions with Group Average.

The table shows for the six marks most deeply profiled and each biological group the average correlation of ChromImpute predictions with the observed data compared to the correlation if the prediction was based on all other observed data sets for the mark within the group. The difference in the correlation between the two corresponding columns is also shown. The evaluation is based on just chr10. These results demonstrate that in almost all cases the ChromImpute predictions show better correspondence to the observed data than predictions based on the group average.

a AUC for Classifying Pairs of Experiments as of the Same Group Taking a Weighted Average of Observed and Imputed Data

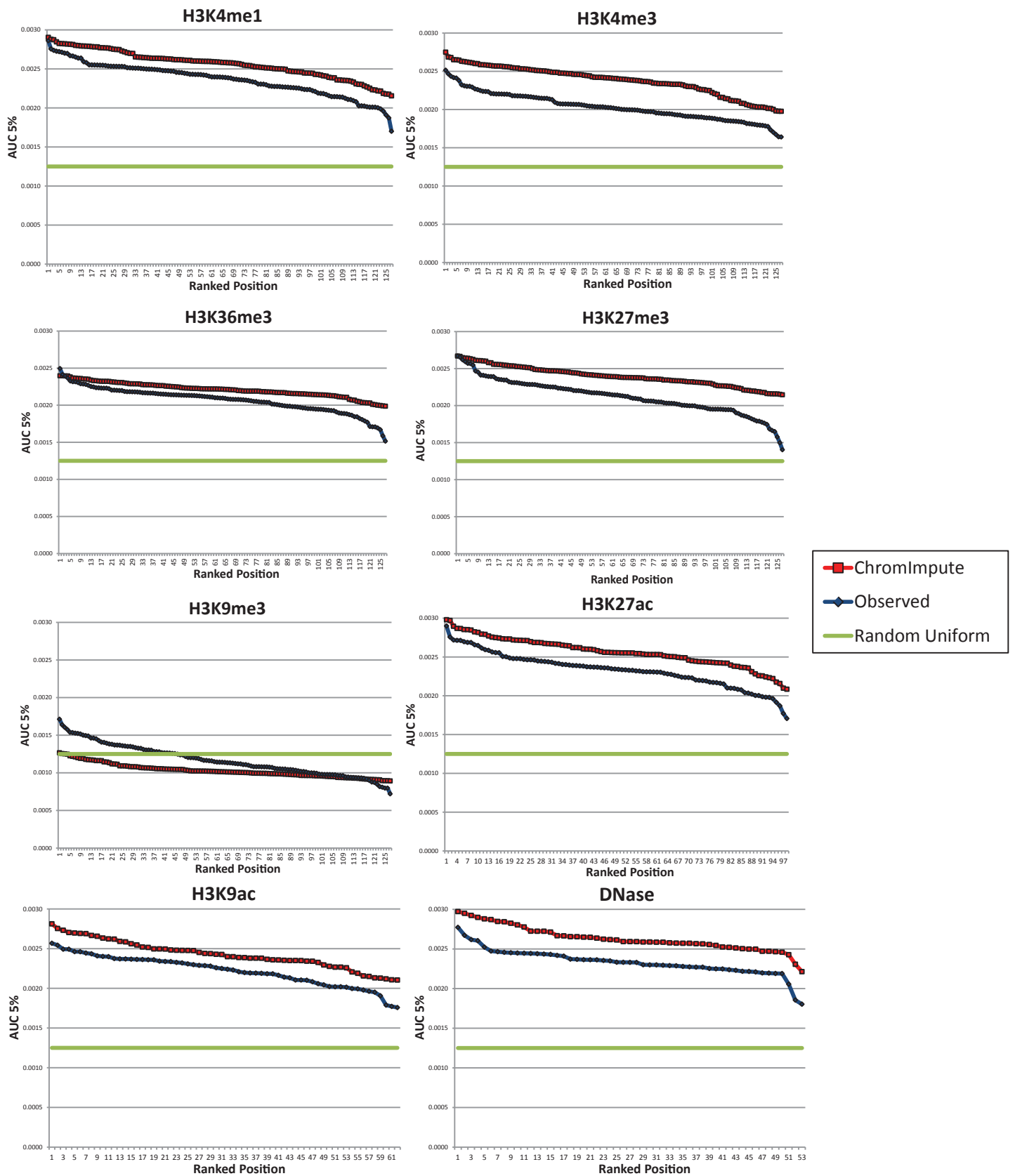


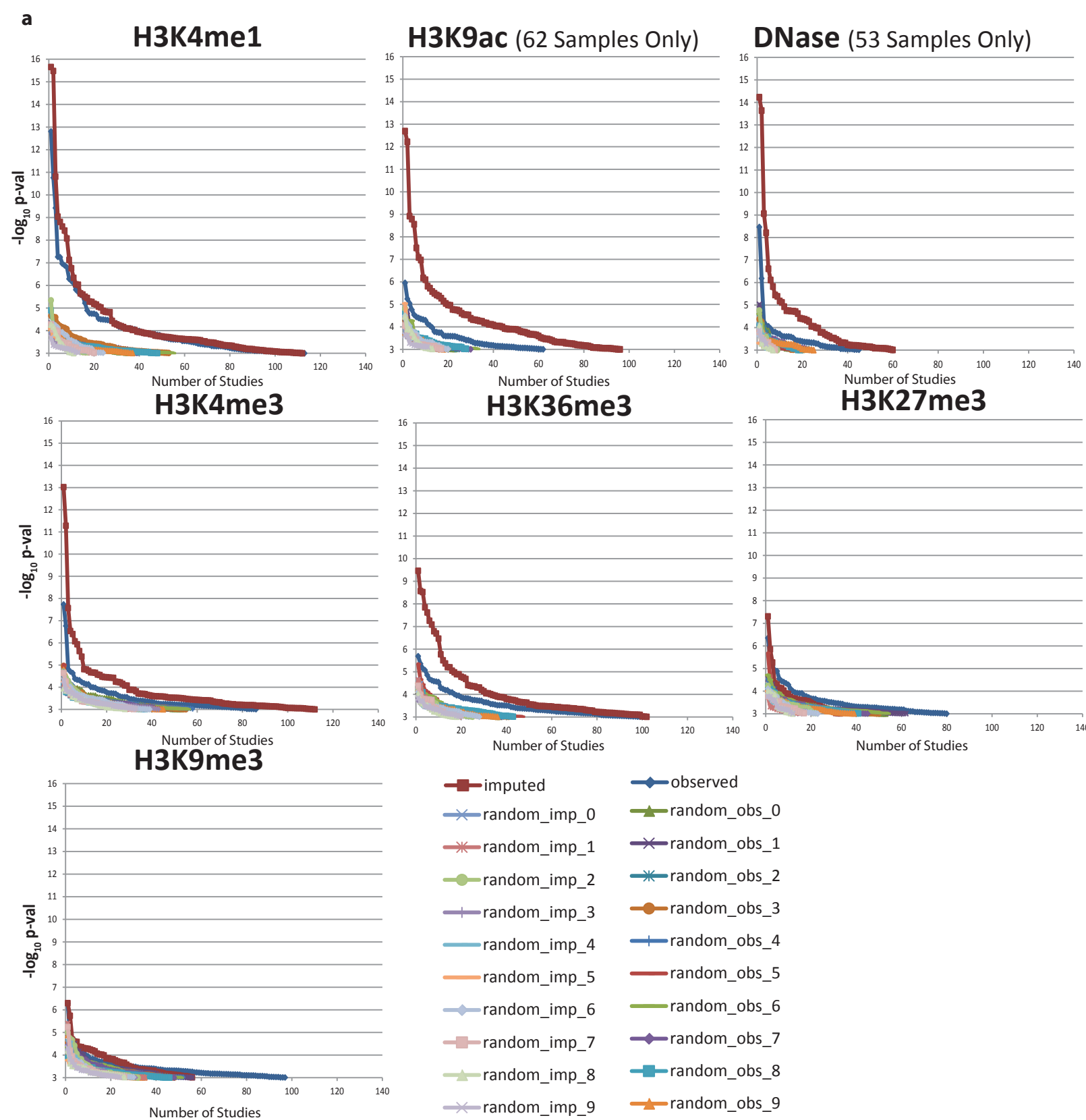
b AUC for Classifying Pairs of Experiments as of the Same Anatomy Taking a Weighted Average of Observed and Imputed Data



Supplementary Figure 22: Weighted Average Based Predictions of Same Group and Anatomy Pairs.

This figure extends the analysis shown in **Fig. 3f** and **Fig. S20a** by showing what the AUC results would be if a weighted average of the observed and imputed data is taken. The weight of the imputed data is shown on the x-axis, with a weight of 0 reducing to the observed data and a weight of 1 reducing to the imputed data. Results for the weights in increments of 0.1 are shown. This shows for all marks except DNA-methylation, the AUC obtained with all weight on the imputed data is either the best or close to the best.

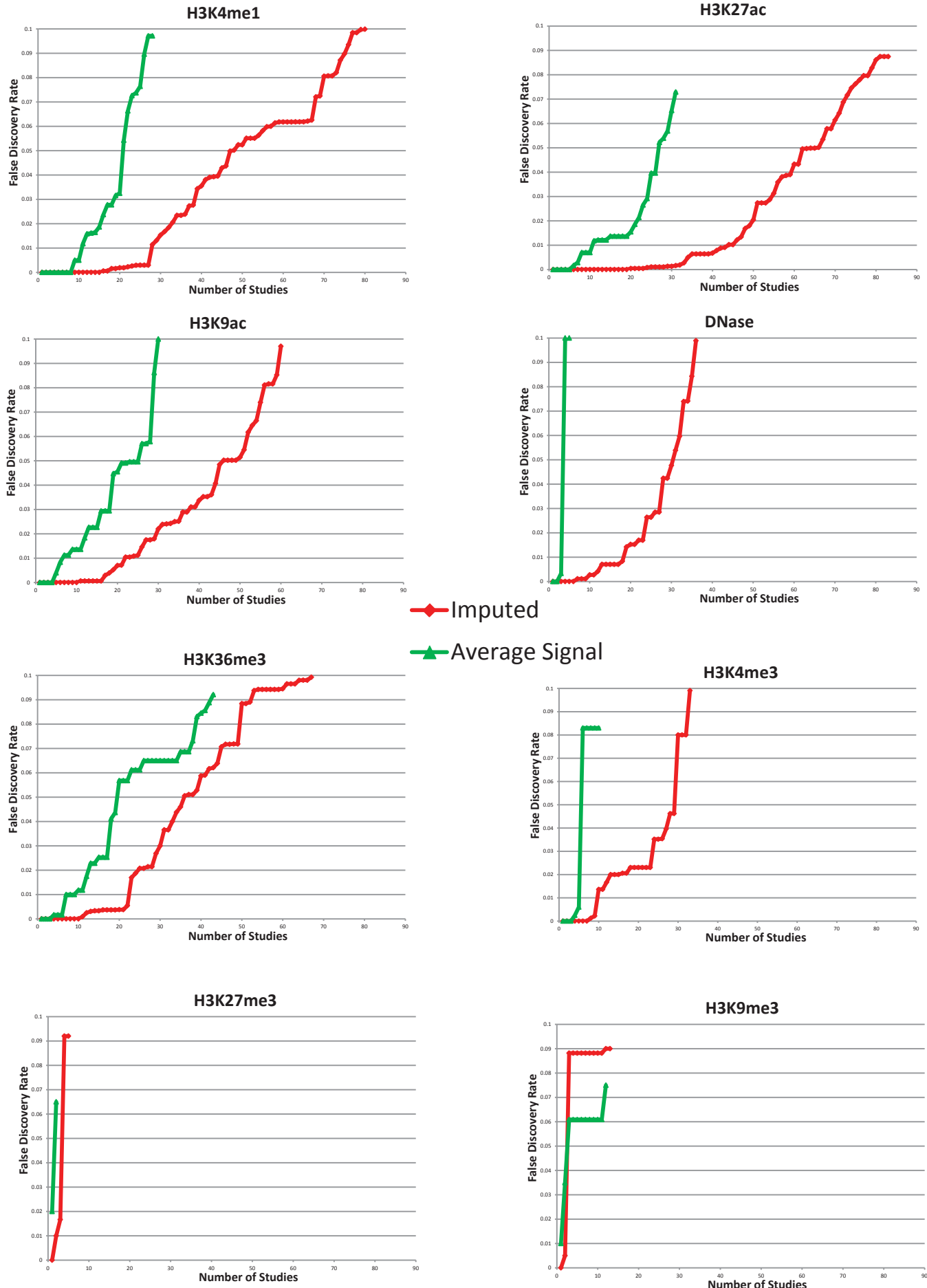


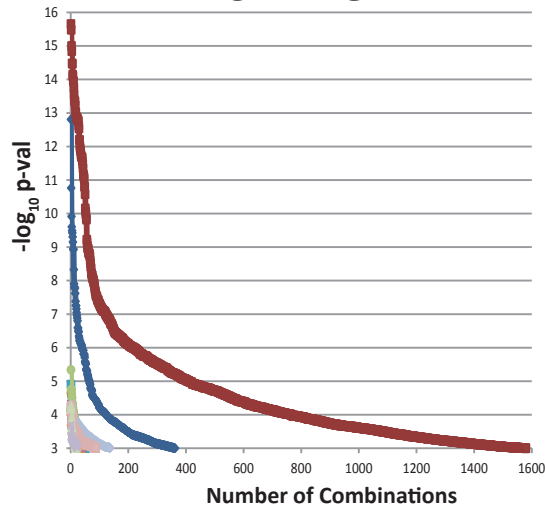
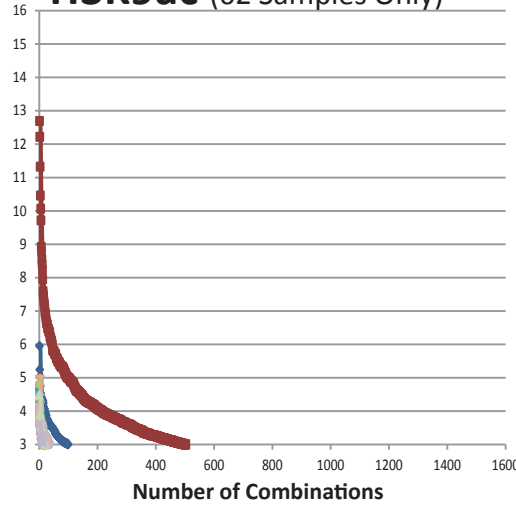
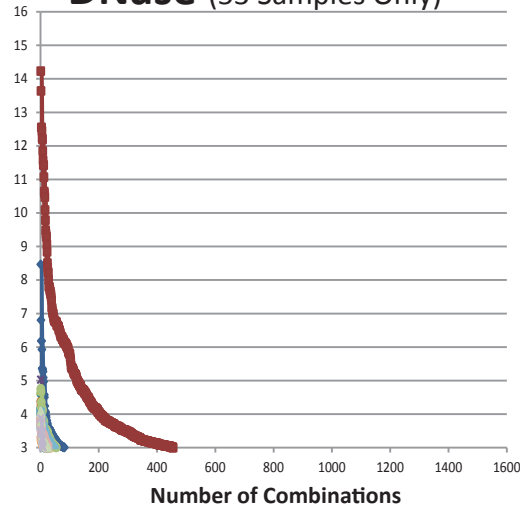
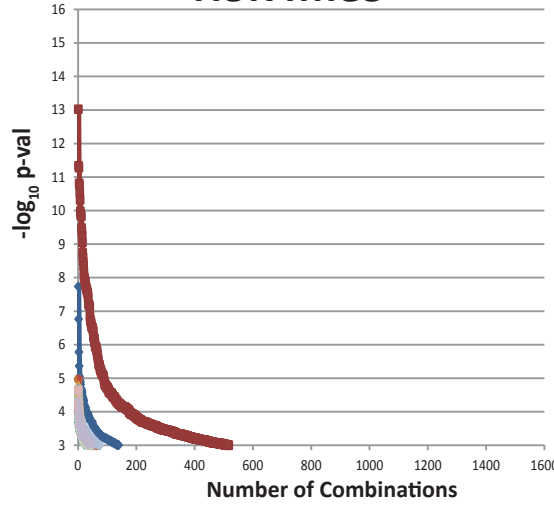
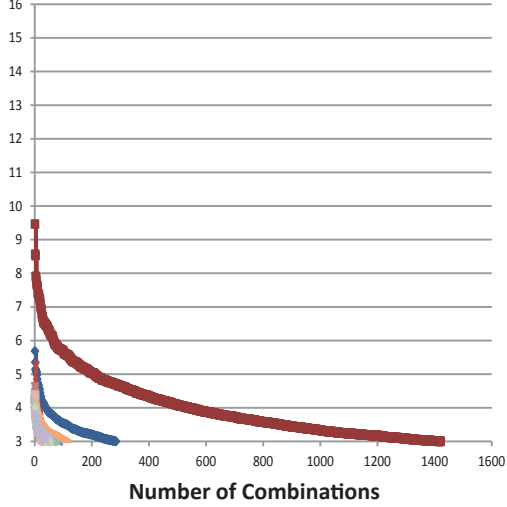
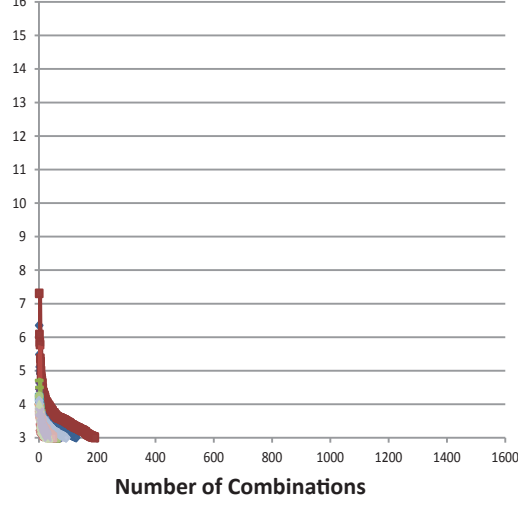
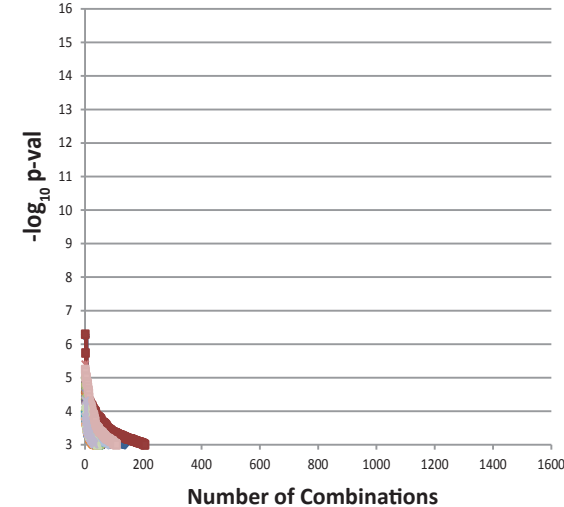


Supplementary Figure 24:

Imputed and Observed Data Correspondence with Genome-wide Association Studies (GWAS) – Max Sample.

(a) Similar to Fig. 4a but for the other Tier-1 marks. The x-axis shows the number of studies for which there was at least one sample for which the indicated mark signal was significantly different for the study identified SNPs compared to a background of all GWAS Catalog SNPs at a significance level indicated on the y-axis based on a Mann-Whitney U test (see Methods). This is shown based on the imputed and observed data with the actual GWAS catalog, along with the observed and imputed data based on ten randomizations of the GWAS catalog. For H3K9ac and DNase the comparison was limited to only those samples where both imputed and observed data is available. (b) Shows for each of the Tier-1 marks the number of studies based on the imputed data that are estimated to be significant in at least one sample restricting to those samples with observed data available at an estimated false discovery rate below 10%, and in comparison based on averaging the observed signal across all samples (see Methods).

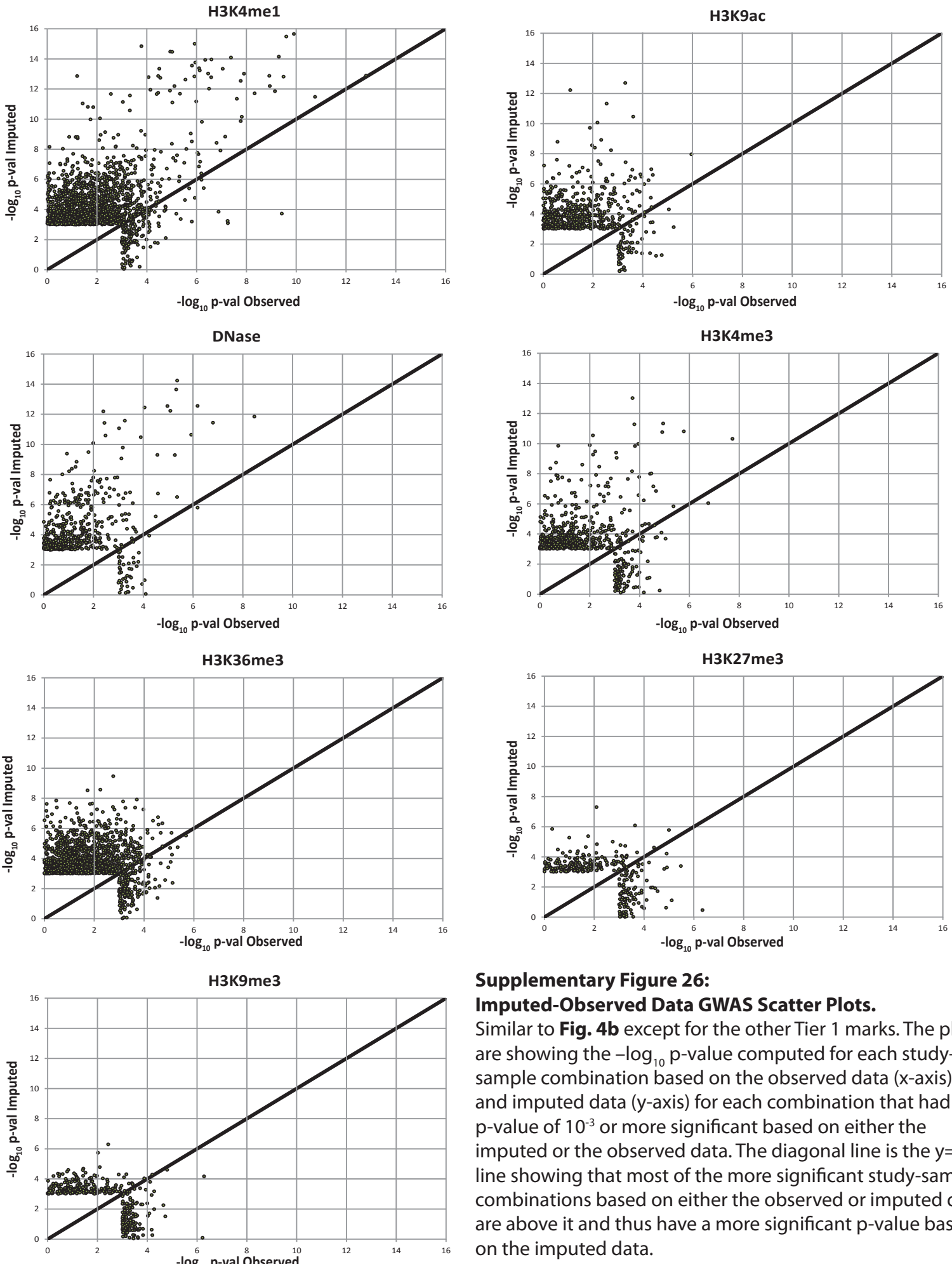
b

H3K4me1**H3K9ac (62 Samples Only)****DNase (53 Samples Only)****H3K4me3****H3K36me3****H3K27me3****H3K9me3**

- imputed
- observed
- random_imp_0
- random_obs_0
- random_imp_1
- random_obs_1
- random_imp_2
- random_obs_2
- random_imp_3
- random_obs_3
- random_imp_4
- random_obs_4
- random_imp_5
- random_obs_5
- random_imp_6
- random_obs_6
- random_imp_7
- random_obs_7
- random_imp_8
- random_obs_8
- random_imp_9
- random_obs_9

Supplementary Figure 25:**Imputed and Observed Data Correspondence with GWAS – Sample-Study Combinations.**

The same as Fig S24a except based on all combinations of studies and samples, and not just the most significant one per study. The x-axis shows the number of combinations that reached the significance level indicated on the y-axis. This is shown based on the imputed data and observed data with the actual GWAS catalog, along with the observed and imputed data based on ten randomizations of the GWAS catalog.



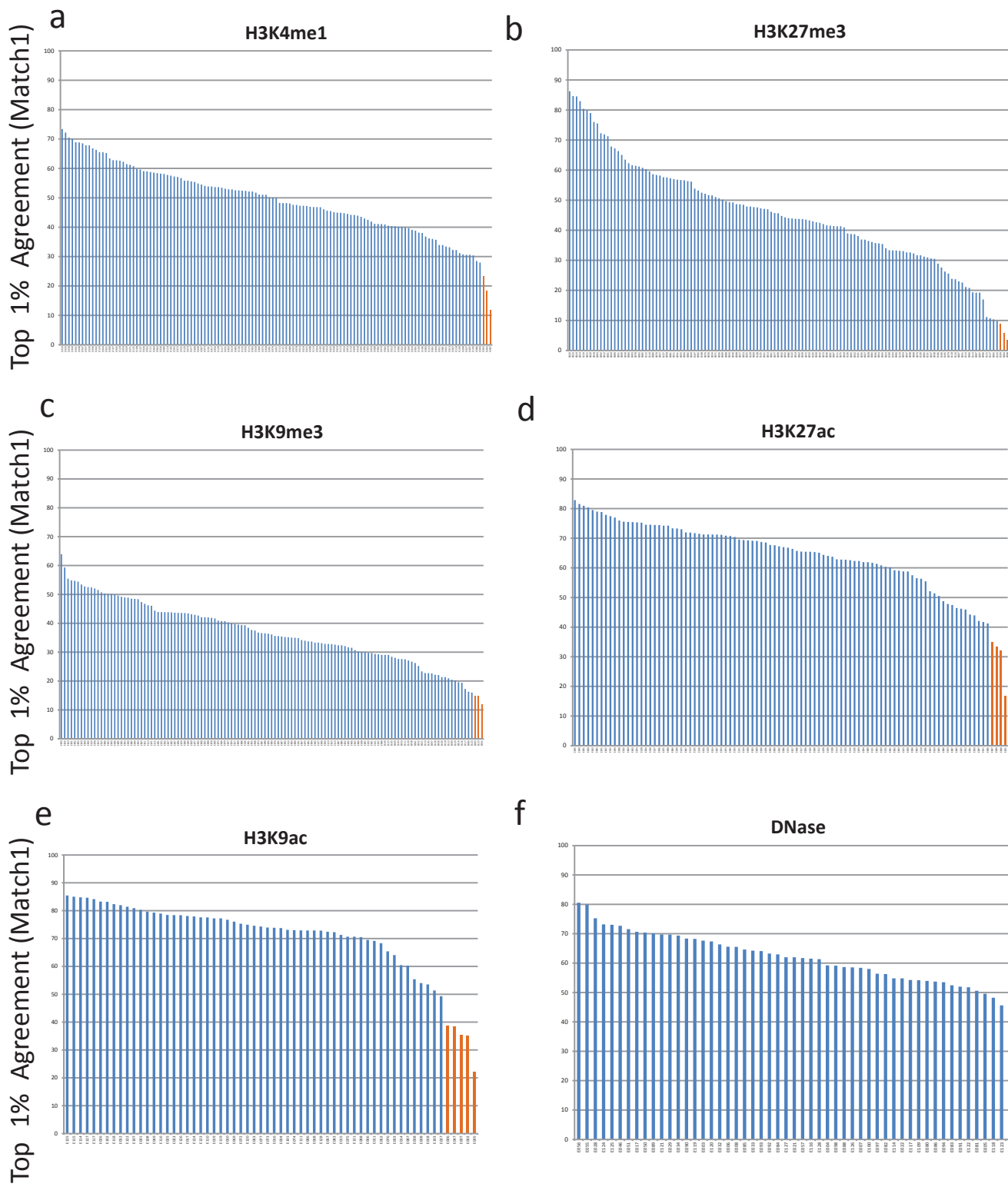
**Supplementary Figure 26:
Imputed-Observed Data GWAS Scatter Plots.**

Similar to **Fig. 4b** except for the other Tier 1 marks. The plots are showing the $-\log_{10}$ p-value computed for each study-sample combination based on the observed data (x-axis) and imputed data (y-axis) for each combination that had a p-value of 10^{-3} or more significant based on either the imputed or the observed data. The diagonal line is the $y=x$ line showing that most of the more significant study-sample combinations based on either the observed or imputed data are above it and thus have a more significant p-value based on the imputed data.

		H3K4me3								H3K9me3								H3K27ac									
		Match1	GWCorr	Poisson	SPOT	FindPeaks	NSC	RSC	PromRecov	Match1		GWCorr	Poisson	SPOT	FindPeaks	NSC	RSC	Match1		GWCorr	Poisson	SPOT	FindPeaks	NSC	RSC	Read Depth	
Match1	1.00	0.88	0.37	0.46	0.51	0.38	0.35	0.77	0.35	Match1	1.00	0.94	0.24	0.44	0.51	0.26	-0.13	0.09	Match1	1.00	0.92	0.44	0.46	0.46	0.41	0.14	-0.14
GWCorr	0.88	1.00	0.29	0.35	0.39	0.31	0.35	0.67	0.40	GWCorr	0.94	1.00	0.22	0.30	0.38	0.13	-0.16	0.23	GWCorr	0.92	1.00	0.39	0.38	0.38	0.28	0.16	-0.10
Poisson	0.37	0.29	1.00	0.98	0.97	0.78	0.39	0.59	-0.23	Poisson	0.24	0.22	1.00	0.28	0.28	0.21	0.07	-0.09	Poisson	0.44	0.39	1.00	0.96	0.97	0.77	0.14	-0.27
SPOT	0.46	0.35	0.98	1.00	1.00	0.83	0.43	0.60	-0.23	SPOT	0.44	0.30	0.28	1.00	0.93	0.84	0.24	0.55	SPOT	0.46	0.38	0.96	1.00	0.99	0.83	0.09	-0.35
FindPeaks	0.51	0.39	0.97	1.00	1.00	0.83	0.43	0.63	-0.18	FindPeaks	0.51	0.38	0.28	0.93	1.00	0.71	0.12	-0.43	FindPeaks	0.46	0.38	0.97	0.99	1.00	0.83	0.10	-0.30
NSC	0.38	0.31	0.78	0.83	0.83	1.00	0.50	0.32	-0.24	NSC	0.26	0.13	0.21	0.84	0.71	1.00	0.54	-0.43	NSC	0.41	0.28	0.77	0.83	0.83	1.00	0.19	-0.39
RSC	0.35	0.35	0.39	0.43	0.43	0.50	1.00	0.22	-0.06	RSC	-0.13	-0.16	0.07	0.24	0.12	0.54	1.00	0.03	RSC	0.14	0.16	0.14	0.09	0.10	0.19	1.00	0.03
PromRecov	0.77	0.67	0.59	0.60	0.63	0.32	0.22	1.00	0.23	PromRecov	0.09	0.23	-0.09	-0.55	-0.43	-0.43	0.03	1.00	PromRecov	0.14	-0.10	-0.27	-0.35	-0.30	-0.39	0.03	1.00
Read Depth	0.35	0.40	-0.23	-0.23	-0.18	-0.24	-0.06	0.23	1.00	Read Depth									Read Depth								
		H3K36me3								H3K4me1								DNase									
		Match1	GWCorr	Poisson	SPOT	FindPeaks	NSC	RSC	GeneRecov	Match1		GWCorr	Poisson	SPOT	FindPeaks	NSC	RSC	Match1		GWCorr	Poisson	SPOT	FindPeaks	NSC	RSC	Read Depth	
Match1	1.00	0.93	0.34	0.34	0.36	0.07	0.02	0.57	0.49	Match1	1.00	0.93	0.26	0.34	0.38	0.25	-0.22	0.16	Match1	1.00	0.86	0.15	0.17	0.22	0.20	-0.27	0.16
GWCorr	0.93	1.00	0.46	0.30	0.40	-0.13	-0.09	0.77	0.55	GWCorr	0.93	1.00	0.22	0.22	0.25	0.08	-0.22	0.33	GWCorr	0.86	1.00	0.02	0.01	0.17	0.19	-0.47	0.06
Poisson	0.34	0.46	1.00	0.89	0.95	0.36	0.25	0.74	-0.05	Poisson	0.26	0.22	1.00	0.94	0.93	0.82	0.33	-0.19	Poisson	0.15	0.02	1.00	0.97	0.91	0.75	0.17	0.14
SPOT	0.34	0.30	0.89	1.00	0.95	0.66	0.40	0.47	-0.22	SPOT	0.34	0.22	0.94	1.00	0.99	0.89	0.23	-0.26	SPOT	0.17	0.01	0.97	1.00	0.90	0.78	0.24	0.16
FindPeaks	0.36	0.40	0.95	0.95	1.00	0.45	0.30	0.65	-0.08	FindPeaks	0.38	0.25	0.93	0.99	1.00	0.86	0.21	-0.23	FindPeaks	0.22	0.17	0.91	0.90	1.00	0.92	-0.04	0.08
NSC	0.07	-0.13	0.36	0.66	0.45	1.00	0.71	-0.19	-0.26	NSC	0.25	0.08	0.82	0.89	0.86	1.00	0.40	-0.19	NSC	0.20	0.19	0.75	0.78	0.92	1.00	-0.13	0.00
RSC	0.02	-0.09	0.25	0.40	0.30	0.71	1.00	-0.09	-0.01	RSC	-0.22	-0.22	0.33	0.23	0.21	0.40	1.00	-0.08	RSC	-0.27	-0.47	0.17	0.24	-0.04	-0.13	1.00	0.21
GeneRecov	0.57	0.77	0.74	0.47	0.65	-0.19	-0.09	1.00	0.40	GeneRecov	0.16	0.33	-0.19	-0.26	-0.23	-0.19	-0.08	1.00	GeneRecov	0.16	0.06	0.14	0.16	0.08	0.00	0.21	1.00
Read Depth	0.49	0.55	-0.05	-0.22	-0.08	-0.26	-0.01	0.40	1.00	Read Depth									Read Depth								
		H3K27me3								H3K9ac								DNase									
		Match1	GWCorr	Poisson	SPOT	FindPeaks	NSC	RSC	Read Depth	Match1	GWCorr	Poisson	SPOT	FindPeaks	NSC	RSC	Read Depth	Match1	GWCorr	Poisson	SPOT	FindPeaks	NSC	RSC	Read Depth		
Match1	1.00	0.94	0.36	0.63	0.69	0.47	0.30	0.17	0.17	Match1	1.00	0.92	0.40	0.45	0.59	0.44	0.02	0.03	Match1	1.00	0.86	0.15	0.17	0.22	0.20	-0.27	0.16
GWCorr	0.94	1.00	0.31	0.49	0.55	0.35	0.31	0.27	0.27	GWCorr	0.92	1.00	0.29	0.33	0.45	0.31	0.12	0.10	GWCorr	0.86	1.00	0.02	0.01	0.17	0.19	-0.47	0.06
Poisson	0.36	0.31	1.00	0.79	0.74	0.59	0.48	-0.26	0.31	Poisson	0.40	0.29	1.00	0.97	0.93	0.84	0.20	-0.27	Poisson	0.40	0.29	1.00	0.97	0.93	0.84	0.20	-0.27
SPOT	0.63	0.49	0.79	1.00	0.98	0.85	0.46	-0.36	0.73	SPOT	0.45	0.33	0.97	1.00	0.96	0.89	0.14	-0.27	SPOT	0.45	0.33	0.97	1.00	0.96	0.89	0.14	-0.27
FindPeaks	0.69	0.55	0.74	0.98	1.00	0.83	0.45	-0.23	0.74	FindPeaks	0.59	0.45	0.93	0.96	1.00	0.90	0.13	-0.23	FindPeaks	0.44	0.31	0.84	0.89	0.90	1.00	0.18	-0.32
NSC	0.47	0.35	0.59	0.85	0.83	1.00	0.58	-0.28	0.45	NSC	0.30	0.31	0.48	0.46	0.45	0.58	1.00	-0.01	NSC	0.02	0.12	0.20	0.14	0.13	0.18	1.00	-0.31
RSC	0.30	0.31	0.48	0.46	0.45	0.58	1.00	-0.01	0.30	RSC	0.17	0.27	0.26	0.36	0.23	0.28	0.01	1.00	RSC	0.03	0.10	0.27	0.27	0.23	0.32	0.32	1.00
Read Depth									Read Depth									Read Depth									

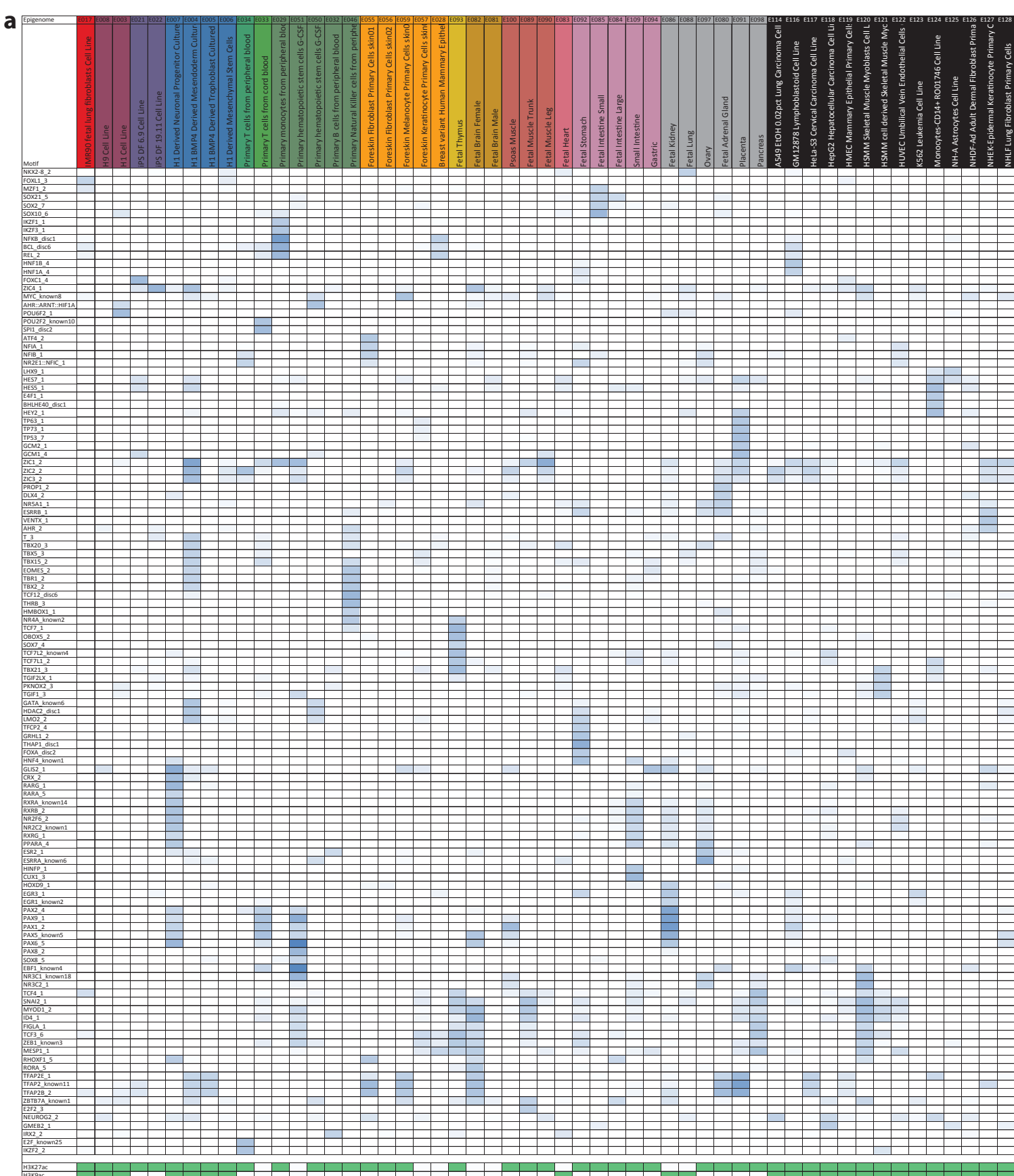
Supplementary Figure 27: Quality Control (QC) Metric Correlations.

These tables show for each of the Tier-1 marks the Pearson correlation between all the general quality control measures evaluated. The table illustrates the two imputation based quality measures (Match 1, GWCorr) consistently correlate highly with each other, and to a lesser extent with the five non-imputation based general QC measures evaluated (SPOT, Poisson, FindPeaks, NSC, and RSC) along with read depth suggesting the imputation metrics could potentially provide additional unique information for quality control. For H3K36me3 and H3K4me3 the tables also contain correlations with a metric that leveraged relevant gene annotation information, AUC at a 5% false positive rate for recovering gene bodies (GeneRecov) and +/-2KB TSS regions (PromRecov) respectively, for which the imputation QC measures are among the best correlated.



Supplementary Figure 28: Distribution of Imputation Top 1% Agreement Scores.

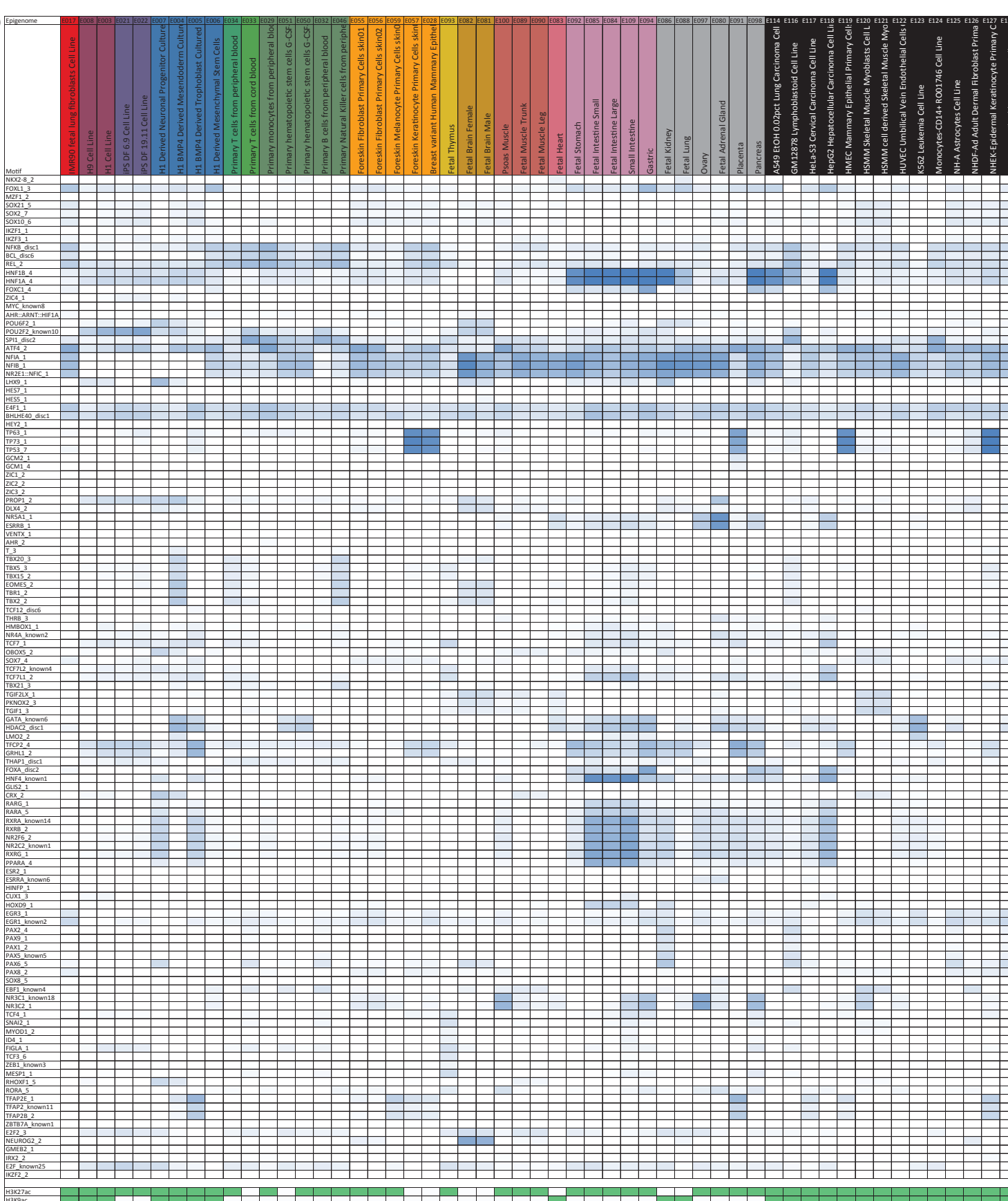
Similar to **Fig. 5b** except the figure shows the distribution across samples of top 1% signal location agreement percentages between the observed and corresponding imputed data for **(a)** H3K4me1 **(b)** H3K27me3 **(c)** H3K9me3 **(d)** H3K27ac **(e)** H3K9ac and **(f)** DNase. Shown in brown are observed datasets with an imputation agreement score more than two standard deviations below average for the mark. See also **Table S3** for the agreement scores and samples.



Supplementary Figure 29: Motif Enrichments in Locations of Unexpected DNase signal.

(a) The heatmap shows sequence motif enrichments occurring in locations with unexpected DNase signal, which was defined here as places where the observed DNase signal was above 5, but the imputed signal was below 1. Motif enrichments are shown in \log_2 relative to control as computed using a previous described motif enrichment program⁵⁷. The background locations for computing the motif enrichments were locations that had an observed signal above 5. The rows correspond to different motifs, and columns different samples with observed DNase data available. Only motifs which had an enrichment value of at least 1 in at least one sample are shown. If multiple motifs corresponding to the same factor were available only the one with the maximum enrichment for any sample is shown. Along the bottom row is indicated which acetylations marks were available in the sample which could affect the expected signal. **(b)** The same heatmap as in a, but for comparison showing the motif enrichment for locations that had an observed signal above 5, used in the background for computing the enrichments in a, relative to a genome-wide background.

-3 0 3



3

0

-3

a Root position

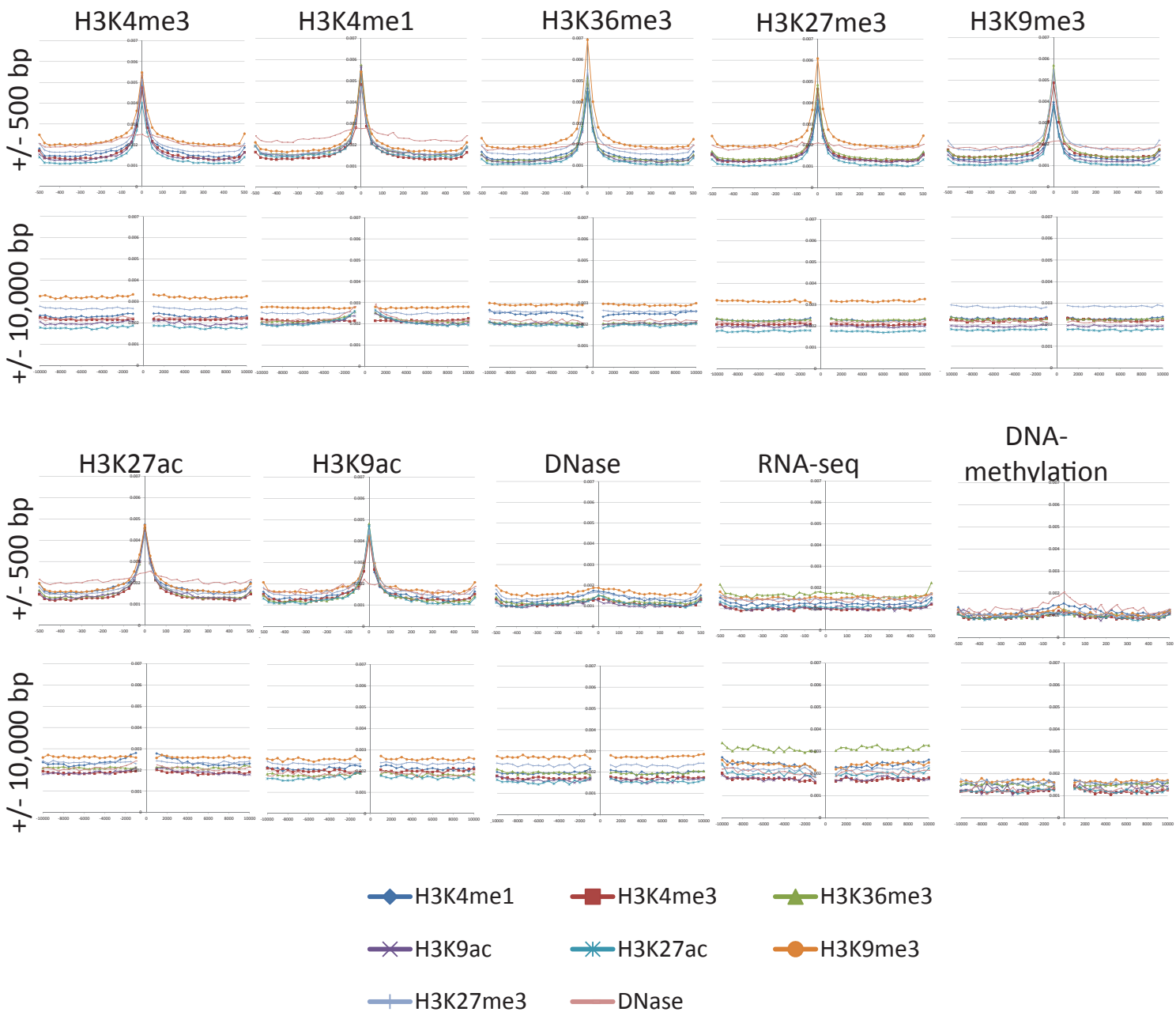
Main Imputation			Imputation on Seven Deep Samples Only			
Mark	Feature #1	Feature #2	Mark	Feature #1	Feature #2	
H3K27me3	KNN 10 by Global H3K4me1	KNN 10 by Global H3K27ac	KNN 10 by Global H3K9ac	H3K27me3	KNN 3 by Global H3K27ac	KNN 2 by Global 2 H3K18ac
H3K36me3	KNN 10 by Global H3K4me1	KNN 10 by Global H3K4me3	KNN 9 by Global H3K4me3	H3K36me3	H3K4me2 center	KNN 4 by Global H3K27ac
H3K4me1	KNN 10 by Local H3K27ac	H3K27ac center	KNN 10 by Local H3K9ac	H3K4me1	H3K27ac center	H3K18ac center
H3K4me3	KNN 5 by Global H3K4me1	KNN 10 by Local H3K9ac	KNN 3 by Global H3K4me1	H3K4me3	KNN 3 by Local H3K4me2	KNN 2 by Global DNase
H3K9me3	KNN 10 by Global H3K4me1	KNN 10 by Global H3K4me3	KNN 10 by Global H3K27ac	H3K9me3	KNN 4 by Global H2BK120ac	KNN 4 by Global H3K27me3
H3K27ac	KNN 2 Global H3K4me1	H3K9ac center	KNN 1 by Global H3K4me1	H3K27ac	H2BK5ac center	H4K5ac center
H3K9ac	H3K4me3 center	H3K27ac center	KNN 10 by Local H3K4me3	H3K9ac	H3K4me3 center	H3K18ac center
DNase	KNN 1 by Global H3K4me3	KNN 2 by Global H3K4me3	KNN 5 by Global H3K4me1	DNase	KNN 2 by Global H2BK15ac	KNN 2 by Global H4K91ac
H3K4me2	H3K4me3 center	KNN 7 by Local H3K4me3	KNN 4 by Global H3K4me1	H3K4me2	H3K4me3 center	KNN 3 by Global H3K18ac
H2A.Z	KNN 5 by Local H3K4me2	KNN 7 by Global H3K27ac	KNN 8 by Local H3K4me2	H2A.Z	H4K8ac center	H3K4me2 center
H3K79me2	KNN 5 by Local H3K36me3	KNN 6 by Local H3K27ac	KNN 3 by Global DNase	H3K79me2	H4K20me1 center	H3K4ac center
H4K20me1	H3K36me3 center	KNN 10 by Global H3K4me1	KNN 10 by Local H3K36me3	H4K20me1	H3K79me2 center	H4K8ac center
H2AK5ac	H3K18ac center	H3K4me1 center	H2BK12ac center	H2AK5ac	H3K18ac center	H2BK12ac center
H2BK120ac	H3K18ac center	H3K27ac center	H4K91ac center	H2BK120ac	H3K18ac center	H4K91ac center
H2BK5ac	H3K27ac center	H4K5ac center	H3K18ac center	H2BK5ac	H3K27ac center	H4K5ac center
H3K18ac	H4K5ac center	H3K14ac center	H3K4ac center	H3K18ac	H4K5ac center	H3K14ac center
H3K23ac	H3K14ac center	H3K18ac center	H4K5ac center	H3K23ac	H3K14ac center	H3K18ac center
H3K4ac	H3K18ac center	H3K9ac center	H3K18ac center	H3K4ac	H3K18ac center	H4K5ac center
H3K79me1	H3K79me2 center	KNN 4 by Global H3K9ac	KNN 5 by Global H3K9ac	H3K79me1	H3K79me2 center	H3K14ac center
H4K8ac	H4K5ac center	H3K18ac center	H3K9ac center	H4K8ac	H4K5ac center	H3K18ac center
H2BK12ac	H3K18ac center	KNN 4 by Global H3K4me1	H4K91ac center	H2BK12ac	H3K18ac center	H4K91ac center
H3K14ac	H3K18ac center	H3K27ac center	H4K91ac center	H3K14ac	H3K18ac center	H4K91ac center
H4K91ac	H3K18ac center	H3K27ac center	KNN 4 by Global H3K27ac	H4K91ac	H3K18ac center	H2BK12ac center
H2BK15ac	H3K18ac center	H2BK12ac center	H3K27ac center	H2BK15ac	H3K18ac center	H2BK12ac center
H3K0me1	H2AK5ac center	H3K4me1 center	H4K20me1 center	H3K9me1	H2AK5ac center	H3K23ac center
H2BK20ac	H3K4me1 center	H2BK12ac center	H2BK120ac center	H2BK20ac	H2BK12ac center	H2BK120ac center
H3K56ac	H3K27ac center	H4K5ac center	H4K8ac center	H3K56ac	H4K5ac center	H3K27ac center
H4K5ac	H3K27ac center	H4K8ac center	H3K9ac center	H4K5ac	H4K8ac center	H3K27ac center
H3K23me2	H3K4me3 center	H3K4me2 center	H4K20me1 center	H3K23me2	H3K4me2 center	H3K56ac center
H2A9ac	H2A.Z center	H3K9ac center	H3K27ac center	H2A9ac	H2A.Z center	H3K9ac center
H3T11ph	H3K4me1 center	H2BK12ac center	H3K18ac center	H3T11ph	H2BK12ac center	H3K18ac center
H4K12ac	H4K8ac center	H2A.Z center	H3K4me3 center	H4K12ac	H4K8ac center	
DNAseq	KNN 4 by Global H3K4me1	KNN 6 by Global DNase	KNN 4 by Global H3K27ac	DNAseq	KNN 4 by Global H3K27ac	KNN 3 by Global H3K9me3
RNA-seq	KNN 3 by Global H3K27ac	KNN 5 by Global H3K9ac	KNN 2 by Global H3K4me3	RNA-seq	KNN 1 by Global H3K9ac	KNN 2 by Global H3K4me3

b All positions

Main Imputation			Imputation on Seven Deep Samples Only		
Mark	Feature #1	Feature #2	Mark	Feature #1	Feature #2
H3K27me3	H3K9me3 center	H3K36me3 center	H3K27me3	H3K9me3 center	H3K4me2 center
H3K36me3	H3K9me3 center	H3K27me3 center	H3K36me3	H3K9me3 center	H4K20me1 center
H3K4me1	H3K4me3 center	H3K9ac center	H3K4me1	H3K4me2 center	H2A.Z center
H3K4me3	H3K9me3 center	H3K9ac center	H3K4me3	H3K9me3 center	H3K36me3 center
H3K9me3	H3K36me3 center	H3K27me3 center	H3K9me3	H3K36me3 center	H3K4me3 center
H3K27ac	H3K4me1 center	H3K9me3 center	H3K27ac	H3K4me2 center	H3K23ac center
H3K9ac	H3K4me3 center	H3K27ac center	H3K9ac	H3K4me2 center	H3K4me1 center
DNase	KNN 1 by Local H3K4me1	KNN 1 by Local H3K9me3	DNase	H3K9me3 left 7000	KNN 1 by Local H3K27ac
H3K4me2	H3K4me3 center	H3K4me1 center	H3K4me2	H3K9ac center	H2BK5ac center
H2A.Z	H3K9me3 center	H3K27me3 center	H2A.Z	H3K9me3 center	H3K4me1 center
H3K79me2	H3K9me3 center	H3K36me3 center	H3K79me2	H4K20me1 center	H3K9me3 center
H4K20me1	H3K36me3 center	H3K27me3 center	H4K20me1	H3K79me2 center	H3K36me3 center
H2AK5ac	H3K9me1 center	H3K9me3 center	H2AK5ac	H2BK15ac center	H3K79me2 center
H2BK120ac	H3K9me1 center	H3K4me3 center	H2BK120ac	H2BK15ac center	H3K4ac center
H2BK5ac	H3K27ac center	H3K36me3 center	H2BK5ac	H4K5ac center	H3K27ac center
H3K18ac	H3K9me1 center	H3K4me1 center	H3K18ac	H2BK120ac center	H4K5ac center
H3K23ac	H3K9ac center	H4K20me1 center	H3K23ac	H4K20me1 center	H3K56ac center
H3K4ac	H3K9me1 center	H3K27ac center	H3K4ac	H4K8ac center	H4K91ac center
H3K79me1	H3K9me1 center	H3K36me3 center	H3K79me1	H4K20me1 center	H3K36me3 center
H4K8ac	H2A.Z center	H3K9me1 center	H4K8ac	H2A.Z center	H3K56ac center
H2BK12ac	H3K9me3 center	H3K27ac center	H2BK12ac	H2BK5ac center	H4K91ac center
H3K14ac	H3K4me1 center	H3K9me3 center	H3K14ac	H2BK120ac center	H3K18ac center
H4K91ac	H3K9me1 center	H3K36me3 center	H4K91ac	H2BK12ac center	H2BK120ac center
H2BK15ac	H3K9me1 center	H3K9me3 center	H2BK15ac	H2BK120ac center	H3K14ac center
H3K9me1	H3K79me1 center	H3K9ac center	H3K9me1	H3K79me2 center	H2AK5ac center
H2BK20ac	H3K9me3 center	H3K9me1 center	H2BK20ac	H2BK120ac center	H2AK5ac center
H3K56ac	H4K20me1 center	H3K27ac center	H3K56ac	H3K23ac center	H4K20me1 center
H4K5ac	H3K27ac center	H3K4me3 center	H4K5ac	H2BK5ac center	H3K56ac center
H3K23me2	H3K9me3 center	H2A.Z center	H3K23me2	H3K56ac center	H3K4me2 center
H2A9ac	H3K9me3 center	H3K36me3 center	H2A9ac	H3K9me3 center	H3K9me3 right 25
H3T11ph	H3K27ac center	H3K4me3 center	H3T11ph	H3K27ac center	H2A.Z center
H4K12ac	H3K4me1 center	H3K36me3 center	H4K12ac	H3K9me3 center	H3K4me3 center
DNAseq	KNN 2 Global H3K27ac	KNN 2 by Global H3K27me3	DNAseq	KNN 4 by Local H3K9me3	KNN 2 by Local DNase
RNAseq	H3K36me3 left 10000	H3K36me3 right 5000	RNAseq	H3K36me3 left 3000	H3K36me3 right 4000

Supplementary Figure 30: Top Used Features.

(a) (left) The table shows for imputing each mark in the main imputation the top three ranking features in terms of proportional usage as the root feature in the regression trees. Proportional usage in the root was determined as the fraction of times the feature was selected as the root feature for any regression tree built for the mark out of the number of times the feature was eligible for selection. The marks are color coded based on acetylation, methylation, or other. The features are color coded based on if it is the same mark in a sample determined based on local distance, based on global distance, or an acetylation, methylation, or other in the same sample. (right) The same as on the left but for the imputation restricted to the seven samples with deep mark coverage. **(b)** (left) The table shows for imputing each mark in the main imputation the top three ranking features in terms of proportional usage as a feature anywhere in the regression trees. Proportional usage here was determined as the fraction of times the feature was used at any split node in the tree out of the total number of split nodes for which the feature was eligible to be selected. The color coding was the same as in part **a**. (right) The same as on the left but for the imputation restricted to the seven samples with deep mark coverage.



Supplementary Figure 31: Feature Usage Relative to Position.

The figure displays for predicting each of the Tier-1 marks, RNA-seq, and DNA-methylation a plot showing the relative usage of Tier-1 mark signal features at each 25bp position within 500bp of the target position (x-axis) based on the proportion of times it was selected as a split feature in a node anywhere in the tree out of the number of times it was eligible for selection (y-axis), and then directly below that the same plot, but now showing features from 500bp up until 10kb spaced at 500 base pair intervals.

a

state	H3k9me3	H3k36me3	H4k20me1	H3k79me2	H3k4me1	H3k27ac	DNase	H3k9ac	H3k4me3	H3k4me2	H2A.Z	H3k27me3
1	0.2	0.1	0.5	8.9	1.3	92.8	89.5	88.6	96.5	89.1	79.1	0.4
2	0.3	0.7	2.5	12.5	96.1	99.1	78.1	86.2	95.6	99.9	74.7	0.7
3	0.9	0.5	2.6	17.5	88.0	13.0	29.7	44.8	91.8	98.9	70.8	2.9
4	3.9	9.6	10.2	98.6	23.2	92.9	55.6	97.9	99.6	96.4	68.2	12.3
5	0.3	1.2	3.5	59.5	2.5	0.8	0.4	1.9	0.1	0.6	0.3	0.0
6	0.2	33.6	37.7	82.2	0.8	0.9	0.6	0.8	0.1	0.5	0.1	0.1
7	0.4	78.7	5.5	4.2	0.4	0.9	0.5	0.6	0.1	0.1	0.2	0.1
8	0.3	7.3	1.7	2.2	0.2	0.1	0.2	0.1	0.0	0.1	0.1	0.0
9	0.8	34.3	35.8	97.6	82.5	59.2	22.1	59.6	78.9	97.6	3.9	0.3
10	1.0	75.9	38.9	64.8	58.1	37.0	14.5	11.9	2.6	14.7	2.9	0.6
11	0.4	5.1	25.3	89.1	69.7	10.7	9.6	6.0	1.4	29.1	2.6	0.1
12	0.6	2.5	2.6	12.0	91.0	95.4	47.7	41.5	6.1	63.1	29.9	0.4
13	0.5	0.1	2.0	0.5	89.0	26.8	64.7	7.4	7.4	67.6	47.1	0.8
14	0.4	0.3	1.3	1.8	59.2	1.9	1.6	0.8	0.2	7.7	5.6	1.1
15	1.4	0.6	0.3	1.2	13.2	3.7	1.8	4.5	1.8	9.6	56.5	1.7
16	0.5	1.0	0.5	2.8	18.1	58.1	30.7	5.6	0.9	9.7	2.4	0.4
17	0.5	0.2	1.5	0.2	10.2	1.8	94.5	0.7	0.2	5.5	9.4	0.7
18	67.4	60.5	7.5	29.7	2.1	1.5	2.3	2.0	9.1	2.3	2.2	2.3
19	59.1	0.8	0.2	0.4	0.3	0.2	0.7	0.3	1.3	0.4	1.3	2.1
20	5.1	0.0	0.0	0.0	0.0	0.0	0.0	0.1	0.1	0.1	0.1	0.1
21	0.6	0.4	0.7	7.9	3.3	6.2	45.5	33.4	77.5	82.8	42.8	1.4
22	4.1	1.4	7.4	1.7	54.9	6.1	31.8	17.1	43.9	78.5	40.3	84.7
23	1.5	0.2	2.0	0.0	0.6	0.2	0.5	0.2	0.1	0.3	1.1	45.8
24	0.3	0.1	0.2	0.1	0.0	0.1	0.0	0.2	0.0	0.1	0.7	1.1
25	0.3	0.0	0.0	0.0	0.0	0.0	0.0	0.0	0.0	0.0	0.1	0.1

b

Average Genome % DNase Present	Average Genome % DNase Missing	Log_2 Present/Missing
0.30	0.41	-0.43
0.23	0.30	-0.38
0.17	0.19	-0.18
0.17	0.08	1.02
3.79	3.77	0.01
2.00	2.40	-0.26
1.99	2.05	-0.04
6.53	5.62	0.22
0.18	0.09	0.93
0.36	0.28	0.36
0.75	0.83	-0.14
0.55	0.56	-0.01
0.40	0.24	0.72
1.08	0.99	0.12
0.39	0.25	0.64
0.52	0.62	-0.26
0.66	0.01	6.06
0.22	0.22	-0.02
1.34	1.17	0.19
7.63	6.38	0.26
0.25	0.28	-0.13
0.30	0.23	0.38
2.75	1.97	0.48
33.42	30.69	0.12
34.03	40.36	-0.25

Supplementary Figure 32: Chromatin State Model with 12-Marks Using Observed Data.

(a) The emission parameters for a chromatin state model learned directly on the Tier-1 and 2 observed data across 127 samples after applying the ChromHMM default binarization and treating as missing cases in which a mark was not available in a sample. **(b)** The first columns show the average percent of the genome assigned to each state for samples where DNase is present, the next column when DNase is absent, and the last column shows the log base two of the ratio between these two columns. This demonstrates that the percentage of the genome assigned to a state associated with DNase (State 17) is highly dependent on whether DNase data was available in the sample.

a

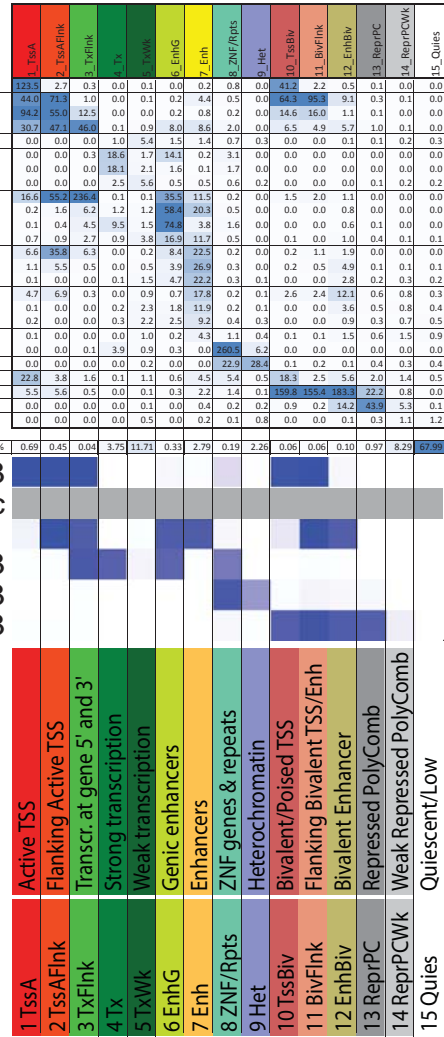
25-state model using 12-marks imputed across 127-samples

	1_TssA	2_PromU	3_PromD1	4_PromD2	5_TxS	6_TxW	7_TxWk	8_TxReg	9_TxReg5'	10_TxEnh5'	11_TxEnh3'	12_TxEnhW	13_EnhA1	14_EnhA2	15_EnhAF	16_EnhW1	17_EnhW2	18_EnhAc	19_DNase	20_ZNF/Rpts	21_Het	22_PromP	23_PromBiv	24_ReprPC	25_Quies
Genome %	0.4	0.1	0.0	5.0	0.4	89.3	92.3	96.5	99.9	99.1	86.4	3.5	0.18												
CG/GC/hg19																									
Exons_Gencodev10.hg19																									
Genes_Gencodev10.hg19																									
Introns_Gencodev10.hg19																									
TSS_Gencodev10.hg19																									
TES_Gencodev10.hg19																									
ZNF_genes																									
ZNF_Bgenes																									
Conserved																									
DNA Methylation Imputed																									
DNA Methylation Observed																									
RNA-seq Observed																									
RNA-seq Imputed																									

b Enrichment for 127-samples

15-state '5-Core-Marks'

Observed Model

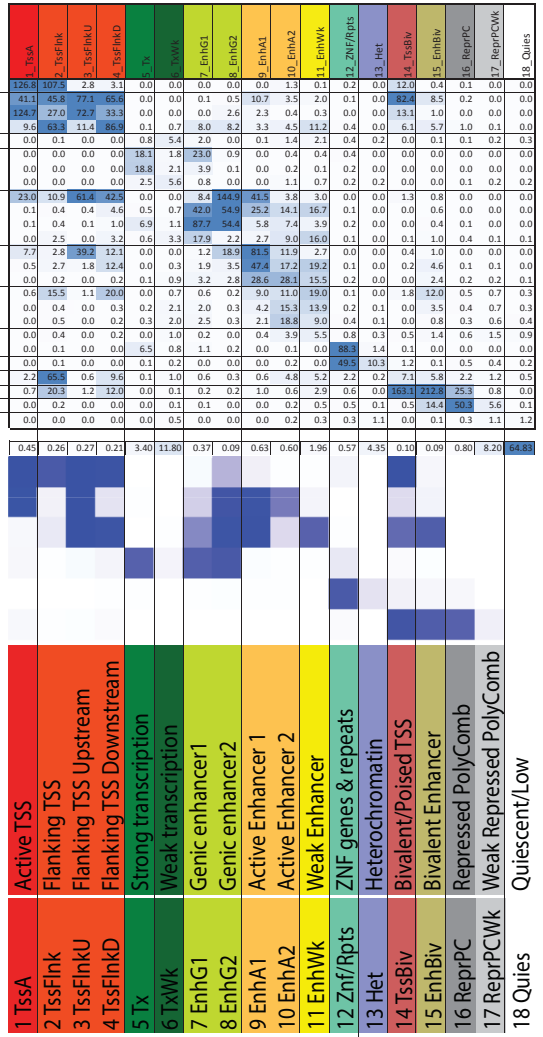


c

Enrichment for 98-samples

18-state '5-Core-Marks+H3K27ac'

Observed Model



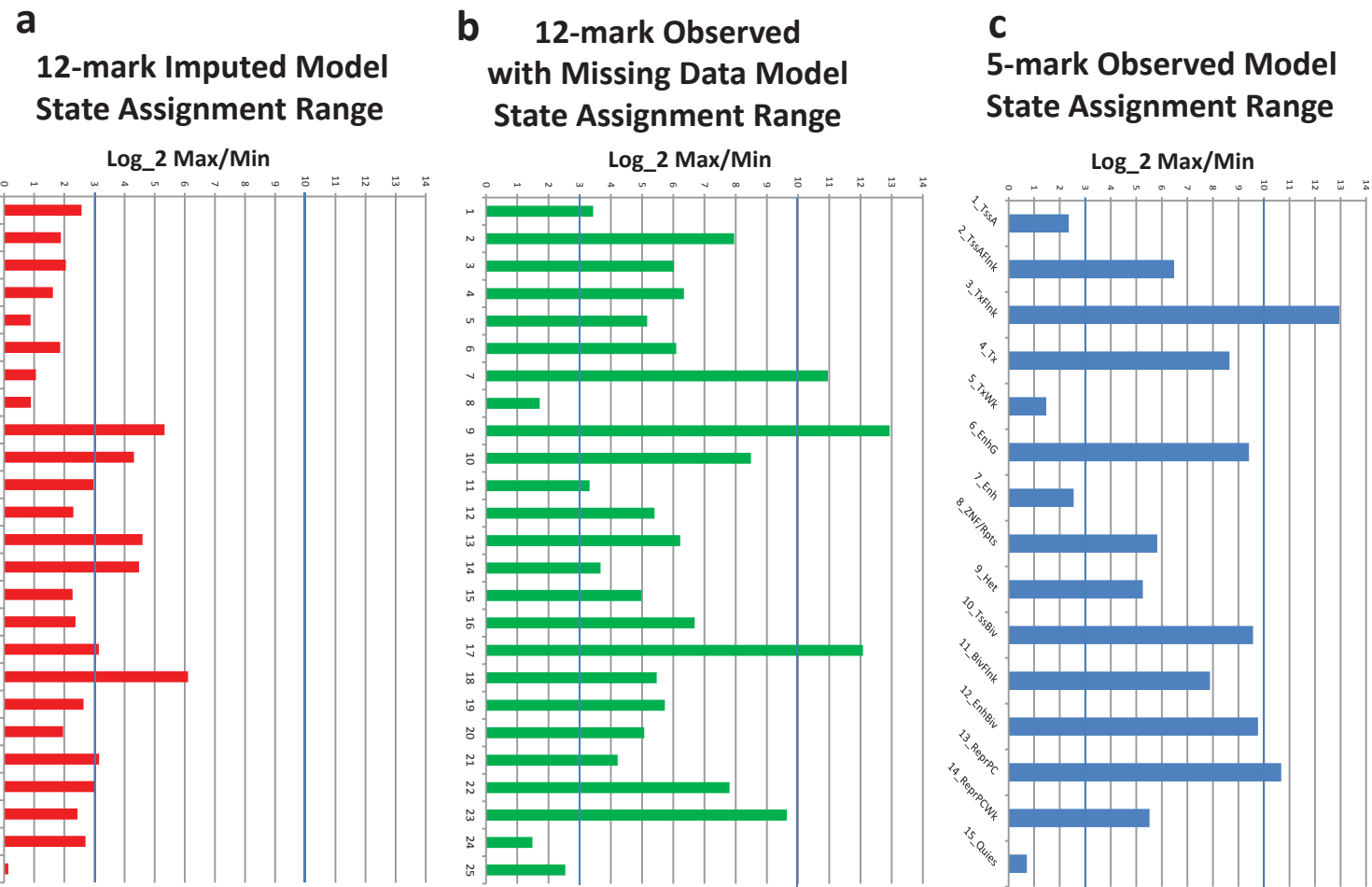
d

	1_TssA	2_PromU	3_PromD1	4_PromD2	5_TxS	6_TxW	7_TxWk	8_TxReg	9_TxReg5'	10_TxEnh5'	11_TxEnh3'	12_TxEnhW	13_EnhA1	14_EnhA2	15_EnhAF	16_EnhW1	17_EnhW2	18_EnhAc	19_DNase	20_ZNF/Rpts	21_Het	22_PromP	23_PromBiv	24_ReprPC	25_Quies
Genome %	0.18	97.6	10.1	1.3	0.6	3.5	2.5	96.9	9.4	3.6	5.9	0.03	0.13	0.6	0.7										
CG/GC/hg19																									
Exons_Gencodev10.hg19																									
Genes_Gencodev10.hg19																									
Introns_Gencodev10.hg19																									
TSS_Gencodev10.hg19																									
TES_Gencodev10.hg19																									
ZNF_genes																									
ZNF_Bgenes																									
Conserved																									
DNA Methylation Imputed																									
DNA Methylation Observed																									
RNA-seq Observed																									
RNA-seq Imputed																									

Supplementary Figure 33:

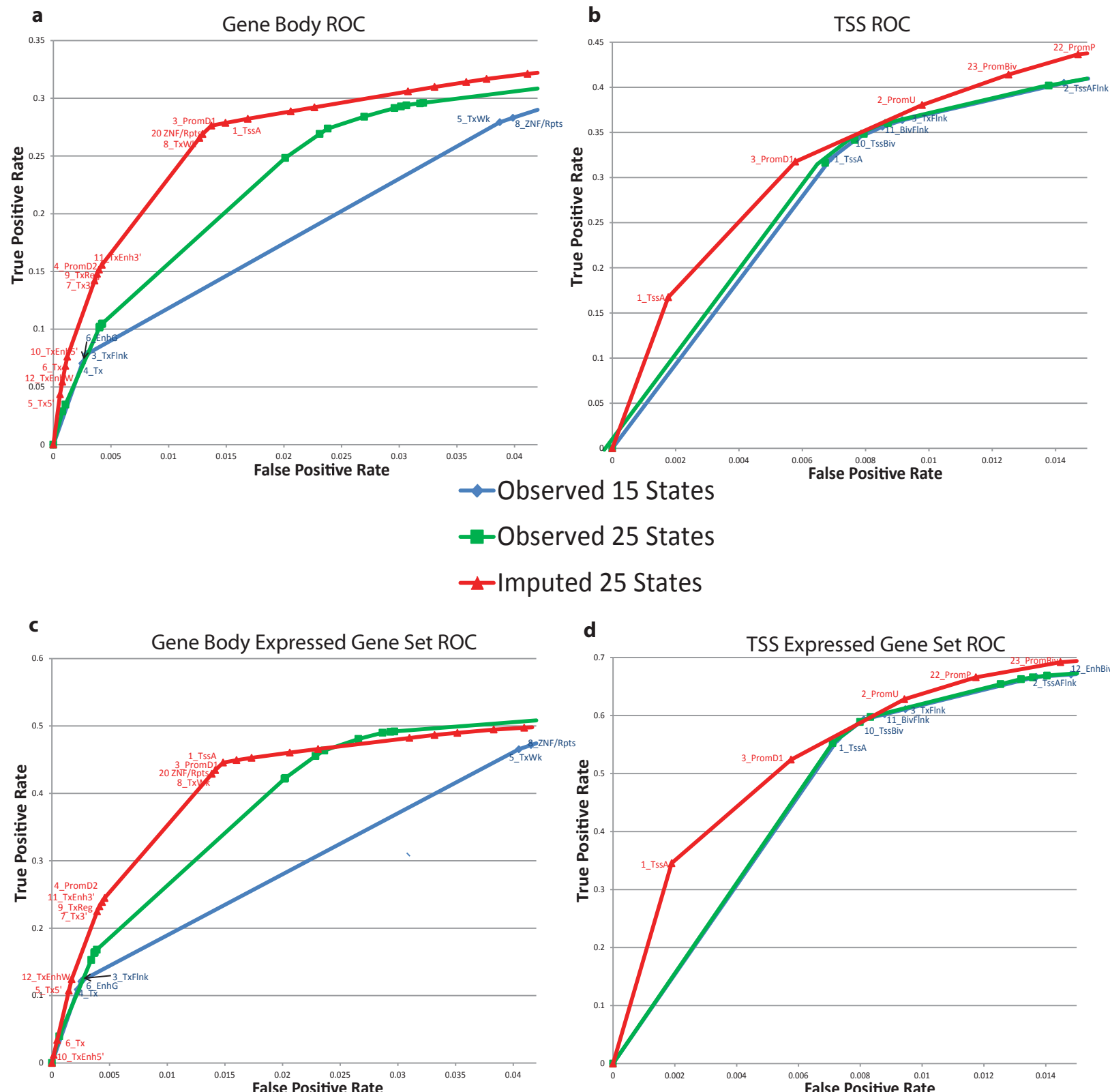
Enrichments of 12-mark Imputation Based Chromatin State Model.

(a) The emission parameters for the 25-state 12-mark imputation based model followed by the median percent of the genome across samples assigned to each state. (b) The median enrichments of the state assignments of the imputed data based model for the state assignments of a 15-state model based on observed data for five core marks (H3K4me1, H3K4me3, H3K9me3, H3K27me3, H3K36me3) from (Roadmap Epigenomics Consortium et al, 2015)¹⁰. The bottom row shows the median state assignment percentages. Below it is a heatmap of the emission parameters and state descriptions from (Roadmap Epigenomics Consortium et al, 2015)¹⁰. H3K27ac was not used in this model and is grayed out in the heatmap. (c) Similar to b except comparing state assignments for the imputation model for the state assignments of a 18-state model based on the core marks plus H3K27ac restricted to the 98 samples in which it was defined, also from (Roadmap Epigenomics Consortium et al, 2015)¹⁰. (d) Median state overlaps from Fig. 6c here with numeric details. All values are fold enrichments except the column after the state label is genome % and the last four columns report average signal values for observed and imputed DNA-methylation at CGs or RNA-seq data as indicated.



Supplementary Figure 34: Comparison of Chromatin State Model State Assignment Coverage Ranges.

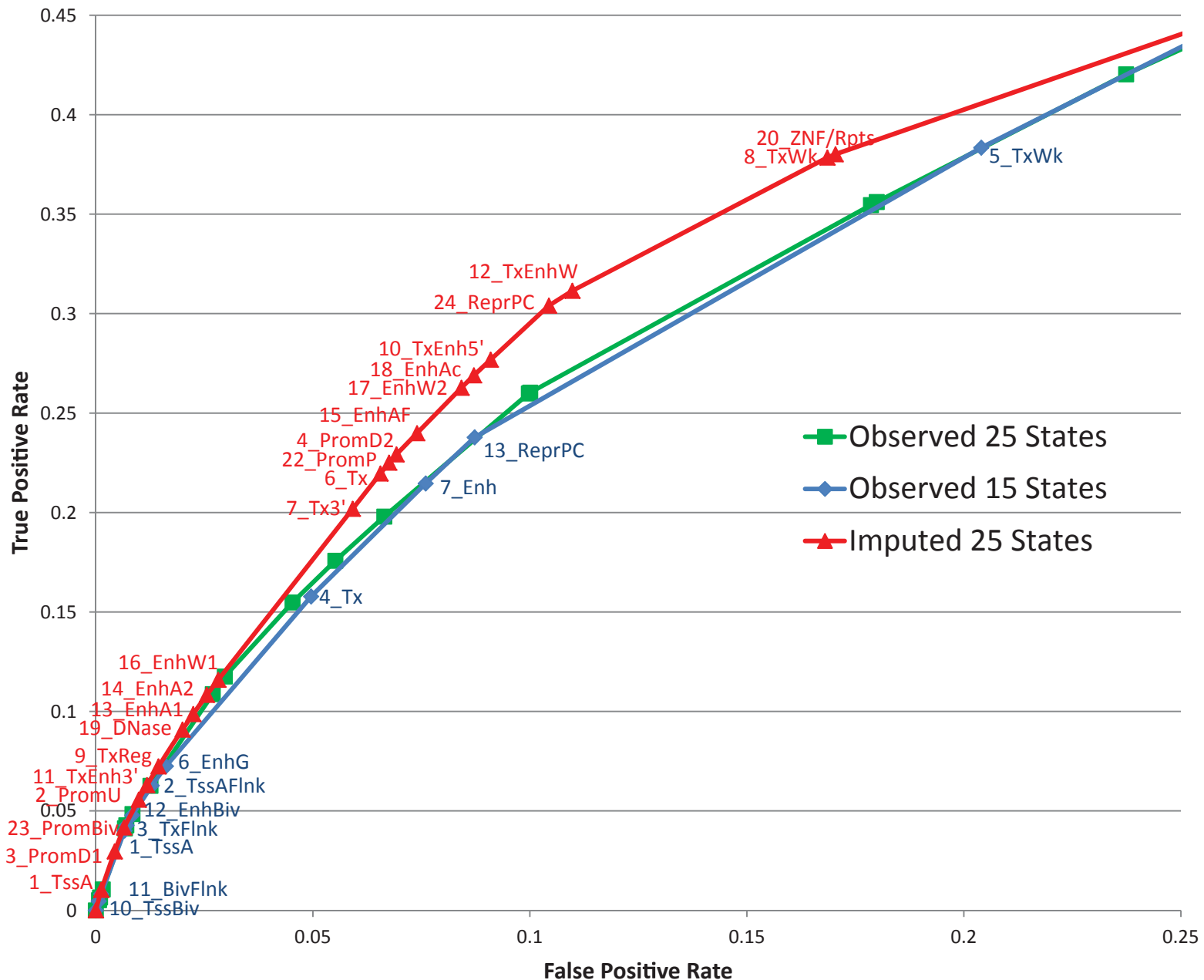
The graphs shows for three different models and each state the range of percentage of the genome assigned to each state in terms of log base two ratio of the maximum genome percentage for any sample divided by the minimum genome percentage. The three models are **(a)** 25-state imputation based model based on the 12 Tier-1 and 2 marks. **(b)** 25-state observed data model based on the 12 Tier-1 and 2 marks treating marks as missing data for some samples (**Fig. S32**). **(c)** 15-state observed data model based on 5-core marks mapped in every sample¹⁰ (also see **Fig. S33** for emission parameters). The graphs indicate that the chromatin states inferred based on the imputed data have a more consistent fraction of the genome assigned across samples than based on the observed data.



Supplementary Figure 35: Comparison of Chromatin State Models at Recovering Annotated Gene Features

(a) The plot compares the chromatin state agreement with annotated genes for the 25-state model based on imputed data for 12-marks, the 15-state model based on observed data for 5-marks¹⁰, and a 25-state model based on observed data for 5-marks learned in the same way as the 15-state model. The plot shows for each model a portion of the best possible ROC curve for recovering bases overlapping annotated genes based on a single ordering of states used across all samples. Predictions are made for each sample and the ROC curve represents the combined results. Labeled on the ROC curve are the top prioritized states for the 25-state imputed and the 15-state observed models at the cumulative true positive and false positive rate after making predictions based on the indicated state is included. (b) The same plot as in a but for annotated transcription start sites. (c), (d) The same as a and b, but based on a set of expressed genes (see Methods) and only using samples with gene expression data available.

Conserved Elements ROC

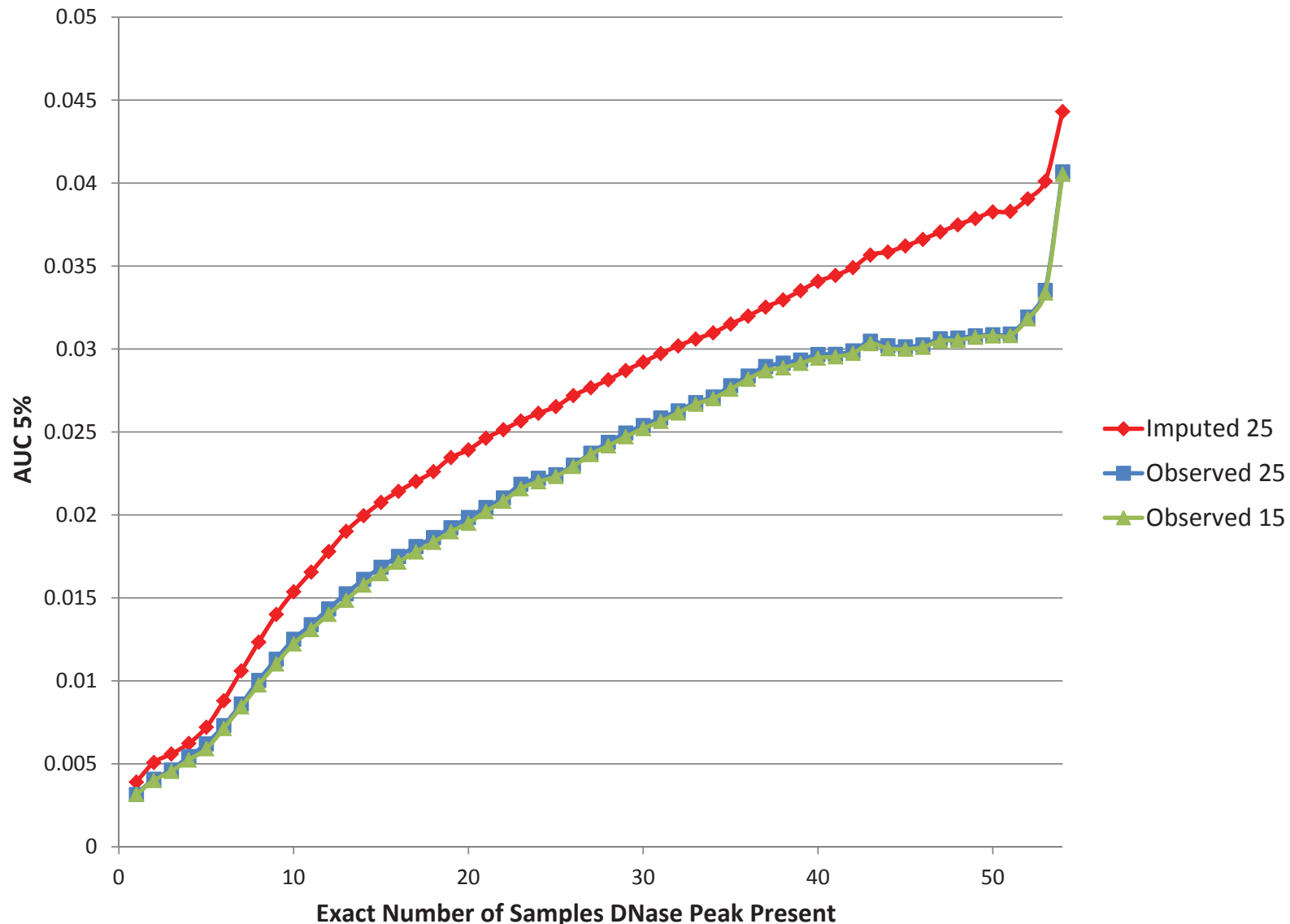


Supplementary Figure 36:

Comparison of Chromatin State Models at Recovering Evolutionarily Conserved Elements.

A similar plot to those shown in Fig. S35, but for recovering conserved elements based on the SiPhy-pi measure^{38,53}.

Osteoblasts DNase Peak Recovery

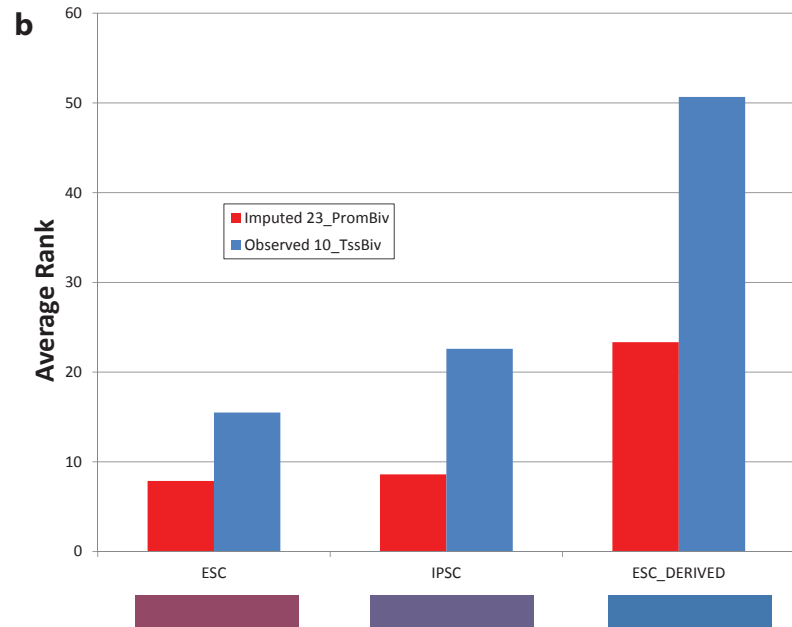


Supplementary Figure 37: Chromatin State Correspondence with Osetoblast DNase Sites.

The figure reports the AUC up to a false positive rate of 5% for chromatin state models recovering bases covered by a DNase site in Osteoblast cells corresponding to sample E129. The bases are stratified based on the number of samples that had a DNase peak overlapping it including this dataset in Osteoblast cells. Locations which had a DNase peak, but did not overlap the number of samples being evaluated were excluded for the specific evaluation. This DNase dataset was based on a different DNase protocol³⁹ than the other datasets and thus was not included in the processed data in (Roadmap Epigenomics Consortium et al, 2015)¹⁰ or used for the imputation here, and E129 otherwise did not have a DNase dataset associated with it. The three chromatin state models being compared are the imputed 25-state model, the observed 15-state model based on the 5-core marks¹⁰ and an observed 25-state model which was generated in the same way as the observed 15-state model except for having a different number of states. In order to generate the ROC curve to compute an AUC 5% value the chromatin states were ordered based on the greatest fold enrichment for the Osteoblast DNase peak bases. This figure demonstrates that the imputed model was better able to recover bases covered by DNase peaks from this data, though this difference generally increased for DNase peaks which were observed in increasing numbers of other samples.

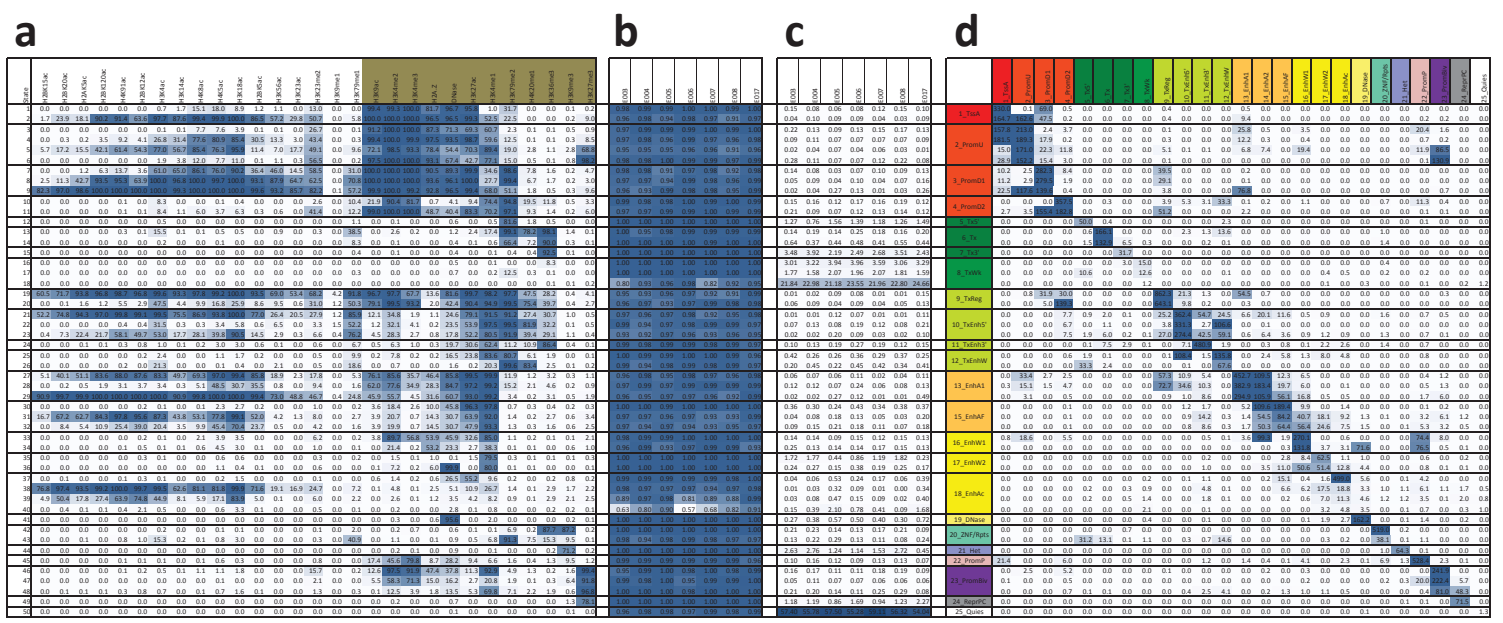
a Imputed Model 23_PromBiv Observed Model 10_TssBiv

Ranking	Imputed Model 23_PromBiv	Observed Model 10_TssBiv
1	E004_IPS-15b Cell Line	E018_IPS-15b Cell Line
2	E004_HUES48 Cell Line	E020_IPS-20b Cell Line
3	E020_IPS-20b Cell Line	E018_HUE564 Cell Line
4	E010_IPS-18 Cell Line	E001_ES-3 Cell Line
5	E002_ES-WAT Cell Line	E118_HepG2 Hepatocellular Carcinoma Cell Line
6	E010_HUES6 Cell Line	E015_HUE56 Cell Line
7	E010_HUES64 Cell Line	E019_IPS-1 Cell Line
8	E011_NESC Derived CD164+ Endoderm Cultured Cells	E014_HUE548 Cell Line
9	E008_H9 Cell Line	E012_NESC Derived CD56+ Ectoderm Cultured Cells
10	E003_H1 Cell Line	E070_Brain Germinal Matrix
11	E024_ES-CSF4 Cell Line	E003_H1 Cell Line
12	E012_NESC Derived CD56+ Ectoderm Cultured Cells	E057_Forekkin Keratinocyte Primary Cells skin02
13	E001_ES-5 Cell Line	E002_Fetal Brain Females
14	E004_H1 BMP4 Derived Mesendoderm Cultured Cells	E008_H9 Cell Line
15	E007_H1 Derived Neurogenin Progenitor Cultured Cells	E011_NESC Derived CD164+ Endoderm Cultured Cells
16	E021_IPS Df6-9 Cell Line	E092_Fetal Stomach
17	E008_H9 Derived Neurogenin Progenitor Cultured Cells	E112_Thymus
18	E008_Fetal Muscle Trunk	E078_Duodenum Smooth Muscle
19	E002_IPS Df6-19.11 Cell Line	E002_ES-WAT Cell Line
20	E001_Placenta	E004_Fetal Intestine Large
21	E002_Fetal Stomach	E002_Forekkin Fibroblast Primary Cells skin02
22	E010_Fetal Undifferentiated Cells	E003_Fetal Intestine Small
23	E004_Forekkin Fibroblast Primary Cells skin02	E013_NESC Derived CD56+ Mesendoderm Cultured Cells
24	E010_NESC Derived CD56+ Mesendoderm Cultured Cells	E103_Fetal Heart
25	E004_Fetal Heart	E004_Fetal Muscle Leg
26	E004_Fetal Muscle Leg	E004_Fetal Muscle Leg
27	E001_Fetal Brain Males	E111_Stomach Smooth Muscle
28	E002_Primary Hematopoietic stem cells	E002_Brain Hippocampus Moltke
29	E002_Placenta Ammon	E058_Forekkin Keratinocyte Primary Cells skin02
30	E002_Fetal Adrenal Gland	E008_Brain Cerebellar Gyrus
31	E003_Fetal Thymus	E005_Forekkin Fibroblast Primary Cells skin02
32	E008_Fetal Lung	E003_Primitive T cells from cord blood
33	E008_Fetal Kidney	E005_Adipose Derived Mesenchymal Stem Cell Cultured Cells
34	E004_Forekkin Melanocyte Primary Cells skin01	E010_Rectal Mucosa Donor 29
35	E007_Brain Germinal Matrix	E077_Duodenum Mucosa
36	E002_Primary Hematopoietic stem cells short term culture	E008_Fetal Kidney
37	E118_HepG2 Hepatocellular Carcinoma Cell Line	E107_Skeletal Muscle Male
38	E003_Primary T cells from cord blood	E002_Brain Dorsolateral Prefrontal Cortex
39	E003_Primary neutrophils from peripheral blood	E007_Brain Inferior Temporal Lobe
40	E120_KG62 Leukemia Cell Line	E010_Possas Muscle
41	E005_H1 BMP4 Derived Trophoblast Cultured Cells	E075_Colonic Mucosa
42	E007_Breast Myoepithelial Primary Cells	E005_Fetal Muscle Leg
43	E004_Fetal Intestine Large	E122_NHEK Epidermal Keratinocyte Primary Cells
44	E004_Primary T helper naïve cells from peripheral blood	E003_Fetal Melanocyte Female
45	E005_Fetal Intestine Small	E076_Colon Smooth Muscle
46	E113_Spleen	E009_Fetal Muscle Trunk
47	E001_Primary B cells from cord blood	E000_Fetal Adrenal Gland
48	E112_Thymus	E114_AS49_E010_H0.02oct Lung Carcinoma Cell Line
49	E006_Colon Smooth Muscle	E002_Primary mononuclear cells from peripheral blood
50	E110_Stomach Mucosa	E012_Rectal Mucosa Donor 31
51	E003_Primary T helper naïve cells from peripheral blood	E009_H9 Derived Neuronal Progenitor Cultured Cells
52	E002_Primary monocytes from peripheral blood	E001_Forekkin Melanocyte Primary Cells skin03
53	E042_Primary T helper 17 cells PMA1-stimulated	E129_Osteoblast Primary Cells
54	E005_Adipose Nuclei	E120_HSMM Skeletal Muscle Myoblasts Cell Line
55	E111_Stomach Smooth Muscle	E008_Brain Anterior Caudate
56	E006_H1 Derived Mesenchymal Stem Cells	E009_Forekkin Melanocyte Primary Cells skin01
57	E007_H9 Cell Line	E077_Myoblasts Cell Line Derived Adipocyte Cultured Cells
58	E004_Cardionectin derived primary cultured neurospheres	E003_Mesenchymal Stem Cell Cultured Cells
59	E077_Duodenum Mucosa	E121_BMSC derived Skeletal Muscle Myotubes Cell Line
60	E004_Primary T cells from peripheral blood	E007_Pancreatic Islets
61	E003_Primary T cells from peripheral blood	E007_H9 Derived Pancreatic Progenitor Cultured Cells
62	E078_Duodenum Smooth Muscle	E074_NHEK-Like CD14+ R001746 Cell Line
63	E002_Primary B cells from peripheral blood	E128_NHFL Lung Fibroblast Primary Cells
64	E004_Primary T regulatory cells from peripheral blood	E129_NHA-Astrocytes Cell Line
65	E004_Primary T helper cells from peripheral blood	E003_Primary mesenchymal stem cells derived Chondrocyte Cultured Cells
66	E002_Primary mononuclear cells from peripheral blood	E121_H9 Cell derived Adipocyte Nuclei
67	E001_Brain Females	E122_Cardionectin derived primary cultured neurospheres
68	E004_Cardionectin derived primary cultured neurospheres	E004_Primary T regulatory cells from peripheral blood
69	E007_Duodenum Mucosa	E010_H9 Derived Neuron Culture Cells
70	E003_Primary T helper naïve cells from peripheral blood	E109_Small Intestine
71	E118_HMEC Mammary Epithelial Primary Cells	E001_Skeletal Muscle Female
72	E102_Skeletal Muscle Female	E005_Left Ventricle
73	E004_Primary T helper memory cells from peripheral blood 1	E002_Brain Anterior Caudate
74	E005_Primary Hematopoietic stem cells G-CSF-mobilized Female	E022_IPS-Df6-18 Cell Line
75	E073_Brain Dorsolateral Prefrontal Cortex	E106_Sigmoid Colon
76	E004_Primary T killer memory cells from peripheral blood	E005_H1 BMP4 Derived Trophoblast Cultured Cells
77	E002_Primary T killer memory cells from peripheral blood	E005_H9 Derived Adipose Fibroblast Primary Cells
78	E001_Skeletal Muscle Male	E004_Cardionectin derived primary cultured neurospheres
79	E004_Forekkin Fibroblast Primary Cells skin01	E074_Primary T regulatory cells from peripheral blood
80	E002_Primary T helper memory cells from peripheral blood 2	E004_Primary T killer memory cells from peripheral blood
81	E118_HMEC Mammary Epithelial Primary Cells	E010_H9 Derived Neuron Culture Cells
82	E102_Skeletal Muscle Female	E109_Small Intestine
83	E004_Primary T helper memory cells from peripheral blood 1	E005_Left Ventricle
84	E005_Primary Hematopoietic stem cells G-CSF-mobilized Female	E002_Brain Anterior Caudate
85	E073_Brain Dorsolateral Prefrontal Cortex	E106_Right Ventricle
86	E004_Primary T killer memory cells from peripheral blood	E116_GM12878 Lymphoblastoid Cell Line
87	E002_Primary T killer memory cells from peripheral blood	E005_Primary T cells effectomerically enriched from peripheral blood
88	E010_Right Ventricle	E003_Cortico derived primary cultured neurospheres
89	E004_Brain Substantia Nigra	E122_HUVEC Umbilical Vein Endothelial Cells Cell Line
90	E012_H9 Derived lung fibroblasts Cell Line	E001_Placenta Ammon
91	E004_Brain Substantia Nigra	E003_Cortico derived primary cultured neurospheres
92	E004_Brain Substantia Nigra	E122_HUVEC Umbilical Vein Endothelial Cells Cell Line
93	E117_Hela-S3 Cervical Carcinoma Cell Line	E001_Placenta Ammon
94	E010_Rectal Mucosa Donor 29	E001_Primary B cells from cord blood
95	E007_Brain Angular Gyrus	E001_Primary neutrophils from peripheral blood
96	E002_Brain Inferior Temporal Lobe	E009_Primary T helper naïve cells from peripheral blood
97	E009_Brain Cingulate Gyrus	E005_Primary hematopoietic stem cells
98	E114_AS49_E010_H0.02oct Lung Carcinoma Cell Line	E001_Primary T helper cells PMA1-stimulated
99	E002_Brain variant Human Mammary Epithelial Cells (vHMEC)	E001_Primary T killer memory cells from peripheral blood
100	E004_Gastric	E004_Primary T killer memory cells from peripheral blood
101	E124_Monocyte-D14+ R001746 Cell Line	E006_H9 Derived Mesenchymal Stem Cells
102	E001_Forekkin Melanocyte Primary Cells skin03	E003_Primary monocytes from peripheral blood
103	E115_Dnd1 T Cell Leukemia Cell Line	E019_HMEC Mammary Epithelial Primary Cells
104	E102_Rectal Mucosa Donor 31	E009_Ovary
105	E007_Brain Angular Gyrus	E005_Aorta
106	E127_NHEK Epidermal Keratinocyte Primary Cells	E002_Primary T helper 17 cells PMA1-stimulated
107	E002_Mesenchymal Stem Cell Derived Adipocyte Cultured Cells	E003_Primary T killer memory cells from peripheral blood
108	E006_Lung	E007_Primary T killer naïve cells from peripheral blood
109	E124_NHA-Astrocytes Cell Line	E009_Placenta Ammon
110	E120_NHFL Lung Fibroblast Primary Cells	E009_Placenta Ammon
111	E002_Adipose Derived Mesenchymal Stem Cell Cultured Cells	E003_Primary hematopoietic stem cells G-CSF-mobilized Female
112	E002_Mesenchymal Stem Cell Derived Chondrocyte Cultured Cells	E003_Primary monocytes from peripheral blood
113	E002_Mesenchymal Stem Cell Derived Chondrocyte Cultured Cells	E003_Primary T helper naïve cells from peripheral blood
114	E007_Brain Hippocampus Midline	E003_Primary T killer memory cells from peripheral blood
115	E122_HUVEC Umbilical Ven Endothelial Cells Cell Line	E008_Lung
116	E121_H9 Cell derived Skeletal Muscle Myoblasts Cell Line	E002_Primary T cells from peripheral blood
117	E120_HSMM Skeletal Muscle Myoblasts Cell Line	E008_Primary Natural Killer cells from peripheral blood
118	E008_Forekkin Keratinocyte Primary Cells skin03	E004_Right Atrium
119	E009_Esophagus	E003_Fetal Heart
120	E120_HSMM Skeletal Muscle Myoblasts Cell Line	E003_Soleus
121	E120_Osteoblast Primary Cells	E117_Hela-S3 Cervical Carcinoma Cell Line
122	E008_Bone Marrow Derived Cultured Mesenchymal Stem Cells	E115_Dnd1 T Cell Leukemia Cell Line
123	E120_NHDF-Ad Adult Dermal Fibroblast Primary Cells	E003_Primary T helper memory cells from peripheral blood 2
124	E009_Mouse Satellite Cultured Cells	E006_Liver
125	E009_Left Ventricle	E004_Primary T helper memory cells from peripheral blood 1
126	E104_Right Atrium	E004_Gastric
127	E004_Aorta	E008_Pancreas



Supplementary Figure 38:
Comparison of Sample Ranking for Bivalent State.

(a) On left the 127 samples are ranked based on the relative amount of genome assigned to state 23_PromBiv a bivalent promoter state from a chromatin state mode learned from the imputed data (**Fig. 6c**). On the right the same samples are ranked, but based on the presence of a bivalent promoter state (10_TssBiv) from a chromatin state model learned based on the observed data for 5-core marks (**Fig. S33**)¹⁰. The samples are colored based on their biological groups (**Fig. 1**). (b) The figure shows that for samples corresponding to Embryonic Stem Cells (ESC), Induced Pluripotent Stem Cells (iPSC), and ESC derived cells (ESC_DERIVED), which could be expected to have a greater presence of the bivalent state⁴⁰ relative to other samples, the average of their ranks is lower (corresponding to a greater relative presence of the bivalent state) for the imputed model compared to the observed data model. Colors corresponding to each of these three groups is shown below the graph and the individual samples that comprise them have this color in a.



Supplementary Figure 39:

Comparison of 29-mark and 12-mark Imputation Based Chromatin State Models.

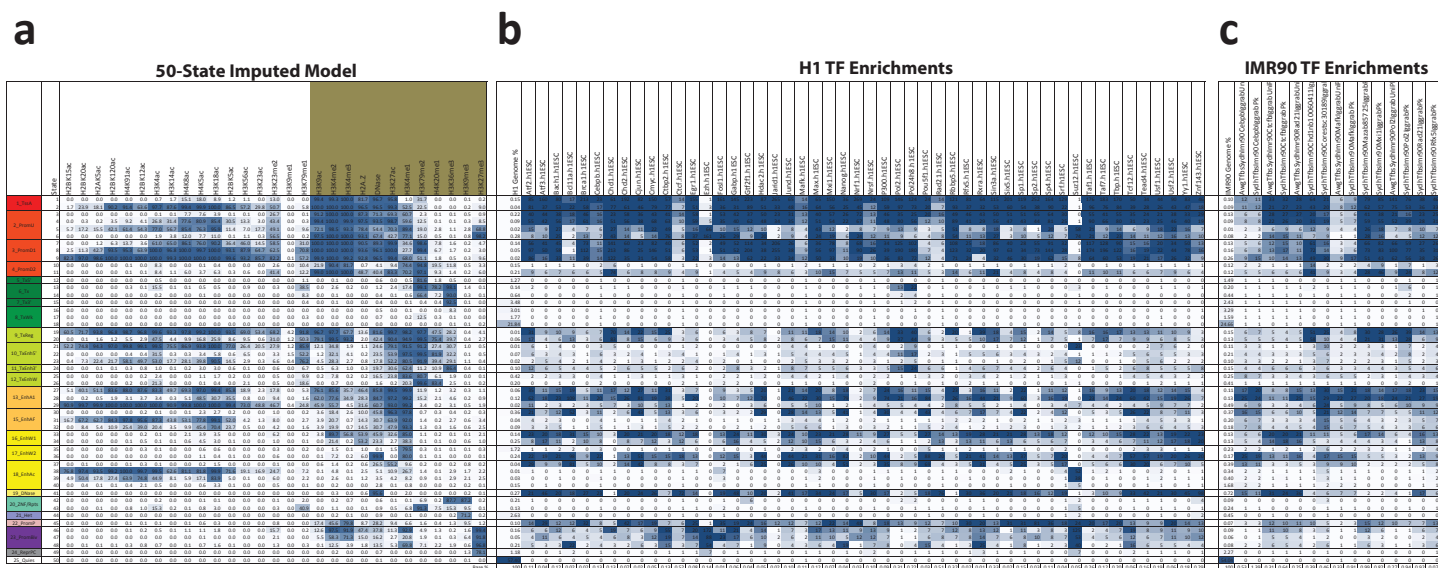
(a) The emission parameters for a 50-state chromatin model learned based on imputed data for 29-marks across the seven samples with deep mark coverage (also see **Fig. 6d**). The marks that are shaded are the Tier-1 and 2 marks. **(b)** The heatmap shows the correlation of the emission parameters with the frequency each mark was found at locations assigned to the state for each of the seven samples. **(c)** The percentage of the genome assigned to each state in the seven samples used to learn the model. **(d)** The median fold enrichment of each state across the seven samples for each state of a 25-state model learned based on the imputed data for the Tier-1 and 2 marks (**Figs. 6c and S33**). The states of the 50-state model have been grouped based on their maximum enrichment for states of this 25-state model.

a

		Best match 25-state			
	Date				
1_TshA	3	0.0	0.0	0.0	0.0
	2	1.7	23.9	18.1	50.2
2_PromU	3	0.0	0.0	0.0	0.0
	4	0.0	0.3	0.2	3.5
3_PromD1	5	5.7	17.2	15.5	42.1
	6	0.0	0.0	0.0	0.0
4_PromD2	7	0.0	0.0	1.2	6.3
	8	2.5	11.3	42.7	95.5
5_TxS	9	82.3	97.8	98.0	100.0
	10	0.0	0.0	0.0	0.0
6_Tx	11	0.0	0.0	0.0	0.0
	12	0.0	0.0	0.0	0.0
7_Tx3'	13	0.0	0.0	0.0	0.0
	14	0.0	0.0	0.0	0.0
8_TxWk	15	0.0	0.0	0.0	0.0
	16	0.0	0.0	0.0	0.0
9_TxReg	17	0.0	0.0	0.0	0.0
	18	60.5	71.7	39.8	36.8
10_TxEnhS'	19	52.2	74.8	94.3	97.0
	20	0.0	0.0	0.0	0.0
11_TxEnh3'	21	0.0	0.0	0.0	0.0
	22	0.4	7.3	22.4	21.7
12_TxenhW	23	0.0	0.0	0.1	0.3
	24	0.0	0.0	0.0	0.0
13_EnhA1	25	0.0	0.0	0.0	0.0
	26	0.0	0.1	1.6	1.2
15_EnhAP	27	5.1	40.1	51.1	83.6
	28	0.0	0.2	0.5	1.9
16_EnhW1	29	0.0	0.0	0.0	0.0
	30	0.0	0.0	0.0	0.0
17_EnhW2	31	0.0	0.0	0.0	0.0
	32	0.0	0.0	0.0	0.0
18_EnhAc	33	0.0	0.0	0.0	0.0
	34	0.0	0.0	0.0	0.0
19_Dnase	35	0.0	0.0	0.0	0.0
	36	0.0	0.0	0.0	0.0
20_ZNF/Rpts	37	0.0	0.0	0.0	0.0
	38	76.8	97.4	93.5	99.2
21_Het	39	4.9	50.4	17.8	27.4
	40	0.0	0.4	0.1	2.1
22_PromP	41	0.0	0.0	0.0	0.0
	42	0.0	0.0	0.0	0.0
23_PromBiv	43	0.0	0.1	0.0	1.0
	44	0.0	0.0	0.0	0.0
24_ReRPC	45	0.0	0.0	0.0	0.0
	46	0.0	0.0	0.0	0.0
25_Quies	47	0.0	0.0	0.1	0.0
	48	0.0	0.1	0.1	0.3
26	49	0.0	0.0	0.0	0.0
	50	0.0	0.0	0.0	0.0

b

		Genomic %													
		Exons	introns	UTR5	UTR3	TSS	2kbp	5kbp	10kbp	20kbp	50kbp	1M	2M	DNA_Methyl_Observed	RNA-seq_Observed
1_TshA	0.10	93.8	0.0	1.4	0.7	3.8	2.7	3.8	4.1	4.0	0.0	0.1	0.6	0.9	0.0
2_PromU	0.09	80.2	9.2	1.3	0.7	3.1	4.0	4.7	8.6	2.6	3.5	0.1	0.2	0.3	0.4
3_PromD1	0.13	34.9	5.0	1.1	0.8	3.2	2.5	27.8	8.4	2.6	3.5	0.1	0.2	0.3	0.4
4_PromD2	0.07	58.7	7.5	1.2	0.7	3.2	2.6	45.4	8.8	3.3	4.2	0.1	0.1	0.4	0.6
5_TxS	0.08	58.1	6.5	1.3	0.9	3.9	2.6	4.13	7.0	1.0	3.6	0.2	0.2	0.5	0.5
6_Tx	0.11	85.3	8.1	1.5	1.0	3.7	2.5	25.4	8.7	1.2	5.4	0.1	0.1	0.3	0.4
7_Tx3'	0.09	64.2	9.2	1.3	1.4	4.0	2.9	41.5	10.0	5.3	4.9	0.0	0.1	1.2	1.3
8_TxWk	0.07	89.3	11.8	1.4	1.1	4.1	3.0	46.0	10.0	4.3	5.8	0.0	0.1	1.5	1.6
9_TxReg	0.12	73.7	8.5	1.4	0.9	3.0	2.6	5.6	1.4	3.1	3.0	0.3	0.3	0.7	0.8
10_TxEnhS'	0.04	41.4	0.0	0.0	0.0	0.0	0.0	0.0	0.0	0.0	0.0	0.0	0.0	0.0	0.0
11_TxEnh3'	0.08	2.68	1.27	0.2	1.6	5.0	2.2	2.7	2.8	2.8	0.9	0.9	1.0	1.0	1.0
12_TxenhW	0.22	30.0	0.2	1.1	1.2	0.9	1.3	0.6	1.0	0.7	1.0	0.9	0.1	0.1	0.1
13_EnhA1	0.02	8.66	4.2	1.7	1.7	3.7	2.3	4.4	4.9	2.0	3.5	0.5	0.8	1.0	1.0
14_EnhAP	0.04	16.8	5.4	2.0	1.7	6.3	3.8	3.1	3.0	3.0	3.0	0.9	0.9	1.1	1.1
15_EnhAF	0.04	44.1	5.1	2.0	1.7	9.0	2.4	2.9	3.9	2.5	3.5	1.0	1.1	1.0	1.1
16_EnhW1	0.02	2.68	1.27	0.2	1.6	5.0	2.2	2.7	2.8	2.8	0.9	0.9	1.0	1.0	1.0
17_EnhW2	0.15	1.07	1.2	0.9	0.9	1.0	1.3	1.8	2.1	1.7	1.7	0.8	0.8	0.3	0.7
18_EnhAc	0.08	1.06	0.6	0.3	0.3	0.7	0.9	1.2	1.4	1.2	1.2	0.5	0.5	0.7	0.7
19_Dnase	0.29	17.9	7.4	1.4	1.6	7.6	4.4	3.0	3.2	1.9	3.6	0.8	0.8	1.3	1.5
20_ZNF/Rpts	0.02	0.18	0.8	2.0	2.4	0.7	0.9	1.1	1.8	2.1	1.9	0.8	0.8	0.1	0.4
21_Het	0.02	0.12	0.5	2.0	2.3	0.6	0.8	0.7	1.2	1.4	0.7	0.9	0.1	0.1	0.4
22_PromP	0.01	0.08	0.17	1.3	1.3	1.1	1.7	1.5	3.3	2.5	1.1	2.8	0.5	0.2	0.4
23_PromBiv	0.02	0.12	0.2	1.0	1.0	0.4	0.5	0.5	0.6	0.6	0.6	0.6	0.6	0.6	0.6
24_ReRPC	0.02	0.08	0.17	1.2	1.2	1.2	1.4	1.4	1.6	1.6	1.6	1.6	1.6	1.6	1.6
25_Quies	0.02	0.08	0.17	1.2	1.2	1.2	1.4	1.4	1.6	1.6	1.6	1.6	1.6	1.6	1.6



Supplementary Figure 41: Chromatin State Transcription Factor Binding Enrichments.

(a) The same emission parameters of the same expanded mark chromatin state model based on imputed data shown in **Fig. 6d** and **Fig. S39-40**. **(b)** The heatmap shows the H1 chromatin state fold enrichment for a collection of H1 ENCODE transcription factor binding datasets based on the uniform processed peak calls², which was curated in (Roadmap Epigenomics Consortium et al, 2015)¹⁰. The first column gives the chromatin state percentages and the last row the genome coverage of the peak call dataset. **(c)** The same heatmap but for the IMR90 chromatin states and a collection of ENCODE transcription factor binding in IMR90 cells². The table shows data for ten different datasets, based on the lab provided peak calls. For five of the data sets there was also available uniformly processed peak calls² indicated by the 'Awg' prefix and their enrichments are also shown.

Relative Top 1% Agreement and 0.25-concordance for DNA-methylation

a

Relative Coefficient of Determination

b

Supplementary Figure 42: Feature Subset Performance for Seven Samples with Deep Mark Coverage.

(a) An extension of the table shown in **Fig. 6a**. The table reports for various feature subsets (rows) the relative average imputation performance for different marks (columns) compared to an imputation conducted using all features. The imputation was done based on only data for the seven samples with deep mark coverage and making no distinctions between Tier-1-3 marks. The feature subsets include using only same sample features as the target, only same mark features from other samples, and all features that can be computed for various subsets of the mark subsets specified, or restricted to same sample features for the mark subset if indicated. The imputation performance is computed based on the agreement in top 1% signal on chr10, except for the DNA methylation which is based on the % of predictions within 0.25 of the observed data on chr10. In italics are those cases in which the target mark is also a mark of the row, but was not used for its imputation. The last two columns show the average performance of the feature subset over all target marks and specifically for acetylations. For the purpose of computing these averages for mark subsets if the target mark is part of the mark subset of the row then a value of 1 is used for the target mark. The mark subset evaluations involving H3K79me2 are limited to five samples where H3K79me2 is present. In gray are values which could not be predicted based on the method. **(b)** The same as **a** except based on the coefficient of determination, which was used here instead of the correlation coefficient so the relative agreement would be meaningful.

a

b

C

Core + mark

Core + mark	
Core Marks	
+H3K18ac	
+H4K91ac	
+H3K79me2	
+H2BK120ac	
+H4K85c	
+H3K4ac	
+H4K5ac	
+H3K14ac	
+H2AK5ac	
+H2BK20ac	
+H2BK5ac	
+H2BK15ac	
+H3K79me1	
+H4K20me1	
+Dline	
+H3K56ac	
+H3K27ac	
+H3K23ac	
+H4A-Z	
+H3K9ac	
+H3K23me2	
+H3K4me2	
+H3K9me1	
82	75 80 79 79 79 79 71 82 65 82 78 76 83 77 80 82 86 82 88 79 83 90 71 87 82
0	7 24 0 14 23 8 24 7 15 10 11 16 11 1 0 8 0 8 0 5 0 0 1 0
41	49 45 55 45 44 45 51 45 48 45 44 47 45 52 47 40 47 40 45 53 57 37 50 41
0	34 7 1 9 7 24 7 29 7 2 2 4 0 1 0 2 2 4 3 0 0 1 0
3	50 43 3 38 35 43 53 50 40 38 16 17 14 11 9 3 4 7 9 16 4 4 4 3 3
58	53 50 58 58 58 58 57 55 57 58 58 58 58 57 58 66 58 49 84 88 94 59 70 58
6	41 8 34 8 10 34 12 24 21 8 8 6 7 4 8 15 9 6 14 7 9 6 6
1	53 72 32 45 72 55 63 59 30 61 11 69 5 50 1 2 62 1 51 1 1 27 1
14	40 45 9 51 45 40 42 40 43 61 77 46 73 24 17 28 48 31 47 23 24 36 17 14
26	35 29 40 29 30 35 24 36 31 28 29 32 28 27 21 24 51 31 54 28 30 59 37 26
34	40 38 53 37 38 42 30 44 37 38 40 37 32 24 41 39 36 38 35 42 25 34 34
8	9 90 9 9 9 9 10 9 9 10 9 24 40 10 8 8 9 13 9 8 7 8
10	11 11 65 11 10 10 22 11 9 10 10 11 10 36 78 12 12 14 10 11 10 10 11 10
8	9 9 77 9 9 10 9 9 9 9 9 34 31 10 9 9 8 11 8 8 8 8
97	96 99 96 96 96 97 96 96 96 96 96 96 96 96 96 96 96 96 96 96 96 96 96 97
90	89 97 90 89 89 89 89 89 89 89 89 89 89 89 93 94 90 90 90 89 89 90 90
9	10 10 91 10 10 8 11 10 10 11 10 30 17 11 10 8 10 14 10 10 9 9
77	79 80 79 78 78 78 78 78 77 78 77 78 78 78 77 79 77 78 77 78 77 78 77
4	28 31 10 30 32 30 22 30 32 31 24 30 24 32 32 6 18 25 10 23 6 28 16 18 6 5
47	43 53 47 43 47 44 39 43 46 47 47 45 47 49 71 40 42 46 57 41 53 41 47 46
0	22 27 3 28 34 28 23 27 26 32 27 27 23 15 1 1 8 7 12 0 4 10 1 0
16	17 17 45 17 17 17 17 10 17 16 17 17 17 37 67 15 14 13 16 18 16 15 19 18
0	18 12 1 10 5 7 2 6 4 6 3 2 2 6 1 1 1 1 0 1 0 0 1 1 0
62	60 70 61 60 61 61 60 61 61 61 61 60 61 68 67 68 62 67 62 61 61 62 63
23	27 28 73 29 29 28 19 29 27 27 30 29 28 46 37 27 26 14 26 44 26 25 21 23
5	6 26 7 7 6 5 7 6 7 7 6 15 82 7 5 7 6 7 6 5 6 5 6 5 6 5
0	21 24 0 24 22 19 22 12 12 14 8 13 6 0 0 0 3 0 2 4 1 1 0 0
20	19 24 19 25 25 23 24 21 23 24 22 19 20 20 29 20 24 20 15 28 19 31 20
1	70 70 1 70 74 75 72 74 73 76 77 79 80 19 2 5 68 8 55 20 32 48 25 2
23	25 21 24 23 30 23 21 31 24 30 20 19 21 21 24 24 18 81 19 19 21 19 26
0	13 38 0 28 29 21 30 10 14 24 21 8 17 0 0 0 9 1 3 0 1 2 1 0
37	35 15 0 22 17 13 13 20 10 16 15 8 4 0 0 0 1 2 1 0 0 1 0
35	36 37 42 37 37 36 39 37 37 37 37 39 37 40 39 32 37 33 37 30 50 36 41 35
1	2 1
84	83 89 83 84 84 84 84 85 84 84 84 85 87 88 89 85 90 85 82 87 84 84 85
0	0 0
3	7 6 4 7 6 6 5 6 5 6 5 5 3 4 8 4 8 3 4 6 4 5 3
0	40 51 1 42 67 63 61 58 50 71 60 56 62 1 1 1 19 1 16 1 1 1 20 1 1
59	58 0 54 10 3 16 4 1 6 24 1 3 0 0 0 0 0 0 0 0 0 0 0 0
2	68 62 3 68 49 42 54 42 37 49 57 35 43 4 4 3 4 16 9 15 4 5 19 5 2
0	0 0
97	97 98 97
3	5 25 4 4 4 4 5 4 4 4 4 4 4 34 6 4 4 3 4 4 4 4 4 3
99	99 99
60	65 65 61 62 66 63 66 63 61 60 63 60 62 65 63 69 61 68 67 66 67
67	72 68 73 67 67 68 74 68 71 69 67 67 67 68 67 68 67 67 70 80 76 71 67
59	60 59 59 59 59 60 59 59 59 59 59 59 59 59 59 63 59 66 63 65 75 79
82	83 82 87 82 82 82 82 82 82 82 82 83 85 82 83 82 82 82 82 82 82 82 82
99	99 99
97	97 97
0	0 0
31	43 42 42 42 41 41 41 40 40 39 38 38 37 37 36 36 35 34 34 34

d

Supplementary Figure 43: Chromatin State Recovery with Different Mark Subsets.

(a) (left) The emission parameters of the same expanded mark chromatin state model on imputed data also shown in **Fig. 6d** and **Fig. S39-40**. (right) An evaluation of chromatin state recovery of this model using all marks of the model except the indicated mark of the column. Shown for each state is the percentage of locations assigned to it based on a maximum-posterior decoding for the full set of marks that would receive the same state assignment based on performing the posterior decoding with the indicated subset of marks. Along the bottom is the minimum state recovery of any state and the average state recovery. Columns are ordered by increasing minimum state recovery. **(b)** The same as **a** except showing the results for the subset of all Tier-1 and 2 marks along with this set extended by the one additional mark indicated in the column. Columns for the extended set are ordered in decreasing order of minimum state recovery. **(c)** The same as **b** except based on the core mark set of H3K4me3, H3K4me1, H3K36me3, H3K9me3, and H3K27me3 instead of the Tier-1 and 2 mark set and the columns are ordered in decreasing average state recovery. **(d)** The same as **c** except showing the chromatin state recovery with only the single mark of the column.